

ENHANCED TRANSDERMAL DRUG DELIVERY OF NSAIDS USING EUTECTIC FORMATION AND A TWO-PHASE LIQUID SYSTEM

by

XUDONG YUAN

(Under the Direction of Anthony C. Capomacchia)

ABSTRACT

The thermodynamic, eutectic and crystalline properties of binary mixtures of selected non-steroidal anti-inflammatory drugs (NSAIDs), enantiomers, eutectic and racemate of ibuprofen were investigated using differential scanning calorimetry (DSC) and X-ray powder diffractometry (XRPD). DSC studies showed that melting points, enthalpy and entropy of fusion of the eutectic were significantly reduced as compared to those of the individual drugs or enantiomers. XRPD indicated that the eutectic did not form a new crystalline structure different from that of pure drugs or enantiomers. Ibuprofen and ketoprofen were selected to study the effect of eutectic formation on membrane permeation using *in vitro* diffusion and snake skin as the model membrane. The presence of aqueous isopropyl alcohol (IPA) was necessary to transform the solid drugs into a two-phase liquid system at ambient temperature. Due to melting point depression by eutectic formation, high drug concentration in the oily phase and maximum thermodynamic activity in the system, the preparation based on the two-phase liquid system showed significantly higher permeation rates of ibuprofen and ketoprofen as compared to other

reference preparations. The stability of the two-phase system was studied and no degradation of drugs was observed. The effects of reduced melting points of the drugs on the flux of membrane permeation were also predicted by two mathematical models based on ideal solution theory and by using enthalpy, entropy, melting point and other thermodynamic parameters. The experimental data of maximum fluxes were not significantly different from the predicted values, suggesting that the changes of maximum fluxes of drugs could be estimated if their melting point depression and other relevant thermodynamic data are available. The eutectic mixture was developed into emulsion, O/W and W/O creams and gel formulations to study the effect of vehicles and formulation types on drug permeation. Drug release testing was conducted to compare the fluxes of ibuprofen and ketoprofen in different formulations and two commercial creams by using the model membrane. The stability of the cream was studied at different temperatures for six months and examined periodically for organoleptic characteristics, content of drugs, particle size and apparent viscosity. The prepared formulation was found to be stable under the condition used.

INDEX WORDS: Ibuprofen; Ketoprofen; NSAIDs; Binary eutectic; Two-phase liquid system; Membrane permeability; Enhanced transdermal drug delivery; Topical formulations.

**ENHANCED TRANSDERMAL DRUG DELIVERY OF NSAIDS USING
EUTECTIC FORMATION AND A TWO-PHASE LIQUID SYSTEM**

by

XUDONG YUAN

B.S., Nanjing University of Traditional Chinese Medicine, China, 1993

M.S., National University of Singapore, Singapore, 1999

A Dissertation Submitted to the Graduate Faculty of The University of Georgia in Partial
Fulfillment of the Requirements for the Degree

DOCTOR OF PHILOSOPHY

ATHENS, GEORGIA

2003

© 2003

Xudong Yuan

All Rights Reserved

**ENHANCED TRANSDERMAL DRUG DELIVERY OF NSAIDS USING
EUTECTIC FORMATION AND A TWO-PHASE LIQUID SYSTEM**

by

XUDONG YUAN

Major Professor: Anthony C. Capomacchia

Committee: James C. Price
D. Robert Lu
Catherine White
John W. McCall

Electronic Version Approved:

Maureen Grasso
Dean of the Graduate School
The University of Georgia
August 2003

DEDICATION
TO
DAD, MOM, SISTER AND MY WIFE
WITH LOVE

ACKNOWLEDGEMENTS

I would like to express my most sincere thanks and gratitude to my major professor Dr. Anthony C. Capomacchia for his support, patience, encouragement and guidance during my various endeavors and hardships in my graduate studies.

I would like to thank Dr. James C. Price, Dr. D. Robert Lu, Dr. Catherine White and Dr. John W. McCall for serving in my advisory committee and their continuous support and help. Especially, I would like to thank Dr. James C. Price for advising me with his detailed explanation and insights that helped me clarify my thoughts. Also I would like to thank Dr. John W. McCall for his financial support in terms of research scholarship in my first two years of graduate study.

I am very grateful of the University of Georgia for the financial support in terms of teaching assistantship and university wide scholarship in the past years.

I would like to dedicate this thesis to my parents, sister and my wife, who have been giving me unconditional love and care, for everything they have done for me.

Last, but definitely not least, I would also like to express my deep appreciation to the help and encouragement I received from my friends wherever they are.

TABLE OF CONTENTS

	Page
ACKNOWLEDGEMENTS	v
CHAPTER	
1 INTRODUCTION AND LITERATURE REVIEW	1
2 THE BINARY EUTECTIC OF NSAIDS AND A TWO-PHASE LIQUID SYSTEM FOR ENHANCED MEMBRANE PERMEATION.....	47
3 PHYSICOCHEMICAL STUDIES OF THE BINARY EUTECTIC OF IBUPROFEN AND KETOPROFEN AND MATHEMATICAL MODELS FOR ENHANCED TRANSDERMAL DELIVERY	79
4 THE PERMEATION AND STABILITY OF IBUPROFEN AND KETOPROFEN IN BINARY EUTECTIC TWO-PHASE LIQUID SYSTEM	112
5 PHYSICOCHEMICAL STUDIES OF ENANTIOMERS, RACEMATE AND EUTECTIC OF IBUPROFEN FOR ENHANCED TRANSDERMAL DELIVERY	140
6 THE FORMULATION OF AND DRUG RELEASE FROM EMULSION, CREAM AND GEL OF THE BINARY EUTECTIC OF IBUPROFEN AND KETOPROFEN	180
7 CONCLUSIONS.....	211
APPENDIX.....	214

DETERMINATION OF CARBAMAZEPINE IN UNCOATED AND FILM- COATED TABLETS BY HPLC WITH UV DETECTION.....	214
---	-----

CHAPTER 1

INTRODUCTION AND LITERATURE REVIEW

1. The structure of skin and drug permeation

The skin is the largest organ in a human body, accounting for over 10% of the whole body mass. It enables the body to interact with its environment and more importantly provides protection. Basically, the human skin consists of the epidermis, dermis and hypodermis embedded with hair shafts and gland ducts (Figure 1.1). The epidermis is the major barrier against drug permeation, and it is comprised of five layers: *stratum corneum* (horny layer), *stratum lucidum*, *stratum granulosum* (granular layer), *stratum spinosum* (spinous layer) and *stratum germinativum* (basal layer). As the cells approach the *stratum corneum* (SC) layer they flatten and their metabolic activity declines. Finally, all the cells in the SC are deceased, anucleate, and metabolically inactive and upward migration continues as cells at the surface desquamate.

The two most important pathways for drugs to permeate through the skin are trans-epidermal pathway and appendageal or shunt route. The overall flux of drugs across the skin is the sum of the individual flux through these parallel pathways, which depend on different physicochemical and geometrical properties (1). It was reported that the available diffusional area of the shunt route is about 0.1% of the total skin area (2,3). Although the fraction of appendages is relatively small, in some cases, these sites might still provide the main portal of entry into the subepidermal layers of the skin for ions (4,5) and large polar molecules (1,6,7). For small nonelectrolyte molecules, it was reported that the shunt route was dominant only in the non-steady-state phase of percutaneous absorption, but makes a negligible contribution to overall flux in the steady-state permeation period (2,3). It was found that the contribution of shunt route in the

steady-state transport of polar and non-polar steroids was less than 10% (8) and there was a poor correlation between appendageal density and percutaneous absorption when different skin regions were compared (9,10). However, some papers also reported that the appendages could be a potential pathway for steady-state permeation of a wide range of drugs (11,12).

Transdermal delivery of drugs is a result of partitioning and diffusion of drug molecules in the SC, viable epidermis, and papillary layer of the dermis, with the microcirculation usually providing an infinite sink (1). The main barrier to permeation of water is in the external layers of the epidermis, particularly the SC (13). And the SC is the rate-limiting barrier to percutaneous absorption of most compounds in most conditions (3,14–18). However, for very lipophilic drugs, the rate-limiting step may change from diffusion through to clearance from the SC (1). The SC has a multilayer structure, in which keratin-rich epidermal cells are imbedded in an intercellular lipid-rich matrix. This two-compartment arrangement has been referred to as a bricks (corneocytes) and mortar (intercellular domain) analogy (Figure 1.2) (19, 20). The SC usually has 15 to 20 layers of corneocytes and the thickness varies from 10 to 15 μm in dry state (21–24). After hydration, the SC swells and may reach to as much as around 40 μm thickness (2). The SC lipids content accounts for 5 to 15% of the dry tissue weight (25–27), which mainly comprise ceramides, cholesterol and fatty acids, together with smaller amounts of cholesteryl sulfate, sterol/wax esters, triglycerides, squalene, n-alkanes, and phospholipids (25,27–30). SC lipids localize mainly in the intercellular space with little in the corneocytes (20, 31,32). Besides lipids, some proteins and enzymes also exist in the intercellular space (33,34). Freeze-fracture electron microscopy studies of the SC

(35,36) showed that intercellular lipids form a bilayers structure (20). The lipids pack into lamellae, with the hydrocarbon chains mirroring each other and the polar groups dissolving in an aqueous layer as shown in Figure 1.2. The intercellular bilayers are in pairs (37) and firmly bind together, possibly by the action of molecules such as acylceramides. Adjacent bilayers may mutually contribute chains to an intermediate structure as a monolayer (37 – 39). Small-angle X-ray diffraction studies (SAXS) of hydrated human SC (40, 41) demonstrated that SC lipids develop in two lamellar structures. In addition, SC intercellular lipids exhibit a phenomenon of complex polymorphism. According to wide-angle X-ray diffraction studies (WAXS) of human SC, lipid alkyl chains arrange into orthorhombic perpendicular and (pseudo)hexagonal packings, with some in the liquid state. Cholesterol may also be present in the form of small crystals in human SC (42, 43). As the result, the SC intercellular domain comprises a mixture of crystalline, lamellar gel, and lamellar liquid crystalline lipid phases. It was reported that intact intercellular lamellae are present at all levels in human SC and their appearance does not differ significantly between different anatomical locations (37, 38).

2. Mathematical models for percutaneous absorption

The transport of molecules through the skin occurs by the process of passive diffusion. The spontaneous diffusional events take place because the system is not at equilibrium, and the laws of thermodynamics dictate that it must move toward such an equilibrium state. This irreversible tendency toward a lower energy state that arises is the

result of increased entropy within the system and can be expressed in terms of a net decrease in the Gibbs free energy of the system under isothermal conditions:

$$\Delta G = \Delta H - T \cdot \Delta S \quad (1)$$

Where ΔG represents the Gibbs free energy change, ΔS is the entropy change of the system, T the temperature (usually is constant), and ΔH the change in enthalpy. The process of diffusion is driven primarily by the increase in entropy associated with movement toward a more disordered system. In more common nonideal cases, the process is accompanied by some change in enthalpy.

In transport process, the flow (or flux, J in $\text{mol} \cdot \text{cm}^{-2} \cdot \text{s}^{-1}$) is related to the velocity of molecular movement (v in $\text{cm} \cdot \text{s}^{-1}$) and the concentration (C in $\text{mol} \cdot \text{cm}^{-3}$) of the molecules in motion:

$$J = C \cdot v \quad (2)$$

A fundamental principle of irreversible thermodynamics is that the flow, at any point in the system, at any instant, is proportional to the appropriate potential gradient. This can be expressed mathematically for a species i as shown in Eq. (3), where $\partial \mu_i / \partial x_i$ is the gradient and L_i is proportionality constant.

$$J_i = -L_i \cdot (\partial \mu_i / \partial x) \quad (3)$$

This equation is a general form of Fick's first law of diffusion. If at constant temperature and pressure then Eq. (4) can be obtained:

$$(\partial \mu_i / \partial x) = (\partial \mu_i / \partial C_i) \cdot (\partial C_i / \partial x) \quad (4)$$

From classic thermodynamics, Eq. (5) can be derived:

$$J_i = (RT / N_A f_i) \cdot [1 + C_i (\partial \ln \gamma_i / \partial C_i)] \cdot (\partial C_i / \partial x) \quad (5)$$

Where γ_i is the activity coefficient, N_A is coefficient related to force acting on the molecule, f_i is the frictional coefficient, R is the gas constant.

Eq. (5) can be simplified as:

$$J_i = -D_i \cdot (\partial C_i / \partial x) \quad (6)$$

Where

$$D_i = (RT / N_A f_i) \cdot [1 + C_i (\partial \ln \gamma_i / \partial C_i)] \quad (7)$$

Eq. (6) is the classic form of Fick's first law of diffusion, which shows that diffusion will stop when the concentration gradient is zero. D_i , the diffusion coefficient, is a function of RT / N_A , which is equal to the molecular kinetic energy ($k_B T$) of the system. Although there is a dependency of D_i on concentration owing to solute – solute interaction, it is small in reality as the effect of concentration decreases with progressively dilute solutions. The relation can be denoted as $C_i \rightarrow 0, D_i \rightarrow RT / N_A$.

Fick's first law relates the rate of change in concentration with time at a given point in a system to the rate of change in concentration gradient at that point. Under non-steady-state conditions, the principle of conservation of mass to describe the transport should be considered. Suppose a thin section of cross-sectional area A and thickness Δx that has a concentration C at position x and time t . The amount of diffusion substance that enters the slab per unit time is $J_{in} \cdot A$, where J_{in} is the flux and the increase in concentration inside the section owing to this influx of material, which has a volume $A \cdot \Delta x$ is given by Eq. 8:

$$dC / dt = J_{in} \cdot A / A \cdot \Delta x = J_{in} / \Delta x \quad (8)$$

However, material is also leaving this section with a finite flux J_{out} and the resulting change in concentration can be expressed as shown in Eq. 9:

$$dC / dt = -J_{out} \cdot A / A \cdot \Delta x = -J_{out} / \Delta x \quad (9)$$

The difference between above two equations is equal to the net rate of change of concentration in the section:

$$dC / dt = (J_{in} - J_{out}) / \Delta x \quad (10)$$

If the Fick's first law is used to describe these fluxes, Eq. 11 can be derived:

$$J_{in} - J_{out} = D \cdot \Delta x \cdot (\partial^2 C_i / \partial x^2) \quad (11)$$

Substituting this into Eq. 10, yields Fick's second law of diffusion as shown in Eq. 12:

$$(\partial C / \partial t) = D \cdot (\partial^2 C_i / \partial x^2) \quad (12)$$

Fick's second law contains partial derivatives because C is a function of both x and t .

If the diffusion occurs through a homogeneous membrane with a constant activity difference and a constant diffusion coefficient, and the diffusive flow begins at the high-concentration donor side, where $C = C_0$ and $x = h$ at all time t . The concentration C , of material at any point x , within the membrane can be calculated as a function of time using the following Eq. 13:

$$C = \frac{C_0 x}{h} + \frac{2}{\pi} \sum_{n=1}^{\infty} \frac{C_0}{n} \cos(n\pi) \sin\left(\frac{n\pi x}{h}\right) \exp\left(\frac{-Dn^2 \pi^2 t}{h^2}\right) \quad (13)$$

where $t = 0$, $C = 0$, and $x = 0$, $C = 0$.

The cumulative mass Q of permeant that passes through a unit area of a membrane in a time t is provided by the following Eq. 14:

$$Q = C_0 h \left[\frac{Dt}{h^2} - \frac{1}{6} - \frac{2}{\pi^2} \sum_{n=1}^{\infty} \frac{(-1)^n}{n^2} \exp\left(\frac{-Dn^2 \pi^2 t}{h^2}\right) \right] \quad (14)$$

A graphic representation of Eq. 14 (Figure 1.3) depicts the time-dependent nature of the total mass transfer Q , through the membrane. As $t \rightarrow \infty$, the exponential term tends to zero; therefore, Eq. 14 approximate to the line described by Eq. 15, which can be

rearranged to Eq. 16. Figure 1.3 shows the line described in equations in relation to the full diffusion curve described by Eq. 14:

$$Q = C_0 h \left[\frac{Dt}{h^2} - \frac{1}{6} \right] \quad (15)$$

$$Q = \frac{DC_0}{h} \left[t - \frac{h^2}{6D} \right] \quad (16)$$

If we put $Q = 0$ into Eq. 16, t can be solved and this yields the value of the time axis intercept known as the lag time (t_{lag}) as described in Eq. 17, which relates it inversely to the diffusion coefficient and directly to the diffusional pathlength. The use of this extrapolation for the calculation of diffusion coefficient is usually used, although the pathlength is unknown for skin, making calculation of absolute values of D difficult.

$$t_{lag} = \frac{h^2}{6D} \quad (17)$$

If Eq. 16 is differentiated relative to time, Eq. 18 is obtained, which is another form of Fick's first law of diffusion describing the flux J at steady state.

$$\frac{dQ}{dt} = J = \frac{DC_0}{h} \quad (18)$$

The partition coefficient $K = C_0 / C_v$, where C_v is the drug concentration in the vehicle, then $C_0 = KC_v$, and Eq. 19 can be obtained:

$$\frac{dQ}{dt} = J = \frac{DKC_v}{h} \quad (19)$$

Suppose a plane sheet of thickness h , for which surfaces, $x = 0$, $x = h$, are maintained at constant concentration C_0 and C_h , respectively. If the diffusion has reached steady state, thus producing a constant concentration gradient across it at all points, provided that D is constant, using Fick's second law of diffusion, Eq. 20 can be obtained:

$$\frac{dC}{dt} = D \frac{D^2C}{Dx^2} = 0 \quad (20)$$

which means the rate of change of the concentration gradient across the membrane is zero. This situation is known as the steady state. If Eq. 20 is integrated relative to x once, Eq. (21) can be obtained:

$$D \frac{dC}{dx} = \text{Constant} \quad (21)$$

This equation shows that the concentration across the membrane reduces linearly with distance (here from C_0 to C_h) and that the rate of transfer of diffusant, the flux J , is the same at all positions within the membrane. This rate is given by Fick's first law, which is:

$$J = D \frac{dC}{dx} = \frac{D(C_0 - C_h)}{h} \quad (22)$$

If the membrane thickness h and the concentration C_0 to C_h are known, D can be measured from the determination of the flux J . Considering sink condition in the receptor solution below the membrane, the value of C_h , the concentration at the inner surface of the membrane is usually approximate as zero. Thus the Eq. 22 can be simplified to Eq. 23, which is identical to Eq. 18:

$$J = \frac{DC_0}{h} \quad (23)$$

Since it is difficult to measure the concentration C_0 (the amount of diffusant in the outermost layer of the membrane) directly, the partition coefficient and the vehicle concentration can be used for calculation instead. Also, it is difficult to measure the diffusional pathlength in skin practically. In addition, the information concerning the individual effects of changes in K and D is often not required. Therefore, a composite

parameter is usually used to replace these values. The permeability coefficient P is thus defined as $P = KD/h$, and this simplifies Eq. 23 further to Eq. 24:

$$J = PC_v \quad (24)$$

This equation is the most basic and frequently used expression in the assessment of membrane permeability. However, it is assumed that the donor concentration is constant and that the diffusion process has reached steady state. Practically this means using a saturated donor solution in the presence of excess permeant, or that the change in donor concentration during the course of the experiment is negligible.

If the diffusion occurs in a homogeneous membrane with a constant donor activity and constant diffusion coefficient, but with an impermeable distal side, the membrane is initially devoid of drug molecules. As diffusion into the membrane occurs, there will be a buildup of drug at the impermeable membrane-crystal interface until saturation is reached at a concentration C_0 (the solubility of the permeant in the membrane). An analytical solution, Eq. 25, describing the buildup of drug at this interface with time can be obtained, using Fick's second law and the relevant initial and boundary conditions (46):

$$\frac{C}{C_0} = 1 - \frac{4}{\pi} \sum_{n=0}^{\infty} \frac{(-1)^n}{2n+1} \exp\left(\frac{-D(2n+1)^2 \pi^2 t}{4h^2}\right) \quad (25)$$

where C is the diffusant concentration at the interface, t is time, D is the diffusion coefficient of the drug, and h is the membrane thickness. There will be an initial period during which drug concentration at the interface increases, followed by an exponential rise to a plateau that represents the saturation of the membrane with drug.

For controlled-release devices that may include transdermal patches, as well as oral and subcutaneous devices, diffusion is out of a precharged homogeneous membrane,

with a constant diffusion coefficient. If a rate-limiting membrane is initially full of material, but no reservoir is present, the following Eq. 26 can be derived (47):

$$M_t = M_\infty \left[1 - \frac{8}{\pi^2} \left(\sum_{n=1}^{\infty} \frac{1}{(2n-1)^2} \right) \exp\left(-\frac{(2n-1)^2 \pi^2 Dt}{4h^2}\right) \right] \quad (26)$$

where M_t is the amount of drug released at time t , M_∞ is the total amount of drug contained in the membrane at $t = 0$. This equation is the full solution for the burst effect without a reservoir and may be applied over the complete time range of an experiment.

Another identical form is also used as shown in Eq. 27.

$$M_t = M_\infty \left[1 - \frac{8}{\pi^2} \left(\sum_{n=0}^{\infty} \frac{1}{(2n+1)^2} \right) \exp\left(-\frac{(2n+1)^2 \pi^2 Dt}{4h^2}\right) \right] \quad (27)$$

The above equations can also be simplified to give both short and long time approximations as shown in the following Eqs. 28 and 29, respectively.

$$M_t = 2M_\infty \left(\frac{Dt}{\pi h^2} \right)^{1/2} \quad (28)$$

$$M_t = M_\infty \quad (29)$$

If the buildup of diffusant in the receptor compartment in which the membrane was initially charged with drug and there was a reservoir present, the solution is shown in Eq. 30 (47):

$$M_t = M_\infty \left[\frac{Dt}{h^2} + \frac{1}{3} - \frac{2}{\pi^2} \sum_{n=1}^{\infty} \frac{1}{n^2} \exp\left(-\frac{n^2 \pi^2 Dt}{h^2}\right) \right] \quad (30)$$

Here, M_∞ is not a finite quantity of drug, because it represents the content of the unchanging reservoir. The short-term approximation of Eq. 30 is the same as Eq. 28, whereas the long-term approximation is as shown in Eq. 31:

$$M_t = M_\infty \left[\frac{Dt}{h^2} + \frac{1}{3} \right] \quad (31)$$

There are numerous cases for which the membrane is not a single homogeneous system and consists of many barriers. For example, the diffusion through laminates, shunt routes (barrier in parallel), barrier with dispersed phases and variable boundary conditions, have different expressions of mathematical models. In addition, the temperature can affect diffusion through a membrane by increasing fluidity or disordering the environment within the SC lipid bilayers (48). The diffusion coefficient itself may be temperature-dependent, and the nature of this dependence can be empirically expressed in a form analogous to the Arrhenius equations for reaction kinetics as shown in Eq. 32:

$$D = D_0 \exp\left[\frac{-E_a}{RT}\right] \quad (32)$$

where D_0 represents the diffusion coefficient at infinite temperature and can be calculated by back-extrapolating a plot of $\ln D$ versus $(1/T)$ to the y -intercept (Eq. 33):

$$\ln D = \ln D_0 - \frac{E_a}{RT} \quad (33)$$

E_a is activation energy and is determined by the nature of the barrier. The above equation appears to hold true in the temperature range over which permeability is generally measured. If skin contains components that are subject to temperature-dependent phase transitions, these equations probably still hold true in the temperature region in which the transition occurs. If D and D_0 are replaced by P and P_0 , respectively, the following Eqs. 34 and 35 can be obtained:

$$P = P_0 \exp\left[\frac{-E_a}{RT}\right] \quad (34)$$

$$\ln P = \ln P_0 - \frac{E_a}{RT} \quad (35)$$

These mathematical interpretations are usually an approximation of the real diffusion process, and can be used under certain conditions.

3. Dermatological drug delivery and formulation

When a dermatological preparation is applied to the skin, the drug is released from the vehicle first, then it penetrates through the skin barrier and therefore achieves its pharmacological effects. Figure 1.4. demonstrates the percutaneous absorption of drug molecules arising from transdermal drug delivery through the skin. Effective therapy should optimize these steps as they are affected by three components: the drug, the vehicle and the skin.

The intact skin is a tough barrier, but chemicals, cuts, abrasions and dermatitis can damage the skin and increase the permeation of drugs through it. There are also other skin conditions affecting drug percutaneous absorption, such as skin age, blood flow, regional skin sites, skin metabolism and species differences. Physiochemical factors, including skin hydration, temperature, pH, diffusion coefficient, drug concentration, partition coefficient, molecular size and shape also play important roles in drug permeation. One of the most important factors is the intrinsic solubility of drug in the skin, this is closely related to the melting point of the drug, the membrane density and molecular weight, drug molecular weight and its entropy of fusion. It has been shown that solid drugs can be transformed into a highly concentrated oily state by depressing the melting points of compounds below ambient temperature (25 °C), and they can be directly emulsified without prior dissolution of the drugs in inert pharmaceutical oils. In

this way, the system provides the maximum thermodynamic activity in the preparation (50, 51). Melting points of a series of anti-emetic drugs have also been shown to be inversely proportional to lipophilicity ($\log P$) and solubility in skin lipid and, therefore, transdermal flux (52). Based on the ideal solution theory, Kasting proposed a relationship between transdermal permeation and melting point of the permeant (55), by which the ideal solubility, S_{ideal} , of a penetrant in the skin lipids can be obtained as:

$$S_{ideal} = \frac{\rho}{1 - \{1 - \exp[\frac{\Delta S_f}{RT}(T_m - T)]\}} \frac{M_l}{M_w} \quad (36)$$

where ρ is the density of the skin lipids and M_l is their average molecular weight. M_w is the molecular weight. T_m is the melting point in degrees Kelvin and ΔS_f is the entropy of fusion of the permeant. The S_{ideal} was then entered into a proposed model to predict a maximum flux (J_m) from molecular weight and melting point:

$$\log(J_m/S_{ideal}) = \log(D_0/h) - (\beta/2.303)v \quad (37)$$

where D_0 is a parameter related to diffusion coefficient D by $D = D_0 \exp(-\beta v)$, where v is molecular van der Waals volume and β is a parameter related to the skin properties. v is the property of the permeant while D_0 and β are properties of the skin. The values of these parameters are estimated, and Eq.37 is simplified as:

$$\log(J_m/S_{ideal}) = 1.80 - (0.0216/2.303) M_w \quad (38)$$

Since the ΔS_f varies slowly with melting point, S_{ideal} increases with decreasing melting point for any given molecular weight. It follows that there should be an increase in transdermal flux with decreasing melting point, all other factors being equal. Again based on ideal solution theory, Touitou proposed a melting temperature-membrane transport (MTMT) concept to predict the relative transdermal fluxes with different melting points (56). The solubility, in terms of mole fraction solute, X , of a permeant in a given solvent, was then related to the melting temperature, T_m , and the enthalpy of fusion, ΔH :

$$\ln X = -\frac{\Delta H}{R} \left(\frac{T_m - T}{T \cdot T_m} \right) \quad (39)$$

where R is the gas constant and T denotes the temperature of the solution. All of the above equations indicate that a depression in the melting point of a permeant would increase its solubility in skin lipids and thus enhance transdermal permeation. Therefore, if the melting point of a drug can be reduced without causing unfavorable changes to other physicochemical parameters, then transdermal flux should be increased accordingly. A method by which the melting point of a compound can be reduced is eutectic formation (53, 54).

After selection of drug candidate to study its transdermal delivery, preformulation should be carried out before formulation development. Preformulation studies permit the rational development of stable, safe and efficacious dosage forms. It usually involves the general description of the drug, calorimetry, polymorphism, hygroscopicity, analytical development, intrinsic stability, solubility and partitioning characteristics and drug delivery characteristics.

There are different types of dermatological formulations, but ointments, emulsions, gels and creams are most frequently used. An ointment is classified as any

semisolid containing fatty material and intended for external application (United States Pharmacopoeia; USP).

There are four types of ointment bases; there are hydrocarbon bases, absorption bases, water-removable bases and water-soluble bases. Only hydrocarbon bases are completely anhydrous. They usually contain straight or branched hydrocarbons with chain length ranging from C₁₆ to C₃₀, and may also contain cyclic alkanes. The preparation of ointment formulations may be as simple as heating all of the constituents to a temperature higher than the melting point of all the excipients and then cooling with constant mixing.

A common characteristic of gels is that they contain continuous structures that provide solid-like properties. Depending on their constituents, they can be clear or opaque, and be polar, hydroalcoholic, or nonpolar. A simple gel is can be made up of water plus semi-synthetic materials (e.g., methylcellulose, carboxymethylcellulose, or hydroxyethylcellulose), or natural gums (e.g., tragacanth, guar, or xanthan), or synthetic materials (e.g., carbomer-carboxyvinyl polymer), or clays (e.g., silicates or hectorite). The viscosity of a gel is generally a function of the amount and molecular weight of the added thickener. If clarity is a major requirement, hydroxypropylmethylcellulose (HPMC) is preferable to methylcellulose (MC). Some cellulose may be incompatible with several salts, and MC and hydroxypropylcellulose (HPC) are incompatible with parabens. And this incompatibility limits the choice of preservatives for semi-solid formulations based on MC and HPC. The presence of oxidative materials (e.g., peroxide, or other ingredients containing peroxide residues) in formulation gelled with cellulose should be avoided because oxidative degradation of the polymer chains may cause a

rapid decrease in formulation viscosity (57). As the branched-chain polysaccharide gums, such as tragacanth, pectin, carageenan, and guar, are of naturally occurring plant origin, they can have widely varying physical properties, depending on their source. They are usually incorporated into semi-solid formulations at concentrations between 0.5 to 10%, contingent on the required viscosity. Tragacanth, a mixture of water-insoluble and water-soluble polysaccharides, is negatively charged in aqueous solution and therefore incompatible with many preservatives when formulated at pH 7 or higher. Xanthan gum, which is produced by bacterial fermentation, is incompatible with some preservatives. In addition, many gums are ineffective in hydroalcoholic gels containing more than 5% alcohol. The natural clay thickeners (e.g., bentonite and magnesium aluminium silicate) are useful for thickening aqueous gels containing cosolvents, such as ethanol, isopropanol, glycerin and propylene glycol. These materials possess a lamellar structure that can be extensively charged. These clays swell in the presence of water because of hydration of the cations and electrostatic repulsion between the negatively charged faces. The rheological properties of these clay dispersions, therefore, are particularly sensitive to the presence of salts. The concentration of clay usually required to thicken formulations is 2 to 10%. The most extensively used thickening agents in the pharmaceutical and cosmetic industries are the carboxyvinyl polymers known as carbomers. These are synthetic high molecular weight polymers of acrylic acid, cross-linked with either allylsucrose or allyl ethers of pentaerythritol. Pharmaceutical grades of these carbomers are available (e.g., Carbopol 981NF; B. F. Goodrich Performance Materials). In the dry state, a carbomer molecule is tightly coiled, but when dispersed in water, the molecule begins to hydrate and partially uncoil, exposing free acidic moieties.

To attain maximum thickening effect the carbomer molecule must be fully uncoiled, and this can be achieved by converting the acidic molecule to a salt with an appropriate neutralizing agent. For formulations containing aqueous or polar solvent, carbomer gellation can be induced by the addition of simple inorganic bases, such as sodium or potassium hydroxide. Less polar or nonpolar solvent systems may be neutralized with amines, such as triethanolamine or diethanolamine, or a number of alternative amine bases (e.g., diisopropanolamine, aminomethyl propanol, tetrahydroxypropyl ethylenediamine, and tromethamine) may be used. Neutralization ionizes the carbomer molecule, generating negative charges along the polymer backbone, and the resultant electrostatic repulsion creates extended three-dimensional structure. The formulation should not be under- or overneutralized, as this will result in viscosity or thixotropic changes (58). Overneutralization will reduce viscosity, as the excess base cations screen the carboxy groups and reduce electrostatic repulsion. Hydrated molecules of carbomer may also be uncoiled in aqueous systems by the addition of 10 to 20% of hydroxyl donors, such as a nonionic surfactant or a polyol, that are able to hydrogen-bond with the polymer. Maximum thickening will not be as instantaneous by using this mechanism as it is with base neutralization and may take several hours. Heating can accelerate the process, but the product should not be heated over 70 °C.

The most common emulsions used in dermatological therapy are creams. These are two-phase preparations in which one phase (the dispersed or internal phase) is finely dispersed in the other (the continuous or external phase). The dispersed phase can have either a hydrophobic-based (oil-in-water creams; O/W), or be aqueous based (water-in-oil creams; W/O). In most pharmaceutical emulsions, the stabilizing agents include

surfactants (ionic or nonionic), polymers (nonionic polymers, polyelectrolytes, or biopolymers), or mixtures of these. The most commonly used surfactant systems are sodium alkyl sulfates (anionic), alkylammonium halides (cationic), and polyoxyethelylene alkyl ethers or polysorbates (nonionic). These are often used alone, or in conjugation with nonionic polymeric, such as polyvinyl alcohol or poloxamer block copolymers, or polyelectrolytes, such as polyacrylic-polymethacrylic acids. There are two ways to stabilize an emulsion system: an increase in the viscosity of the continuous phase, which will reduce the rate of droplet movement, or the establishment of an energy barrier between the droplets. Polyacrylic acid polymers linked to hydrophobic chains (Penmulen; B. F. Goodrich) can be used as primary emulsification systems in O/W formulations and are listed in the USP as carbomer 1342. These materials form very stable emulsions because the polyacrylic acid chain, anchored to the oil droplet by the alkyl methacrylate moieties, considerably increases the surface charge on the oil droplet, forming a strong electrical barrier at the interface. Emulsion stability is further enhanced by an increase in the viscosity of the continuous phase. Ionic surfactants can only be used for O/W emulsions, nonionic surfactants may be used for both O/W and W/O formulations.

An approximate guide to emulsion formulation is provided by the hydrophilic-lipophilic balance (HLB) system that generates an arbitrary number (usually between 0 to 20) that is assigned to a particular surfactant. It is generally recognized that surfactants with HLB values between 4 and 6 are W/O emulsifiers, and those with HLB values between 8 and 18 are O/W emulsifiers. When the cream is formulated, it is composed of at least four phases (Figure 1.5.): bulk water; a dispersed oil phase; a crystalline hydrate;

a crystalline gel phase composed of bilayers of surfactant and fatty alcohol separated by layers of interlamellar-fixed water. A relatively stable emulsion formulation may be prepared from a simple four-component mixture: oil, water, surfactant and fatty amphiphile. In addition to the four principle components, a pharmaceutical emulsion formulation will also contain a drug, and is likely to contain a cosolvent for the drug, a viscosity enhancer, a microbiological preservative system, a pH adjusting – stabilizing buffer, and an antioxidant system. All of these additional components are required so that the formulation is capable of delivering the drugs to the application site at the therapeutic level, free from microbial contamination and is essentially physicochemically stable from the day of manufacture.

All pharmaceutical semisolid formulations that are not sterilized unit-dose products can support the growth of microorganisms. Preservatives are ingredients that prevent or retard microbial growth and protect formulation from spoilage. The most commonly used preservatives in pharmaceutical products are the parabens (alkyl esters of *p*-hydroxybenzoic acid, such as methyl and propyl paraben). Other widely used preservatives in topical formulations include benzoic acid, sorbic acid, benzyl alcohol, phenoxyethanol, chlorocresol, benzalkonium chloride and cetrimide. But the preservatives are intrinsically toxic materials so that a balance must be achieved between antimicrobial efficacy and dermal toxicity. In the cosmetic industry, there is a trend toward preservative-free and self-preserving formulations (60).

4. Non-steroidal anti-inflammatory drugs (NSAIDs) and transdermal drug delivery

Rheumatoid arthritis and related diseases are among the most prevalent diseases in the world. It is estimated that arthritis and related conditions inflict nearly 43 million people in United States, or about one of every six people, making it one of the most prevalent diseases in US. By 2020, as the baby boom generation ages, an estimated 60 million Americans will be affected by arthritis (61). Non-steroidal anti-inflammatory drugs (NSAIDs) have played an important role in treating these diseases (62). In addition, NSAIDs are medications which have the effect of reducing inflammation as well as having analgesic effects.

NSAIDs work by affecting some chemicals in the body which cause inflammation, the prostaglandins. They are most widely administered orally. However, NSAIDs tend to cause stomach irritation, and may even cause duodenal or stomach ulceration. As a result of this side-effect, NSAIDs cannot be used in someone with a history of peptic ulcer. Also they would rarely be used in somebody with heartburn symptoms. In general, the more effective a NSAID is at reducing inflammation, the more likely it is to cause stomach irritation. There are many other potential side effects, but these vary according to the drug chosen and the individual taking it. In addition, some NSAIDs have extensive first-pass effect. To avoid the side effects and first-pass effect associated with the oral administration route, extensive research has been done to develop NSAIDs into transdermal or topical formulations.

Ibuprofen and ketoprofen are among of the most widely used non-steroidal anti-inflammatory drugs (NSAIDs) and a number of topical preparations have been formulated to treat rheumatoid arthritis and related diseases (62). Oral dosage forms of NSAIDs usually upset the stomach and cause nausea. Long-term use might result in stomach ulcer and kidney toxicity. Extensive research has been done to develop topical formulations for these drugs to overcome the adverse effects associated with oral doses. Transdermal application of NSAIDs has been used in Europe for the past 15 years and accounts for 2/3rds of the most frequently prescribed NSAIDs in Germany (63). Over the past 20 years, several topical NSAIDs have been licensed in the UK, and a number of others are available in other countries or are under investigation. There is a growing body of evidence attesting to the efficacy of topical NSAIDs in the treatment of acute soft-tissue injury and chronic soft-tissue overuse lesions. It has been estimated that 30% of the overall cost of treating arthritis in the USA is spent on treating the GI side effects of oral NSAIDs. Extrapolating this figure to the whole of the country results in the startling sum of US\$8.6 bn (64).

The transcutaneous passage of ketoprofen gel topically administered, and its distribution in the inner part of the knee joint has been evaluated. The fluid samples from patients using topical ketoprofen were about 100 times higher in the sampled tissue levels than in the plasma concentration drawn at the same time (65). A topical formulation of ketoprofen 2.5%, corresponding to an oral dose of 375mg, was tested on subjects. Results of the assay showed that the plasma concentration was 2.6% of the daily applied dose. There was no sign of local intolerance (66). Advantages of transcutaneous delivery include GI tract circumvention and avoidance of first-pass metabolism (67). Topically

applied NSAID blood concentrations reach only 5 to 10% of those achieved after oral or IM administration; thus, renal impairment, drug interactions (e.g., warfarin), and adverse GI reactions following topical administration have been considered unlikely (68).

NSAIDs administered as cream, gel or spray, quickly penetrate through the corneal layer at the application site and reach high effective concentrations in subcutis, fasciae, tendons, ligaments and muscles, but lesser quantities in joint-capsule and fluid, indicating direct penetration. Blood levels of topical NSAIDs are extremely low with no systemic side effects. By contrast, oral NSAIDs lead to high blood levels and a high incidence of side effects but to a much lower concentration - only one tenth - in particular soft tissues (69). In 1993, Airaksinen et al. published a randomized, double-blind parallel study investigating the efficacy of ketoprofen 2.5% gel versus placebo in 56 patients with acute, minor, soft tissue injuries (diagnoses not specified); 24 of 29 patients (82.8%) in the ketoprofen group reported improvement compared with 14 of 27 patients (51.8%) in the control group (70). Increasing the amount of drug in the epidermis correlated with an increased inhibition of the inflammation. The topical formulation released more drugs to the skin and produced a greater anti-inflammatory effect (71). Organogels were studied as matrices for the transdermal transport of drugs. Preliminary histological studies showed that the gels have no harmful effect when applied to the skin for prolonged periods. The study concluded that lecithin organogel may be an efficient vehicle for the transdermal transport of various drugs (72).

5. Chiral drugs and transdermal drug delivery

Chirality of drugs is a very common phenomenon and more than 50% of marketed drugs are chiral compounds (79, 80). Over the last twenty years, it has been recognized that the stereochemistry of chiral drugs affects their pharmacological, pharmacokinetic and toxicological actions (73). The term *chirality* was derived from the Greek word *cheir*, for hand, therefore refers to the asymmetry center within a molecule. Chirality is a ubiquitous and fundamental characteristic of biological system (74, 75). The chiral enantiomers share essentially the same physicochemical properties, including refractive index, melting points, boiling points, and solubility. However, the three dimensional structural differences between the enantiomers can lead to significant biochemical differences (76, 77). Although pharmacodynamic, pharmacokinetic, and toxicological differences among the enantiomers of chiral drugs have been reported for many years, racemic drugs have frequently been developed and approved without clinical pharmacological consideration of their chiral components.

It is well known that for a majority of the racemic drugs, the biological activity is associated with one of the enantiomers, and, therefore, any enantioselective permeation would affect the pharmacological activity of the transdermal drug delivery system. Furthermore, development of a single enantiomer, rather than a racemate, may reduce the desired flux values, because only half the total racemate would be required to achieve the desired pharmacological effect. It is important to assess the physiochemical properties and membrane permeation characteristics of enantiomers, racemate and even mixtures of enantiomers in developing transdermal drug delivery systems.

The stratum corneum, the rate-limiting barrier to percutaneous absorption, is made up of several components, such as keratin and ceramides and etc. as described above. Differential binding of enantiomers to keratin or interactions with ceramide may give rise to differences in the permeation profiles of the enantiomers (81). These components may serve as potential sources of chiral discrimination that could result in differential permeation rates, depending upon the stereochemistry of the penetrant molecule. Stereoselective processes were observed within the viable epidermis in contact dermatitis (82, 83) and with skin metabolism (84). Enantiomeric differences on the permeation of R-(+)- and S-(-)- propranolol through the rat skin has been reported. The permeation amount of S-(-)- enantiomers was four times higher than that of R-(+)- propranolol at 12 hours (85). Apart from these intrinsic factors resulting from the chiral nature of the skin, the following extrinsic factors were also implicated in enantioselective permeation across the skin: differences in the physicochemical properties between enantiomers and racemate (86); the presence of stereoselective retardants in the donor vehicle (87); chiral permeation enhancers; and differences in the hydrolysis rates of the prodrugs of the enantiomers in epidermis / dermis (88).

In addition, different melting points of enantiomers, racemate and binary mixtures of R- and S- enantiomers will cause different solubility in the skin lipid, therefore result in different permeation rates. Some studies reported that enantiomers with a lower melting point than their corresponding racemates exhibited higher solubility and consequently higher skin permeation profiles than that of the racemate (86, 89). But in the case of ketorolac acid, the melting point of each enantiomers was 20 °C higher than that of the racemate. Consequently, the solubility of the racemic compound has twice the

solubility of that of the enantiomers. The flux values of the racemate through a synthetic membrane and human cadaver skin were 1.5 times higher than those of the enantiomers (90).

The enantiomers are mirror images of one another, their racemic species can be homochiral (enantiomorphous crystals), made up of molecules of the same handedness, or heterochiral (racemic crystals), consisting of an ordered array of both right- and left-handed molecules (91, 92). And random packing of the enantiomers will result in a solid solution. There are three types of crystalline racemates, which are illustrated in Figure 1.6: (1) conglomerate, (2) racemic compound, and (3) pseudoracemate or solid solution. A conglomerate is an equimolar mixture of two crystalline enantiomers (R and S) that are mechanically separable. This mixture melts as if it were a pure substance and will exhibit a eutectic in its melting point phase diagram. The second type of racemate is a racemic compound, which is also called “true racemate”, is characterized by a crystal form in which two enantiomers coexist in the same unit cell. This is the most commonly encountered type of racemate and it is characterized with two eutectic points in the melting point phase diagram near the vicinity of the pure enantiomers. The third type of racemate is “pseudoracemate”, formed when two enantiomers form a solid solution or mixed crystal. This phenomenon of lacking of chiral recognition is relatively rare (93). In a typical binary phase diagram, the *solidus* curve is a line (or a surface on a ternary phase diagram) that indicates the temperature at which a system becomes completely solid on cooling or at which melting begins on heating under equilibrium conditions; while *liquidus* curve is a line on a binary phase diagram (or surface on a ternary phase diagram) that indicates the temperature at which solidification begins on cooling or at which

melting is completed on heating under equilibrium conditions. The portion of the *liquidus* curve on a binary of racemic compound between the eutectic and the pure enantiomers can be predicted by the simplified Shroder-Van Laar equation (40):

$$\text{Ln}(X_A) = \left[\frac{\Delta H_A^f}{R} \right] \cdot \left[\frac{1}{T_A^f} - \frac{1}{T^f} \right] \quad (40)$$

Where subscripts *R* and *A* denote the values of racemic compound and pure enantiomers, respectively, and superscript *f* denotes the value at the final melting temperatures. The *liquidus* curve between the two eutectic points can be predicted by the Prigogine-Defay equation (41):

$$\text{Ln}[4X_A(1 - X_A)] = \left[\frac{2\Delta H_R^f}{R} \right] \cdot \left[\frac{1}{T_A^f} - \frac{1}{T^f} \right] \quad (41)$$

Eutectic points are taken as the points of intersection of the curve obtained by Eqs. 40 and 41, and a *solidus* line is drawn through the eutectic points. The following equations are used to calculate the thermodynamic parameters when the racemic compound has a higher melting point than that of the pure enantiomers (94):

$$\Delta H_{T_A^f}^R = \Delta H_A^f - \Delta H_R^f + \Delta C_{P_R} (T_R^f - T_A^f) \quad (42)$$

$$\Delta S_{T_A^f}^R = \Delta S_A^f - \Delta S_R^f + R \cdot \text{Ln}(2) + \Delta C_{P_R} \cdot \text{Ln}\left(\frac{T_R^f}{T_A^f}\right) \quad (43)$$

$$\Delta G_{T_A^f}^R = \Delta H_A^f \cdot \left(\frac{T_A^f}{T_R^f} - 1 \right) - T_A^f \cdot R \cdot \text{Ln}(2) + \Delta C_{P_R} \cdot [T_R^f - T_A^f - T_A^f \cdot \text{Ln}\left(\frac{T_R^f}{T_A^f}\right)] \quad (44)$$

where ΔH^R , ΔS^R and ΔG^R are enthalpy, entropy, and free energy changes, respectively, associated with the formation of a racemic compound. The subscript, T_A^f , indicates that these values are calculated at the absolute melting temperature of the enantiomers. ΔH_A^f

is the enthalpy of fusion of the enantiomers, and ΔC_{P_R} is the difference between the heat capacities of the solid and super cooled liquid of the racemic compound. The contribution of the term containing the heat capacities in Eq. 44 is always insignificant and negligible. However, the contribution of the heat capacities term in Eqs. 42 and 43 cannot be neglected (95). ΔG reflects the tendency to form a racemic compound or the stability difference between a racemic compound and the corresponding conglomerate of enantiomers (92).

The MTMT theory can be used to relate the physiochemical properties of enantiomers and racemate to their flux ratios (86) as shown in Eq. 45:

$$\ln\left(\frac{F_{\max \cdot S}}{F_{\max \cdot RS}}\right) = \ln\left(\frac{X_{\max \cdot S}}{X_{\max \cdot RS}}\right) = \frac{\Delta H_{RS}(T_{iRS} - T)}{R \cdot T_{iRS} \cdot T} - \frac{\Delta H_S(T_{iS} - T)}{R \cdot T_{iS} \cdot T} \quad (45)$$

where F_{\max} is the maximum flux; subscripts of S and RS denote enantiomer and racemic compound, respectively; X is the ideal solubility of the drug in terms of mole fraction of solute in a given solvent; T_i is the melting point; ΔH is the enthalpy of fusion; R is the gas constant and T is the solvent temperature. However, MTMT concept assumes that there is no significant intrinsic enantioselectivity in permeation resulting from the chiral nature of skin, and, subsequently, the diffusion coefficient (D) and the partition coefficient (K_m) are the same for each enantiomer and for different mixtures of enantiomers. These parameters are in fact identical only for achiral vehicles or membranes.

6. Objectives of study

The objectives of my studies are described as the follows:

1. To study the eutectic properties of binary mixture of non-steroidal anti-inflammatory drugs (NSAIDs) by using differential scanning calorimetry (DSC) and phase diagrams.
2. To study the thermodynamic and crystalline properties of binary eutectic mixture of ibuprofen with ketoprofen by using DSC and X-ray powder diffractometry (XRPD).
3. To determine the drug concentration in the two-phase liquid system of the binary eutectic mixture of ibuprofen and ketoprofen in the presence of aqueous isopropyl alcohol (IPA) by HPLC.
4. To study the effect of melting point depression by eutectic formation on the membrane permeation and compare this with other reference preparations selected from the phase diagram.
5. To prepare, characterize and compare different topical formulations based on the binary eutectic and study the stability of the selected formulations.
6. To study the thermodynamic and crystalline properties of enantiomers, eutectic and racemate of chiral ibuprofen by using DSC and XRPD.
7. To predict the effect of melting point depression on membrane permeation by using mathematical models based on the ideal solution theory and thermodynamic data obtained from DSC and compare this with the experimental results.

References

1. Barry BW. *Dermatological Formulations, Percutaneous Absorption*. New York: Marcel Dekker, 1983.
2. Scheuplein RJ. Mechanism of percutaneous absorption II. Transient diffusion and the relative importance of various routes of skin penetration. *J Invest Dermatol* 1967; 48:79–88.
3. Scheuplein RJ, Blank IH. Permeability of the skin. *Physiol Rev* 1971; 51: 702–747.
4. Grimnes S. Pathways of ionic flow through human skin in vivo. *Acta Derm Venereol (Stockh)* 1984; 64:93–98.
5. Cornwell PA, Barry BW. The routes of penetration of ions and 5-fluorouracil across human skin and the mechanisms of action of terpene skin penetration enhancers. *Int J Pharm* 1993; 94:189–194.
6. Tregear RT. The permeability of skin to albumin, dextrans and polyvinyl pyrrolidone. *J Invest Dermatol* 1966; 46:24–27.
7. Scheuplein RJ, Blank IH, Brauner GJ, MacFarlane DJ. Percutaneous absorption of steroids. *J Invest Dermatol* 1969; 52:63–70.
8. Siddiqui O, Roberts MS, Polack AE. Percutaneous absorption of steroids: relative contribution of epidermal penetration and dermal clearance. *J Pharmacokin Biopharm* 1989; 17:405–424.

9. Rougier A, Dupuis D, Lotte C, Roguet R, Wester RC, Maibach HI. Regional variation in percutaneous absorption in man: Measurement by the stripping method. *Arch Dermatol Res* 1986; 278:465–469.
10. Rougier A, Lotte C, Maibach HI. In vivo percutaneous penetration of some organic compounds related to anatomic site in humans: Predictive assessment by stripping method. *J Pharm Sci* 1987; 76:451–454.
11. Illel B, Schaefer H, Wepierre J, Doucet O. Follicles play an important role in percutaneous absorption. *J Pharm Sci* 1991; 80:424–427.
12. Lauer AC, Lieb LM, Ramachandran C, Flynn GL, Weiner ND. Transfollicular drug delivery. *Pharm Res* 1995; 12:179–186.
13. Berenson GS, Burch GE. Studies of diffusion of water through dead human skin: the effect of different environmental states and of chemical alterations of the epidermis. *Am J Trop Med Hyg* 1951; 31:842–853.
14. Blank IH. Further observations on factors which influence the water content of the stratum corneum. *J Invest Dermatol* 1953; 21:259–271.
15. Monash S, Blank H. Location and re-formation of the epithelial barrier to water vapor. *Arch Dermatol* 1958; 78:710–714.
16. Hadgraft J. Absorption of materials by or through the living skin. *Int J Cosmet Sci* 1985; 7:103–115.
17. Barry BW. Lipid-protein-partitioning theory of skin penetration enhancement. *J Control Rel* 1991; 15:237–248.

18. Williams AC, Barry BW. The enhancement index concept applied to terpene penetration enhancers for human skin and model lipophilic (oestradiol) and hydrophilic (5-fluorouracil) drugs. *Int J Pharm* 1991; 74:157–168.
19. Michaels AS, Chandrasekaran SK, Shaw JE. Drug permeation through human skin: Theory and in vitro experimental measurement. *AIChE J* 1975; 21: 985–996.
20. Elias PM, Brown BE, Fritsch P, Goerke J, Gray GM, White RJ. Localization and composition of lipids in neonatal mouse stratum granulosum and stratum corneum. *J Invest Dermatol* 1979; 73:339–348.
21. Christophers E, Kligman A. Visualization of the cell layers of the stratum corneum. *J Invest Dermatol* 1964; 42:407–409.
22. Christophers E. Cellular architecture of the stratum corneum. *J Invest Dermatol* 1971; 56:165–169.
23. Anderson RL, Cassidy JM. Variations in physical dimensions and chemical composition of human stratum corneum. *J Invest Dermatol* 1973; 61:30–32.
24. Holbrook KA, Odland GF. Regional differences in the thickness (cell layers) of the human stratum corneum: An ultrastructural analysis. *J Invest Dermatol* 1974; 62:415–422.
25. Lampe MA, Burlingame AL, Whitney J, Williams ML, Brown BE, Roitman E, Elias PM. Human stratum corneum lipids: Characterization and regional variations. *J Lipid Res* 1983; 24:120–130.
26. Raykar PV, Fung M-C, Anderson BD. The role of protein and lipid domains in the uptake of solutes by human stratum corneum. *Pharm Res* 1988; 5: 140–150.

27. Wertz PW, Kremer M, Squier CA. Comparison of lipids from epidermal and palatal stratum corneum. *J Invest Dermatol* 1992; 98:375–378.
28. Lampe MA, Williams ML, Elias PM. Human epidermal lipids: Characterization and modulations during differentiation. *J Lipid Res* 1983; 24: 131–140.
29. Melnik BC, Hollmann J, Erler E, Verhoeven B, Plewig G. Microanalytical screening of all major stratum corneum lipids by sequential high-performance thin-layer chromatography. *J Invest Dermatol* 1989; 92:231–234.
30. Wertz PW, Downing DT. Stratum corneum: biological and biochemical considerations. In: Hadgraft J, Guy RH, eds. *Transdermal Drug Delivery: Developmental Issues and Research Initiatives*. New York: Marcel Dekker, 1989: 1–22.
31. Elias PM, Goerke J, Friend DS. Mammalian epidermal barrier layer lipids: Composition and influence on structure. *J Invest Dermatol* 1977; 69: 535–546.
32. Elias PM, Bonar L, Grayson S, Baden HP. X-ray diffraction analysis of stratum corneum membrane couplets. *J Invest Dermatol* 1983; 80:213–214.
33. Elias PM, Menon GK. Structural and lipid biochemical correlates the epidermal permeability barrier. *Adv Lipid Res* 1991; 24:1–26.
34. Sondell B, Thornell L-E, Egelrud T. Evidence that stratum corneum chymotryptic enzyme is transported to the stratum corneum extracellular space via lamellar bodies. *J Invest Dermatol* 1995; 104:819–823.
35. Elias PM, Friend DS. The permeability barrier in mammalian epidermis. *J Cell Biol* 1975; 65:180–191.

36. Elias PM, McNutt NS, Friend DS. Membrane alternations during cornification of mammalian squamous epithelia: A freeze-fracture, tracer, and thin-section study. *Anat Rec* 1977; 189:577–593.
37. Madison KC, Swartzendruber DC, Wertz PW, Downing DT. Presence of intact intercellular lipid lamellae in the upper layers of the stratum corneum. *J Invest Dermatol* 1987; 88:714–718.
38. Swartzendruber DC, Wertz PW, Kitko DJ, Madison KC, Downing DT. Molecular models of the intercellular lipid lamellae in mammalian stratum corneum. *J Invest Dermatol* 1989; 92:251–257.
39. Downing DT. Lipid and protein structures in the permeability barrier of mammalian epidermis. *J Lipid Res* 1992; 33:301–313.
40. Bouwstra JA, de Vries MA, Gooris GS, Bras W, Brussee J, Ponc M. Thermodynamic and structural aspects of the skin barrier. *J Control Rel* 1991; 15:209–220.
41. Bouwstra JA, Gooris GS, van der Spek JA, Bras W. Structural investigations of human stratum corneum by small-angle x-ray scattering. *J Invest Dermatol* 1991; 97:1005–1012.
42. Bouwstra JA, Gooris GS, de Vries MA, van der Spek JA, Bras W. Structure of human stratum corneum as a function of temperature and hydration: A wide-angle x-ray diffraction study. *Int J Pharm* 1992; 84:205–216.
43. Cornwell PA, Barry BW, Stoddart CP, Bouwstra JA. Wide-angle x-ray diffraction of human stratum corneum: effects of hydration and terpene enhancer treatment. *J Pharm Pharmacol* 1994; 46:938–950.

44. Moghimi HR, Williams AC, Barry BW. A lamellar matrix model for stratum corneum intercellular lipids. II. Effect of geometry of the stratum corneum on permeation of model drugs 5-fluorouracil and oestradiol. *Int J Pharm* 1996; 131:117–129.
45. Human Physiology, Joseph J. Previtte, McGraw-Hill Book Company, 1983, page 507
46. Crank J. *The Mathematics of Diffusion*. 2nd ed. London: Oxford University Press, 1975.
47. Hadgraft J. Calculations of drug release rates from controlled release devices. The slab. *Int J Pharm* 2:177-194, 1979.
48. Potts RO, Francoeur ML. Lipid biophysics of water loss through the skin. *Proc Natl Acad Sci USA* 87:1-3, 1990.
49. Michael E. Aulton. *Pharmaceutics – The Science of Dosage Form Design*. Churchill Livingstone. 2nd edition. Page 509, 2002.
50. Adela, A., Nyqvist-Mayer, Brodin, A. F., Frank, S. G., 1985. Phase distribution studies on an oil-water emulsion based on eutectic mixture of lidocaine and prilocaine as the dispersed phase. *J. Pharm. Sci.* 74: 1192-1195.
51. Brodin, A., Nyqvist-Mayer, A., Wadsten, T., Forslund, B. and Broberg, F., 1984. Phase diagram and aqueous solubility of the lidocaine-prilocaine binary system. *J. Pharm. Sci.* 73: 481-484.
52. Calpena, A. C., Blanes, C., Moreno, J., Obach, R., Domenech. J., 1994. A comparative in vitro study of transdermal absorption of anti-emetics. *J. Pharm. Sci.* 83: 29-33.

53. Ford, J. L., Timmins, P., 1989. *Pharmaceutical thermal analysis*. New York, John Wiley and Sons pp. 47-67.
54. Grant, D., Abougela, I., 1982. Physico-chemical interactions in pharmaceutical formulations. *Anal. Proc.* 19: 545-549.
55. Kasting, G. B., Smith, R. L., Cooper, 1987. E. R. Effects of lipid solubility and molecular size on percutaneous absorption. *Pharmacol. Skin* 1: 138-153.
56. Touitou, E., Chow D. D., Chaw J. R., 1994. *Int. J. Pharm.* 104: 19-28.
57. Dahl T, He G-X, Samuels G. Effect of hydrogen peroxide on the viscosity of a hydroxyethylcellulose-based gel. 1998; *Pharm Res* 15:1137-1140
58. Planas MD, Rodriguez FG, Dominguez MH. The influence of neutralizer concentration on the rheological behavior of a 0.1% Carbopol hydrogel. *Pharmazie* 1992; 47:351-355.
59. Kenneth A. Waters. *Dermatological and Transdermal Formulations*. Marcel Dekker, Inc. 2002. Page 332.
60. Kabara JJ, Orth DS, eds. *Preservative-Free and Self-Preserving Cosmetics and Drugs – Principles and Practice*. New York: Marcel Dekker. 1997
61. Centers for Disease Control and Prevention (CDC), National Center for Chronic Disease Prevention and Health Promotion, Atlanta, GA, USA. *The National Arthritis Action Plan: A Public Health Strategy (NAAP)*, 2002
62. Lawrence, R. C., Helmick, C. G., Arnett, F. C., 1998. Estimates of the prevalence of arthritis and selected musculoskeletal disorders in the United States. *Arth. Rheum.* 41: 778-799.

63. Sift, Ebner, et al. "Use of topical NSAIDs in patients receiving systemic NSAID treatment: A pharmacy-based study in Germany" in J CLIN EPIDEM 1997; 50(2): pp. 217-218.
64. Grahame R, "Transdermal Non-Steroidal Anti-Inflammatory Agents" in BRIT J CLIN PRAC 1995; Vol. 49, No. 1.
65. Ballerini R, et al. "Absorption rate of ketoprofen topically administered in man: comparison between tissue and plasma levels" in J CLIN PHARM RESEARCH 1986; VI: pp. 69-72.
66. Flouvat B, et al. "Pharmacokinetics of ketoprofen in man after repeated percutaneous administration" in ARZNEIMITTELFORSCHUNG 1989; 39(7): pp. 812-815.
67. Russell AL, "Piroxicam 0.5% topical gel compared to placebo in the treatment of acute soft tissue injuries: A double-blind study comparing efficacy and safety" in CLIN INVEST MED 1991; 14: pp. 35-43.
68. Doogan DP, "Topical NSAIDs" in Lancet 1989; 2: pp.1270-1. Also Flouvat B, et al., "Pharmacokinetics of ketoprofen in man after repeated percutaneous administration" in ARZNEIMITTEL-FORSHUNG 1989; 39: pp. 812-815.
69. Chlud K, "Percutaneous therapy of painful arthritis" in THERAPEUTISCHE UMSCHAU 1991; 48(1): pp. 42-45.
70. Airaksinen O, et al., "Ketoprofen 2.5% gel versus placebo in the treatment of acute soft tissue injuries" in INT J CLIN PHARM THER TOXICOL 1993; 31: pp. 561-563.

71. Treffel P, Gabard B, "Feasibility of measuring the bioavailability of topical ibuprofen in commercial formulations" in SKIN PHARM 1993; 6(4): pp. 268-275.
72. Medlars UID 93058480 from J PHARM SCI Vol. 81, No. 9, pp. 871-874.
73. Nation, R. L., Chirality in new drug development – Clinical pharmacokinetic considerations, Clin. Pharmacokinet., 27, 249, 1994.
74. Popa R., A sequential scenario for the origin of biological chirality. J. Mol. Evol., 44, 121, 1997.
75. Liu, W. M., Remarks on origins of biomolecular asymmetry, Orig. Life, 12, 205, 1982.
76. Coutts, R.T. and Baker, G. B., Implications of chirality and geometric isomerism in some psychoactive drugs and their metabolites, Chirality, 1, 99, 1989.
77. Hutt, A.J. and Tan, S.C., Drug chirality and its clinical significance, Drugs, 52, 1, 1996.
78. Chrom, W.R., Effects of chirality on pharmacokinetics and pharmacodynamics, Am. J. Hosp. Pharm., 49, S9, 1992.
79. Li, Z.J. and Grant, D. J. W., Relationship between physical properties and crystal structures of chiral drugs, J. Pharm. Sci., 86, 1073. 1997.
80. Millership, J.S. and Fitzpatrick, A., Commonly used chiral drugs: A survey, Chirality, 5, 573, 1993.
81. Heard, C.M. and Brain, K.R., Does solute stereochemistry influence percutaneous penetration?, Chirality, 7, 305, 1995.

82. Bebezra, C., Stampf, J., Brbier, P., and Ducombs, G., Enantiospecificity in allergic contact dermatitis, *Contact Dermatitis*, 13, 110, 1985.
83. Papageorgiou, C., Stampf, J.L., and Benezra, C., Allergic contact dermatitis to tulips: An example of enantiospecificity, *Arch. Dermatol. Res.*, 280, 5, 1988.
84. Weston, A., Hodgson, R.M., Hewer, A.J., Kuroda, R., and Grover, P.L., Comparative studies of the metabolic activation of chrysene in rodent and human skin., *Chem. Biol. Interact.*, 54 (2), 223, 1985.
85. Miyazaki, K., Kaiho, F., Inagaki, A., Dohi, M., Hazemoto, N., Haga, M., Hara, H., and Kato, Y., Eanantiomeric difference in percutaneous penetration of propranolol through rat excised skin., *Chem. Pharm. Bull.*, 40, 1075, 1992.
86. Tuitou, E., Chow, D. D., and Lawter, J.R., Chiral β -blockers for transdermal delivery, *Int. J. Pharm.*, 104, 19, 1994.
87. Heard, C.M., and Suedee, R., Stereoselective adsorption and trans-membrane transfer of propranolol enantiomers using cellulose derivatives. *Int. J. Pharm.*, 139, 15, 1996.
88. Zahir, A., Kunta, J. R., Khan, M.A., and Reddy, I.K., Effect of menthol on permeability of optically active and racemic propranolol across guinea pig skin, *Drug. Dev. Ind. Pharm.*, 24, 77, 1998.
89. Kommuru, T.R., Khan, M.A., and Reddy, I.K., Racemate and enantiomers of ketoprofen: Phase diagram, thermodynamic studies, skin permeability, and use of chiral permeation enhancers, *J. Pharm. Sci.*, 87, 833, 1998.

90. Roy, S.D., Chatterjee, D.J., Manoukian, E., and Divor, A., Permeability of pure enantiomers of ketorolac through human cadaver skin, *J. Pharm. Sci.*, 84,987,1995.
91. Li, Z.J. and Grant, D.J.W., Relationship between physical properties and crystal structures of chiral drugs. *J. Pharm. Sci.*, 86, 1073, 1997.
92. Collet, A., Ziminiski, L., Garcia, C., and Vigne-Maeder, F., Chiral discrimination in crystalline enantiomers systems: Fact, interpretations, and speculations, in *NATO ASI Series – Supramolecular Stereochemistry*, Siegel, J.S., Ed., The Netherlands, Kluwer Academic, 1995, 91.
93. Roozeboon, H.W. B., *Phys. Chem.*, 28, 494, 1899.
94. Leclercq, M., Collet, A., and Jacques, J., Study of mixtures of optical antipodes- XII, *Tetrahedron*, 32, 821, 1976.
95. Dwivedi, S.K., Sattari, S., Jamali, F., and Mitchell, A.G., Ibuprofen racemate and enantiomers: Phase diagram, solubility and thermodynamic studies, *Int. J. Pharm.*, 87, 95, 1992.

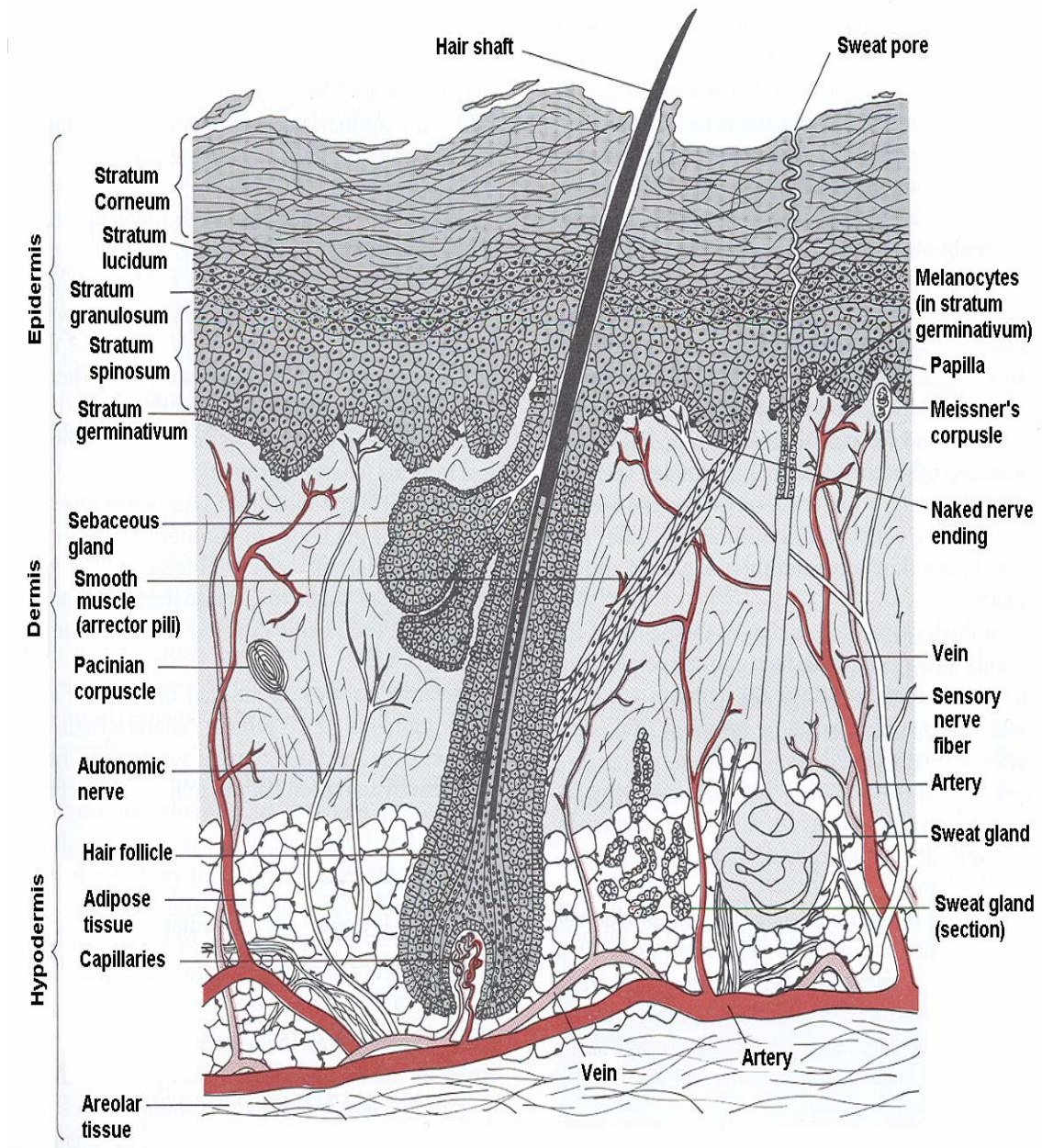


Figure 1.1. Composite diagram of the skin and its tissue layers. (45)

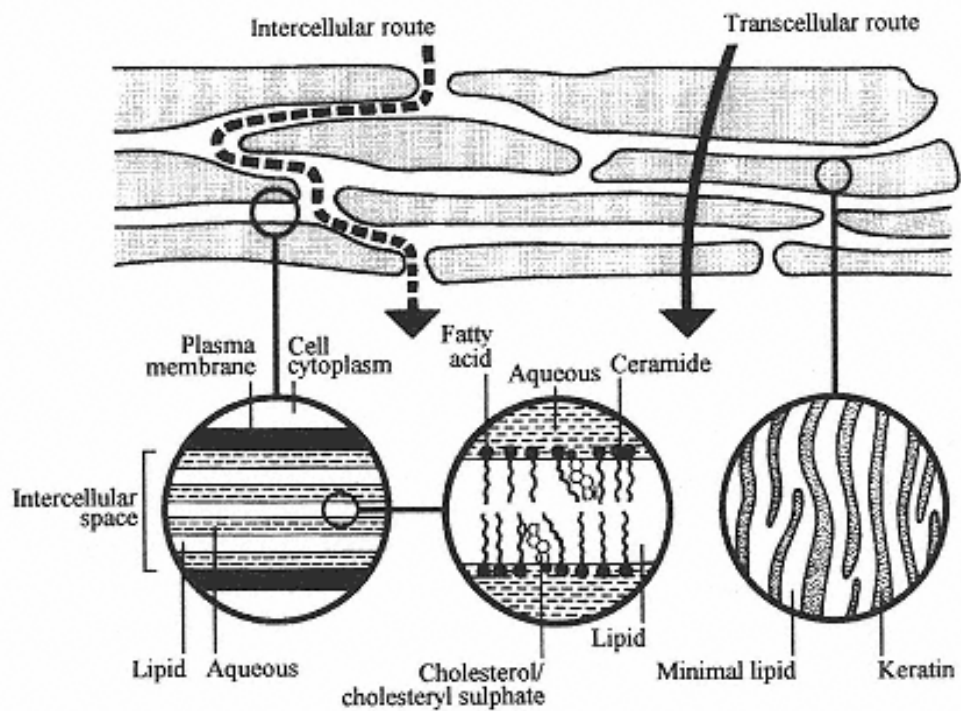


Figure 1.2. Schematic representation of the “brick and mortar” model of the stratum corneum and a very simplified lamellar organization of intercellular domain in which only major stratum corneum lipids are shown. Also illustrated are possible pathways of drug permeation through intact stratum corneum (44).

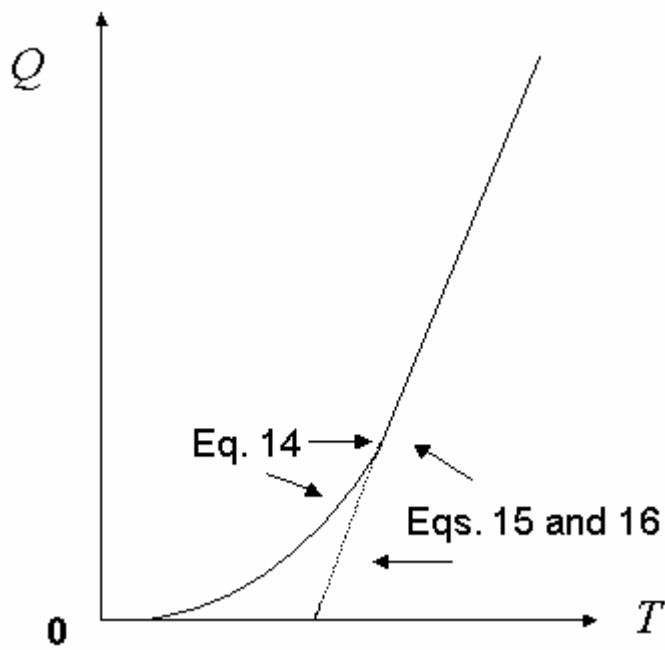


Figure 1.3. Plot of Eq. 14 and Eqs. 15 and 16 representing diffusion (Q , cumulative mass) through a membrane with increasing time (T).

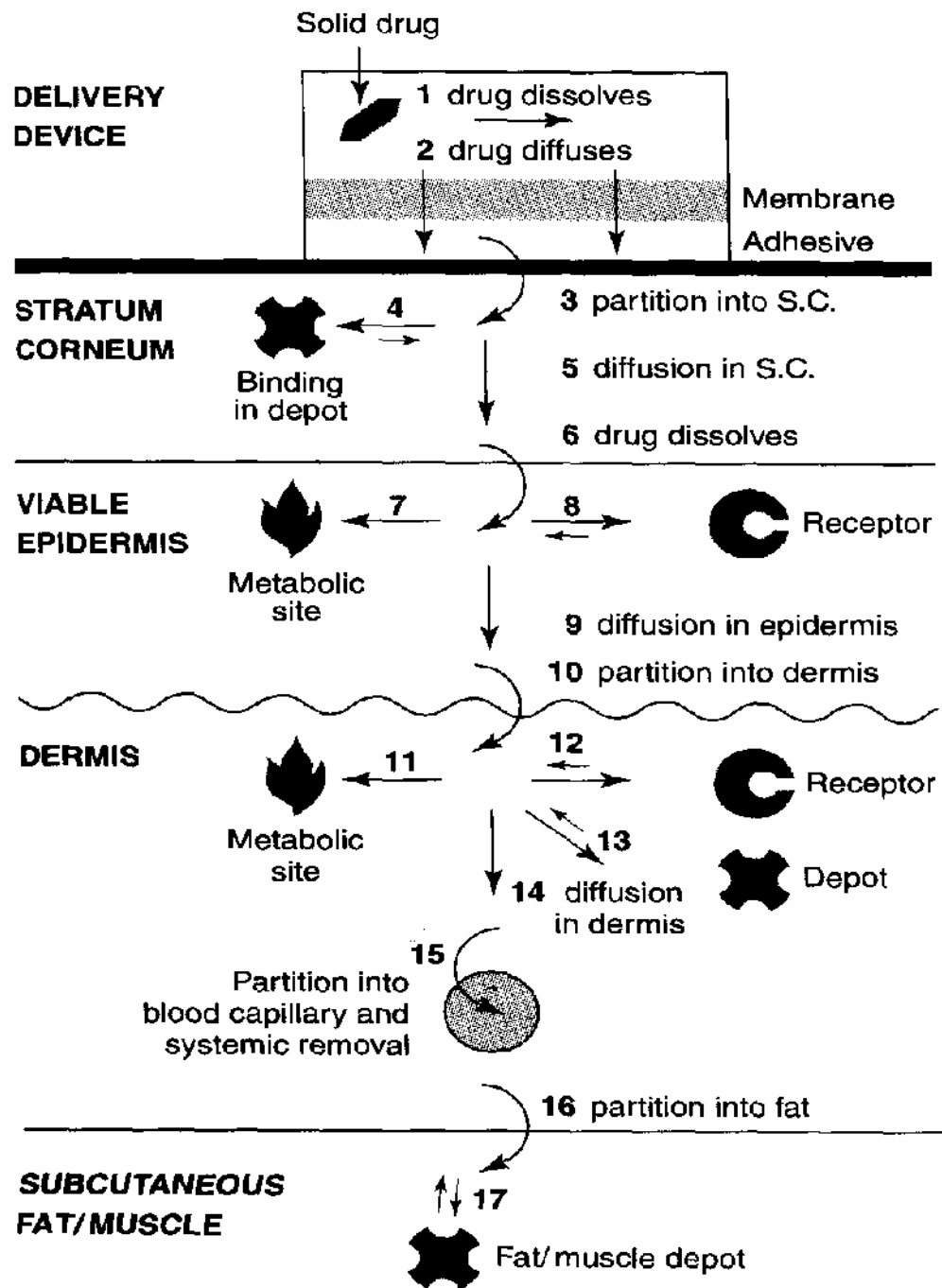


Figure 1.4. Some stages in drug delivery from a transdermal patch (49)

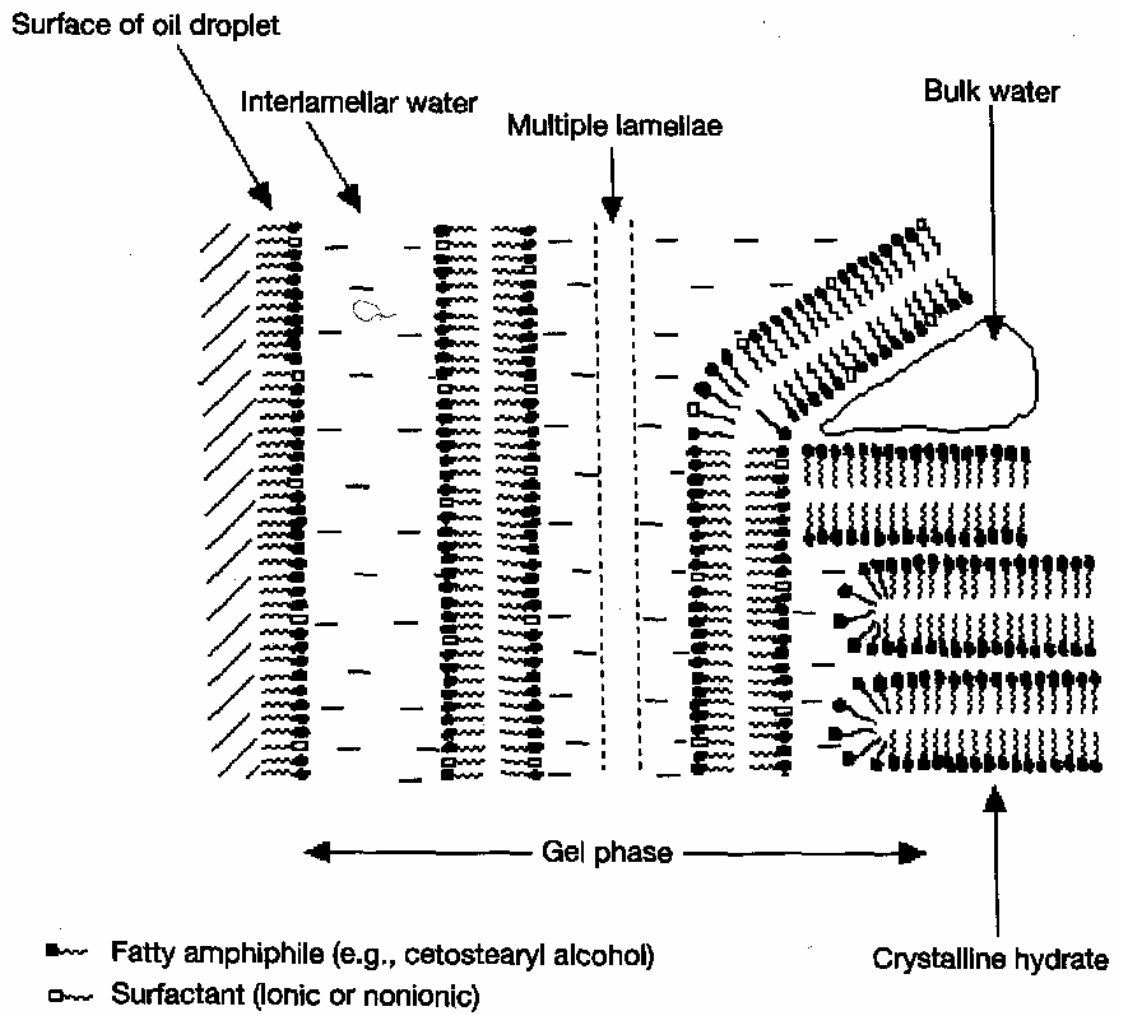


Figure 1.5. The diagram of the structure of a cream with four phases (59)

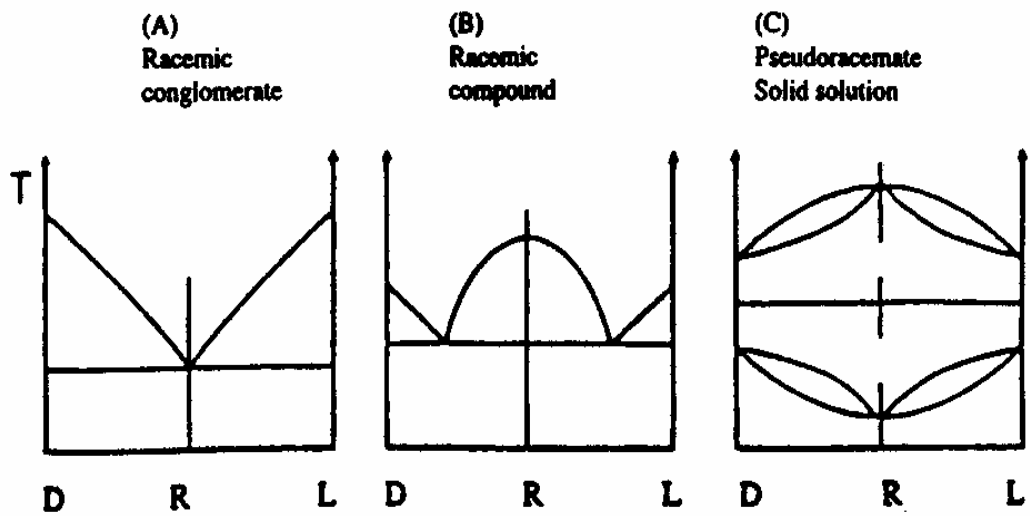


Figure 1.6. Binary phase diagrams illustrating the three fundamental types of crystalline racemates (91).

CHAPTER 2

THE BINARY EUTECTIC OF NSAIDS AND A TWO-PHASE LIQUID SYSTEM FOR ENHANCED MEMBRANE PERMEATION

Yuan, X., Capomacchia, A.C. To be submitted to the Journal of Pharmaceutical
Development and Technology

Abstract

The eutectic properties of binary mixtures of some non-steroidal anti-inflammatory drugs (NSAIDs) with ibuprofen were studied using differential scanning calorimetry (DSC) and phase diagrams. The melting points of several NSAIDs were significantly depressed due to binary eutectic formation with ibuprofen. Ketoprofen and ibuprofen were selected to study the effect of eutectic formation on membrane permeation using Franz diffusion cells and snake skin as the model membrane. The presence of aqueous isopropyl alcohol (aIPA) was necessary to completely transform the solid drugs into an oily state at ambient temperature. As much as 99.6% of the ibuprofen and 88.8% of the ketoprofen added were found in the oily phase of the two-phase liquid system formed when aIPA was added to the eutectic mixture. Due to melting point depression by eutectic formation, high drug concentration in the oily phase and maximum thermodynamic activity in the system, the two-phase liquid system showed enhanced membrane permeation rates of ibuprofen ($37.5 \mu\text{g}/\text{cm}^2/\text{hr}$) and ketoprofen ($33.4 \mu\text{g}/\text{cm}^2/\text{hr}$) as compared to other reference preparations used.

Keywords: NSAIDs; Ibuprofen; Ketoprofen; Isopropyl alcohol; Binary eutectic; Enhanced membrane permeation; Transdermal drug delivery

1. Introduction

Rheumatoid arthritis and related diseases are among the most prevalent diseases in the world. In the U.S. alone, there are over 40 million patients suffering from these diseases, and non-steroidal anti-inflammatory drugs (NSAIDs) have played an important role in treating the diseases^[1]. Long-term use of NSAIDs can result in toxicity to the kidneys and also damage the lining of the stomach, possibly causing ulcers. Thus, transdermal delivery of NSAIDs has been extensively investigated to overcome the adverse effects associated with oral doses of these drugs.

The membrane permeability of drugs in a transdermal formulation depends on many factors, such as type of drug, vehicle composition and additives used, among others. Drug solubility in the skin, which is related to the partition coefficient and melting point of the drug, is particularly important for enhanced dermal permeation. Previous studies have shown that solid drugs that can be transformed into a highly concentrated oily state at ambient temperature (25 °C) exhibited increased skin permeability due to their high thermodynamic activity in the vehicle^[2, 3, 4]. Also, the melting points of different drugs have been shown to be inversely proportional to their lipophilicity and solubility in skin lipids, therefore, affecting the transdermal permeation^[5, 6]. Kasting proposed a relationship between transdermal flux and melting point of the penetrant based on the ideal solution theory^[7], by which the ideal solubility, S_{ideal} , of the penetrant in skin lipids could be calculated:

$$S_{ideal} = \frac{\rho}{1 - \{1 - \exp[\frac{\Delta S_f}{RT} (T_m - T)]\}} \frac{M_1}{MW} \quad (1)$$

where ρ is density of skin lipids, M_l is average molecular weight of skin lipids, MW is molecular weight of the penetrant, T_m is melting point in degrees Kelvin, ΔS_f ($\Delta S_f = \Delta H_f / T_m$) is entropy of fusion of the penetrant and ΔH_f is heat of fusion. S_{ideal} was then entered into a proposed model to predict the maximum flux (J_m) from molecular weight and melting point using:

$$\log (J_m / S_{ideal}) = \log(D_0 / h) - (\beta / 2.303)v \quad (2)$$

where D_0 is a parameter related to diffusion coefficient D by $D = D_0 \exp(-\beta v)$, where v is molecular van der Waals volume and β is a parameter related to the skin properties. v is a property of the permeant while D_0 and β are properties of the skin. For rigid molecules, ΔS_f varies slightly and is approximately 13.5 EU or 56.5 J mol⁻¹ K⁻¹ [8]. According to Equation (1), S_{ideal} increases significantly when the melting point decreases over 10 °C. It also follows that there should be a significant increase in transdermal flux J_m with decreasing melting point, and thus higher S_{ideal} , assuming all other factors being equal. The melting temperature-membrane transport (MTMT) concept [9], again based on the ideal solution theory, has been proposed to predict the relative transdermal fluxes of chiral isomers with different melting points. This concept shows that the ratio of maximum fluxes of enantiomer mixtures is equal to the ratio of their lipid solubility. The solubility, in terms of mole fraction X of a penetrant in a given solvent, was then related to the melting temperature (T_m) and enthalpy of fusion (ΔH) as shown:

$$\ln X = - \frac{\Delta H}{R} \left(\frac{T_m - T}{T \cdot T_m} \right) \quad (3)$$

where R and T are gas constant and temperature of the solution, respectively. These equations clearly show that a reduction in the melting point of a penetrant will increase its solubility in skin lipids and thus enhances transdermal permeation. Therefore, if one can reduce the melting point of a drug without causing unfavorable changes to other physicochemical parameters, then this should enhance transdermal flux. A method by which the melting point of a compound can be reduced by eutectic formation^[10, 11]. Eutectic is a Greek word meaning most fusible or most easily melted. A binary eutectic is a mixture of two compounds which do not interact with each other to form a new chemical entity, but which at certain ratios inhibit crystallization process of one another, resulting in a system with a lower melting point than either of the compounds.

In our studies, several NSAIDs including naproxen, ketoprofen, phenyl salicylate, indomethacin, flurbiprofen were used to form homogeneous mixtures at different ratios with ibuprofen, which has a relatively low melting point (74°C). The eutectic properties of these NSAIDs mixtures were studied by *in vitro* methods in the hope of achieving higher membrane permeation of the compounds. Diffusion studies using shed snake skin were carried out to investigate percutaneous absorption of these drugs in the preparation of binary mixture of ibuprofen with ketoprofen.

2. Materials and methods

2.1 Materials

The following chemicals were obtained from commercial suppliers and used as received: ibuprofen, ketoprofen, naproxen, phenyl salicylate, piroxicam, flurbiprofen, pentobarbital acid (Sigma Chemical Co., St. Louis, MO), isopropyl alcohol (IPA), HPLC grade acetonitrile, monopotassium phosphate, disodium citrate, hydrochloric acid, citric acid, disodium phosphate, dibasic sodium phosphate, phosphoric acid (J. T. Baker Chemical Co., Phillipsburg, NJ). Distilled, deionized water was prepared by a Milli Q system (Millipore Corporation, Bedford, MA). Shed snake skin was donated by the Sandy Creek Nature Center (Athens, GA).

2.2 Differential scanning calorimetry (DSC) of binary mixtures of NSAIDs

Ketoprofen, indomethacin, naproxen, phenyl salicylate and flurbiprofen were selected to prepare eutectic mixtures with ibuprofen. Each drug was mixed with ibuprofen at various weight ratios from 10:90 to 90:10 in a glass test tube, fixing the final total weight at 100 mg. In order to achieve homogenous mixing, the mixtures were dissolved in a solvent consisting of 70% methanol and 30% methylene chloride. The organic solvent was then evaporated using heated vacuum centrifugation for 30 min at 40°C. The residues were left in the refrigerator overnight. Approximately 5 mg each of the resulting mixtures was carefully sealed into aluminum DSC sample pans for thermal analysis. The samples of pure ibuprofen and ketoprofen were not been solvent isolated,

since the DSC thermograms were found to be identical between pure drugs and solvent-isolated drugs. Heat and cool cycles in DSC were done to check if there was any polymorphic transition of binary mixtures. A Perkin Elmer Differential Scanning Calorimeter (Norwalk, CT) equipped with a Perkin Elmer TAC 7/DX thermal analysis controller was used with carrier gas N₂ at pressure of 20 *psi*. Thermograms were obtained at a heating rate of 1 °C/min against an empty reference pan. The scanning temperature ranges were set appropriately according to the melting points of different drugs tested. Perkin Elmer Pyris series software for Windows (Version 3.81) was used to record and analyze the data.

2.3 Composite phase diagram of ibuprofen-ketoprofen-aIPA system

Ibuprofen and ketoprofen are among the most widely used NSAIDs and have relatively low melting points which are respectively 74 °C and 94 °C. They were chosen as model drugs to prepare phase diagrams in the presence of aqueous isopropyl alcohol (IPA). IPA was used in this study because of its complete miscibility with water, common use in cosmetics and proven safety as a pharmaceutical excipient and as a permeation enhancing agent in topical products. Appropriate amounts of ketoprofen were weighed to mix with ibuprofen at different weight ratios from 10:90 to 90:10 in the test tubes keeping the final total weight at 100 mg. One ml citrate buffer (0.05 M, pH 4) was added, then IPA was used to titrate the suspension and the volume was precisely read from the marks on the micro-syringe. The suspension was vortexed until the solid mixture was transformed completely into an oily liquid phase, which was separated out

from the aqueous bulk phase. An optical microscope was used to observe complete transformation of the crystals into an oily state. At this time, a new emulsion system was obtained with oily phase dispersed in external aqueous phase without any remaining crystals in both phases. When the emulsion was further titrated with IPA, a clear homogeneous solution was obtained eventually. At certain ratios, the suspension was transformed completely to a clear homogeneous solution without forming an oily phase and thereafter the two-phase liquid system. To obtain the phase diagram of the system, the volumes of IPA used to completely transform crystals into oil or clear solution and to completely dissolve the oil into the aqueous alcoholic phase were plotted against the IPA percentages (w/w) in the whole system. The total volume of the two-phase system was obtained by transferring the liquid into a micro-syringe and the volume was read precisely from the marks on the syringe.

2.4 Quantification of ibuprofen and ketoprofen in the two-phase liquid system

A binary eutectic system comprising of 40% ibuprofen and 60% ketoprofen was selected to quantitate the amount of each drug in the aqueous and oily phases of the two-phase liquid system formed by titration with IPA using the same method described earlier. More specifically, 80 mg of ibuprofen and 120 mg of ketoprofen were put into a slender glass test tube, followed by the addition of 2 ml of citrate buffer and the appropriate amount of IPA using a micro-syringe. The test tube was sealed and the suspension was vortexed until the solid mixture was completely transformed into an oily state. The tube was then centrifuged (3000 rpm) for 1 hr to make the two phases completely separated.

500 μ l of the aqueous phase was carefully transferred into a 5 ml volumetric flask using a syringe, and 20 % acetonitrile in water was added to make up the sample solution to volume. 200 μ l of this solution was placed in a HPLC autosampler vial, then 1.0 ml of a 20% acetonitrile solution and 20 μ l of the internal standard solution of pentobarbital acid were added and mixed well by vortexing prior to HPLC analysis.

2.5 *In vitro* membrane permeation studies

The permeation rates of ibuprofen and ketoprofen from the select preparations were determined using shed snake skin and Franz diffusion cells. A large whole piece of the skin was cut into small circular pieces of the size that fit the diffusion cells. The skin samples, which were left in the distilled water for 30 min to allow for complete hydration, were mounted onto the diffusion cells with the stratum corneum side facing the donor compartment. Six samples (Table 2.1) were selected from the phase diagram (Figure 2.6) for the *in vitro* permeation studies. The test preparations were poured onto the Franz diffusion cells over the stratum corneum side, and the donor compartments were covered with Parafilm® (American National Can, Neenah, WI). The receptor compartments of the diffusion cells (Dayton Electric Mfg. Co., Chicago, IL) were filled with 0.05 M phosphate buffer (pH 7.4) and were maintained at 32 ± 1.0 °C by circulating water from a thermostat pump (Haake, Model F4391, Berlin, Germany). The receiver phase was continuously stirred at 300 rpm using a star head magnetic stirring bar. The effective diffusion area of the skin was 2.0 cm², and the volume of the receptor compartment was 6.0 cm³. Each test was replicated three times. During 8 hrs of the

diffusion test, 200 μl of the receptor phase was periodically removed and placed into HPLC autosampler vials using a micro-syringe. The receptor phase was immediately replaced with fresh buffer solution. Then, 20 μl of the internal standard solution and 1.0 ml of 20% acetonitrile in water were added into the vial. The vials were capped and vortexed briefly prior to HPLC analysis. The steady state flux, J_{ss} ($\mu\text{g}/\text{cm}^2/\text{hr}$) of ibuprofen and ketoprofen was calculated using Fick's first law:

$$J_{ss} = \Delta M/S \cdot \Delta t = P \cdot C_d = D \cdot K \cdot C_d/h \quad (4)$$

$$D = h^2 / 6 \cdot L \quad (5)$$

where S is the effective diffusion area (cm^2) and $\Delta M/\Delta t$ is the amount of drug penetrating through the membrane per unit time at steady state ($\mu\text{g}/\text{hr}$); P is the permeability coefficient (cm/hr); C_d is the drug concentration in donor phase ($\mu\text{g}/\text{ml}$); D is the diffusion coefficient (cm^2/hr); K is the partition coefficient between vehicle and skin; h is the membrane thickness (cm); and L is the lag time (hr). ANOVA was performed using SAS statistical package (SAS Institute Inc., Cary, NC) to determine significant differences among the J_{ss} values found for different preparations.

2.6 HPLC analysis of ibuprofen and ketoprofen

The Waters HPLC system (Waters, Milford, MA) consisted of a Model 616 solvent delivery pump, a Model 600S controller, a Model 717plus autosampler equipped with a temperature-controlled rack, a photo-diode array UV detector, and a Millennium data station. Ibuprofen, ketoprofen and internal standard pentobarbital acid were

separated on a Waters C18 analytical column (250 × 4.6 mm I.D., 5µm) at ambient temperature. The mobile phase was 50:50 (v/v) acetonitrile : phosphate buffer (0.025 M, pH 2.0). The flow rate was set at 1.0 ml/min. Absorbance was monitored at 223 nm using a photo-diode array UV detector. The automated injection volume was 20 µl for each sample. Separation of ibuprofen, ketoprofen and pentobarbital acid (internal standard) by HPLC was achieved within 10 min run time as shown Figure 2.7. The retention times of ibuprofen, ketoprofen and internal standard were 7.6, 3.3 and 2.3 min, respectively. Weekly calibrations using the peak height ratios of drugs to internal standard were obtained for different concentrations from 20 ng/ml to 2 mg/ml.

3. Results and discussion

3.1 Differential scanning calorimetry (DSC) of binary mixtures of NSAIDs

The DSC thermograms for the mixtures of ibuprofen with ketoprofen (Figures 2.1- 2.5), naproxen, phenyl salicylate or flurbiprofen clearly showed binary eutectic formation between each of ibuprofen combinations. For each of the binary mixtures used, the melting points of the compounds were significantly depressed, and the eutectic melting point for the mixture was identified on the plots. The phase diagrams representing the melting curves against the composition of drugs were also constructed and shown in Figures 2.1 – 2.5. For the ratios of ibuprofen and ketoprofen between 10:90 and 90:10 (w/w), the eutectic melting points ranged from 58 to 61 °C, while the melting points of pure ibuprofen and ketoprofen were 74 °C and 94 °C, respectively. The binary mixtures produced two endothermic peaks, the first one between 58 – 61 °C where initial melting of the mixtures occurred. This point is called the temperature of *solidus* in the

phase diagram. The second peak known as the temperature of *liquidus* was wider and appeared at different positions according to the weight ratios as shown in Figure 2.1. The mixtures of ibuprofen and ketoprofen at the ratios between 40:60 and 60:40 (w/w) showed almost one single merged peak, representing the eutectic melting point. The 40:60 (w/w) ratio was chosen for this study because of the higher anti-inflammatory activity of ketoprofen compared to ibuprofen. When the peak of solidus merged with the peak of liquidus, the peak temperature of merged peaks was sometimes slightly higher than the temperature of solidus because of merging of two peaks, thus up-shifting the peak apex. All the NSAIDs binary mixtures showed similar DSC thermograms, although some peaks of *solidus* or *liquidus* were not clearly visible. For the mixture of ibuprofen and naproxen (m.p., 152 °C), the eutectic point was 69 °C, which occurred at the weight ratio of ibuprofen to naproxen at 20:80. For the mixture of ibuprofen and phenyl salicylate (m.p., 40 °C), the eutectic melting point was 34 °C at the weight ratio of 20:80. The eutectic melting point of ibuprofen and flurbiprofen (m.p., 110 °C) was 63 °C at the weight ratio of 60:40. No polymorphic transition of binary mixtures was observed after heat and cool cycles in DSC.

From Equations (1) and (2) shown earlier, the following Equation (5) could be derived:

$$\log J_m = \log(D_0/h) - (\beta/2.303)v + \log \rho - \log \left\{ 1 - \frac{M_1}{MW} + \exp\left[\frac{\Delta S_f}{RT}(T_m - T)\right] \frac{M_1}{MW} \right\} \quad (5)$$

These equations show that with other conditions being equal the lower the melting point (T_m), the higher the solubility (S_{ideal}) of drugs in skin lipids, and thus the higher the flux (J_m) of drugs through the skin. Since the eutectic formation lowered the melting points of

drugs without modifying their chemical properties, this method was used to enhance the membrane permeation of these compounds in this study.

3.2 Composite phase diagram of ibuprofen-ketoprofen-aIPA system

In order to prepare a topical formulation, ibuprofen and ketoprofen must be in liquid state. It was found that the solid crystals of ibuprofen and ketoprofen could be transformed into an oily state at ambient temperature and formed a two-phase liquid system in the presence of an appropriate amount of aqueous IPA. The analytical data showed that, in the two-phase liquid system, the majority of the drugs were present in the oily phase rather than in the aqueous phase of the system. The drugs in the oily phase should provide the maximum thermodynamic activity, due to the nearly saturated concentration in the oily phase, and thus a very high concentration gradient across the stratum corneum when the oily phase is applied onto the skin surface. The above conditions will create a strong driving force for the compounds to permeate through the membrane. Thermodynamically, this spontaneous process to achieve a new equilibrium state is entropy driven, with a net decrease in Gibbs free energy of the system. In addition, IPA is an enhancer that has been shown to enhance the dermal permeation of many compounds.

In Figure 2.6, the phase diagram of the binary mixture of ibuprofen and ketoprofen in the presence of aqueous IPA showed a lower curve ABCD and an upper curve ACD which respectively represented the complete transformation of the drug crystals into the oily phase and the complete solubilization of the oily phase into the

homogeneous aqueous phase. The phase diagram was then segmented into three regions by the two curves. The lower region under the curve ABCD shows the area where some of the crystals of either ibuprofen or ketoprofen remained. The middle region between the curves ABCD and ACD indicates the coexistence of the oily and aqueous phases. The upper region above ACD displays the region where only the homogeneous aqueous phase is formed. It is interesting to note that the curve ABCD, which corresponds to the volume of IPA used to obtain the two-phase liquid system, has the same pattern as the *liquidus* curve of the melting points of the different mixtures of ibuprofen with ketoprofen. The possible explanation for this phenomenon is that the lower the melting points of the binary mixtures, the lower enthalpy of solubilization required, and thus less aqueous IPA is needed to solubilize the drug crystals into the oily phase. After vortexing the two-phase liquid system vigorously, a fine O/W emulsion was obtained, which could be further developed into topical formulations for enhanced transdermal delivery of these drugs.

3.3 Quantification of ibuprofen and ketoprofen in the two-phase liquid system

The concentrations of ibuprofen and ketoprofen in the aqueous and oily phases of the two-phase liquid system of binary mixture at the eutectic ratio (ibuprofen:ketoprofen = 40:60) were determined by HPLC and shown in Table 2.2. The results showed that the concentration of ibuprofen in the aqueous phase was 0.12 mg/ml, which was only 0.4 % (w/w) of the total ibuprofen in the system. On the other hand, the concentration of ibuprofen in the oily phase was 318.75 mg/ml, which represented 99.6 % (w/w) of the total ibuprofen added. The concentration of ketoprofen in the aqueous phase was close to 5.0 mg/ml, which was 11.2 % (w/w) of the total ketoprofen in the system, while 88.8 % (w/w) remained in the oily phase with the concentration of 426.11 mg/ml. The higher

concentration of ketoprofen in the aqueous phase than that of ibuprofen could be attributed to the more polar nature of ketoprofen molecules. The concentrations of ibuprofen and ketoprofen present in the oily phase were 30.9 % (w/w) and 41.3 % (w/w), respectively. The two drugs together constituted 72.2 % (w/w) of the oily phase. It is clear that no common pharmaceutical oils available could dissolve these drugs at such high concentrations. The majority of the remaining oily phase was probably composed of IPA, since the hydrophilic buffer added could not be dissolved in the hydrophobic oily phase.

3.4 *In vitro* Membrane Permeation Studies

In order to demonstrate the effect of a reduced melting point of the compound on enhanced membrane permeation as shown in above equations, the *in vitro* diffusion profiles of ibuprofen and ketoprofen in the six test preparations (I – VI) selected from the phase diagram (Figure 2.6) were determined using shed snake skin as a model membrane. Due to different solubilities of the drugs and eutectic mixture in the vehicle, obviously, the same thermodynamic activity of drugs could not be achieved if the same solvent or donor concentration were used. In another words, the same thermodynamic activity and the same drug concentration cannot be obtained at the same time for different drugs with different solubilities. Since the thermodynamic activity of a drug in the formulation is very critical for the percutaneous absorption of drugs, several saturated preparations (I, III, V and VI) were used in order to maintain the maximum thermodynamic activity of the drugs in the vehicle. This way, the potential maximum fluxes of drugs in different preparations could be directly compared. Preparation I was a saturated aqueous solution of ibuprofen and ketoprofen in the buffer. III was a saturated aqueous IPA solution of

binary mixture of drugs at the eutectic ratio. V and VI were the saturated aqueous IPA solutions of ibuprofen and ketoprofen, respectively. As described earlier, in the presence of aqueous IPA, the binary eutectic of ibuprofen and ketoprofen formed a two-phase liquid system (II), which might offer enhanced permeation due to high drug concentration and maximum thermodynamic activity in the oily phase. Therefore, II was selected to compare with other preparations. An unsaturated aqueous IPA solution (IV) of binary mixtures of drugs with a higher percentage of IPA was also selected to compare with saturated solution (III) and two-phase liquid system (II) at the same eutectic ratio. The same amounts of drugs (40 mg of ibuprofen, 60 mg of ketoprofen or both) were used in the above preparations (I-VI) in order to compare the fluxes of these compounds directly.

Shed snake skin was used as the model membrane as reported in some previous studies^[4, 12, 13]. From the permeation profiles (Figures 2.8 and 2.9), the steady state fluxes of ibuprofen and ketoprofen were calculated using Fick's first law. The results (Table 2.3) showed that among all of the saturated preparations (I, III, V and VI), the saturated aqueous IPA solution (III) of binary eutectic of drugs gave the highest flux (J_{ss}) of both ibuprofen and ketoprofen. The flux of ibuprofen in III ($25.8 \mu\text{g}/\text{cm}^2/\text{hr}$) was 1.52 – fold higher than that ($17.0 \mu\text{g}/\text{cm}^2/\text{hr}$) in the saturated aqueous IPA solution of ibuprofen (V), and the flux of ketoprofen in III ($25.1 \mu\text{g}/\text{cm}^2/\text{hr}$) was 1.93 – fold higher than that ($13.0 \mu\text{g}/\text{cm}^2/\text{hr}$) in the saturated aqueous IPA solution of ketoprofen (VI). Since III has lower drug concentration than V and VI, the observed phenomenon that III had higher fluxes than V and VI was not caused by variation of donor concentrations, but was due to the enhancing effect of melting point depression by the eutectic formation on membrane permeation as suggested in the Equation (5).

The result also showed that Preparation II, the binary eutectic two-phase liquid system, gave the highest flux (J_{ss}) of both ibuprofen (37.5 $\mu\text{g}/\text{cm}^2/\text{h}$) and ketoprofen (33.4 $\mu\text{g}/\text{cm}^2/\text{h}$) among all the test preparations, regardless of whether they were saturated or unsaturated. The fluxes of ibuprofen and ketoprofen in II increased 3.44 and 4.02 – fold over those in the saturated aqueous solution (I), which were 10.9 and 8.3 $\mu\text{g}/\text{cm}^2/\text{hr}$, respectively. When compared with the saturated aIPA solution (III) of the same binary mixture of drugs, II exhibited 1.45 and 1.33 – fold increases of the fluxes of ibuprofen and ketoprofen, respectively, through the model membrane. II also exhibited 1.96 and 2.21 – fold increases of fluxes of ibuprofen and ketoprofen, respectively, through the skin as compared to those measured from the unsaturated aIPA solution (IV) of the same binary mixture. These increases were attributed to the maximum thermodynamic activity and high drug concentrations in the oily phase to two-phase liquid system and thereafter the high drug concentration gradient created between the two sides of the membrane. Due to the lower thermodynamic activity and concentration in unsaturated aIPA solution, IV had lower fluxes of ibuprofen and ketoprofen (which were 19.1 and 15.1 $\mu\text{g}/\text{cm}^2/\text{hr}$, respectively) than those from the saturated aqueous IPA solution (III).

The differences of the fluxes of ibuprofen and ketoprofen between II and all other preparations were found to be statistically significant ($P < 0.05$) using one-way ANOVA performed by SAS statistical package. In addition, II contained much less IPA than III - VI, which is also desirable for a topical formulation. Therefore, the two-phase liquid system (II) of binary eutectic of ibuprofen and ketoprofen, was a very promising candidate for the enhanced transdermal delivery of these drugs.

4. Conclusion

The eutectic formation of ibuprofen with another NSAID significantly depressed the melting points of these compounds. The addition of aqueous IPA to the binary eutectic mixture completely transformed the solid drugs into the oily state at ambient temperature. The preparation of the two-phase liquid system of these drugs at the eutectic ratio significantly enhanced their membrane permeation as compared to other preparations. The study confirmed that the melting point of the drug is inversely related to its membrane permeation due to increased lipid solubility of the drug when the melting point is depressed. The results suggested that the binary eutectic mixture of NSAIDs and the two-phase liquid system could be used to develop topical formulations of these drugs for enhanced percutaneous absorption.

References

1. Centers for Disease Control and Prevention (CDC), National Center for Chronic Disease Prevention and Health Promotion, Atlanta, GA, USA. The National Arthritis Action Plan: A Public Health Strategy (NAAP), **2002**.
2. Brodin, A.; Nyqvist-Mayer, A.; Wadsten, T.; Forslund, B.; Broberg, F. Phase Diagram and Aqueous Solubility of the Lidocaine-prilocaine Binary System. *J. Pharm. Sci.* **1984**, *73*: 481-484.
3. Nyqvist-Mayer, A. A.; Brodin, A. F.; Frank, S. G. Phase Distribution Studies on an Oil-water Emulsion Based on Eutectic Mixture of Lidocaine and Prilocaine as the Dispersed Phase. *J. Pharm. Sci.* **1985**, *74*: 1192-1195.
4. Kang, L. S.; Jun H.W.; Mani N. Preparation and Characterization of Two-phase Melt Systems of Lidocaine. *Int. J. Pharm.* **2001**, *222* (1): 35-44.
5. Calpena, A. C.; Blanes, C.; Moreno, J.; Obach, R.; Domenech, J. A Comparative In Vitro Study of Transdermal Absorption of Anti-emetics. *J. Pharm. Sci.* **1994**, *83*: 29-33.
6. Kang L. S.; Jun H.W.; McCall J.W. Physicochemical Studies of Lidocaine-menthol Binary Systems for Enhanced Membrane Transport. *Int. J. Pharm.* **2000**, *206* (1-2): 35-42

7. Kasting, G. B.; Smith, R. L.; Cooper E. R. Effects of Lipid Solubility and Molecular Size on Percutaneous Absorption. *Pharmacol. Skin.* **1987**, 1: 138-153.
8. Yalkowski, S. H.; Valvani, S. C. Solubility and Partitioning. I. Solubility of Nonelectrolytes in Water. *J. Pharm. Sci.* **1980**, 69: 912-922.
9. Touitou, E.; Chow D. D.; Lawter J. R. Chiral Beta-blockers for Transdermal Delivery. *Int. J. Pharm.* **1994**, 104: 19-28.
10. Grant, D.; Abougela, I. Physico-chemical Interactions in Pharmaceutical Formulations. *Anal. Proc.* **1982**, 19: 545-549.
11. Ford, J. L.; Timmins, P. *Pharmaceutical Thermal Analysis*; John Wiley and Sons: New York, **1989**, pp. 47-67.
12. Higuchi, T.; Konishi, R. *In Vitro Testing and Transdermal Delivery*, *Therap. Res.* **1987**, (6): 280-288.
13. Itoh T.; Xia J.; Magavi R.; Nishihata T.; Rytting J. H. Use of Shed Snake Skin as a Model Membrane for In Vitro Percutaneous Penetration Studies: Comparison with Human Skin, *Pharmaceutical Res.* **1990**, (7): 1042-1047.

Table 2.1. Composition of selected preparations and fluxes of drugs through the model membrane

Preparation	Concentration of		Concentration of		IPA (%, w/w)
	Ibuprofen (mg)	Ibuprofen (mg/ml)	Ketoprofen (mg)	Ketoprofen (mg/ml)	
I	40.0	N/A *	60.0	N/A *	0.0
II	40.0	28.6	60.0	42.9	22.2
III	40.0	23.7	60.0	35.6	32.8
IV	40.0	20.7	60.0	31.0	40.0
V	40.0	57.0	0.0	N/A	35.0
VI	0.0	N/A	60.0	55.2	36.6

* Preparation I was a suspension of ibuprofen and ketoprofen. The concentrations of the drugs in the system were not measured.

Table 2.2. Concentrations of ibuprofen and ketoprofen in the aqueous (aq.) and oily phases of a selected two-phase liquid system (Preparation II) at 25 °C

Drug	Concentration in aq. phase (mg/ml)	Concentration in oily phase (mg/ml)	% of drug in aq. phase (w/w)	% of drug in oily phase (w/w)	% of total wt. of oily phase (w/w)
Ibuprofen	0.12	318.75	0.39	99.61	30.90
Ketoprofen	4.99	426.11	11.23	88.77	41.30

Table 2.3. Steady state fluxes (J_{ss}) of drugs through the model membrane

Preparation	J_{ss} of Ibuprofen ($\mu\text{g}/\text{cm}^2/\text{hr}$)	J_{ss} of Ketoprofen ($\mu\text{g}/\text{cm}^2/\text{hr}$)
I	10.9	8.3
II	37.5	33.4
III	25.8	25.1
IV	19.1	15.1
V	17.0	N/A
VI	N/A	13.0

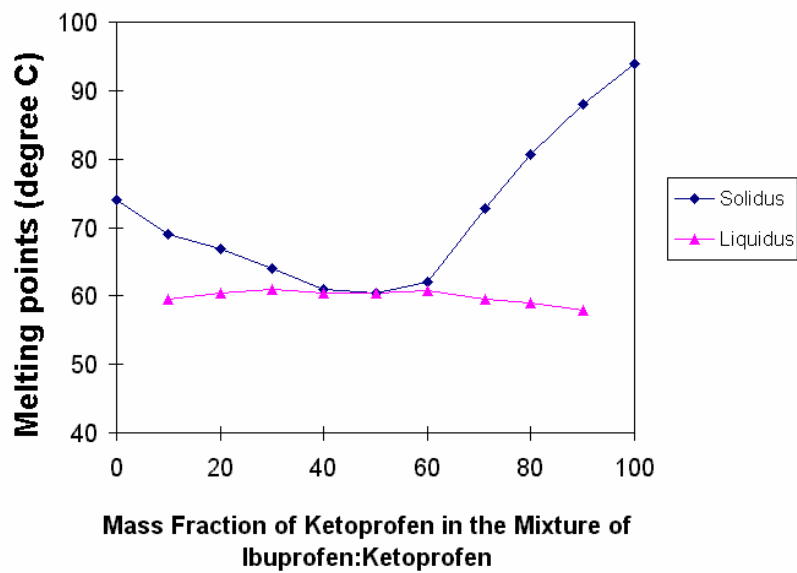
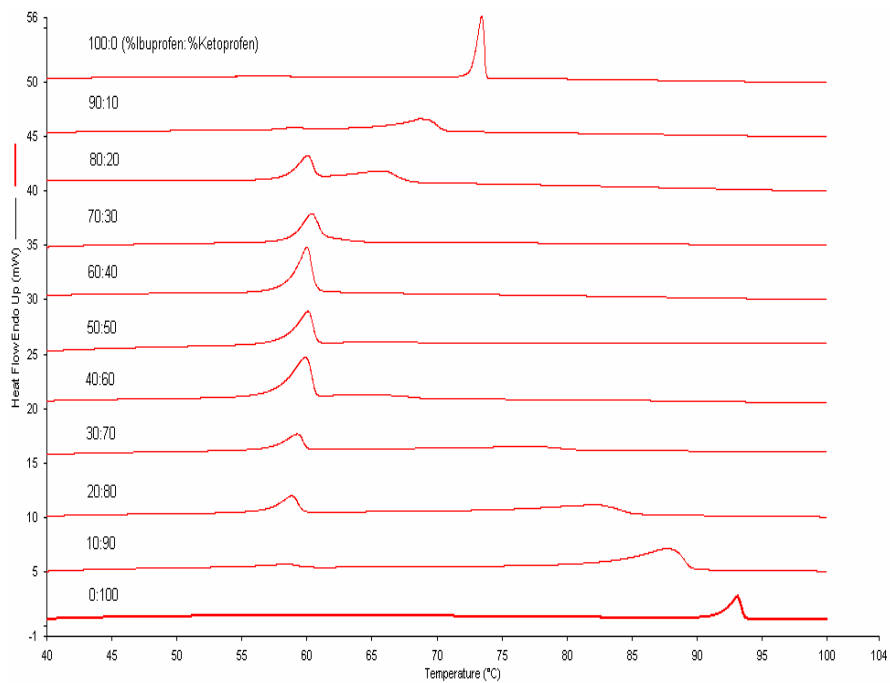
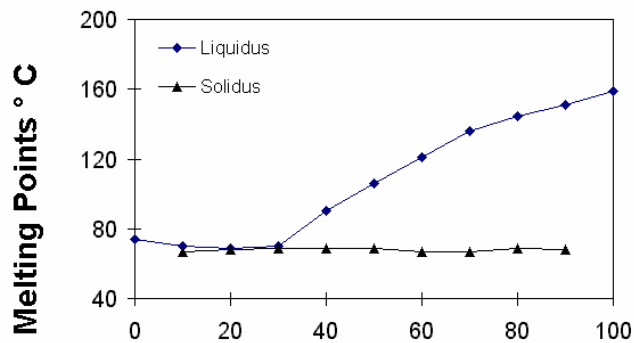
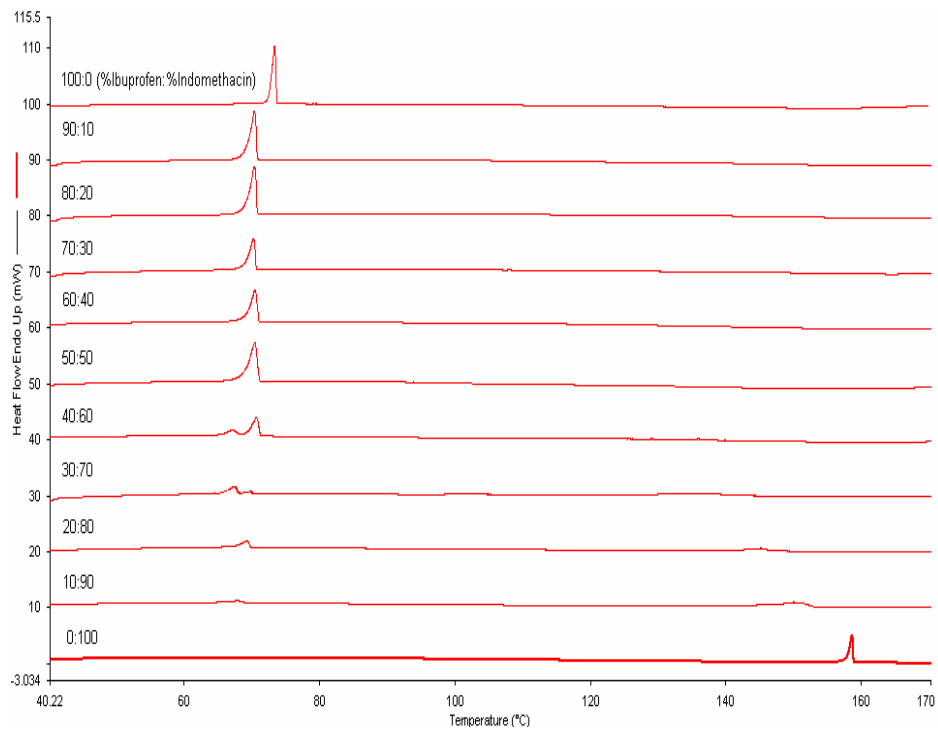


Figure 2.1. DSC thermograms of ibuprofen and ketoprofen mixtures



Mass Fraction (%) of Indomethacin in Mixture of Ibuprofen and Indomethacin

Figure 2.2. DSC phase diagram of ibuprofen and indomethacin mixtures

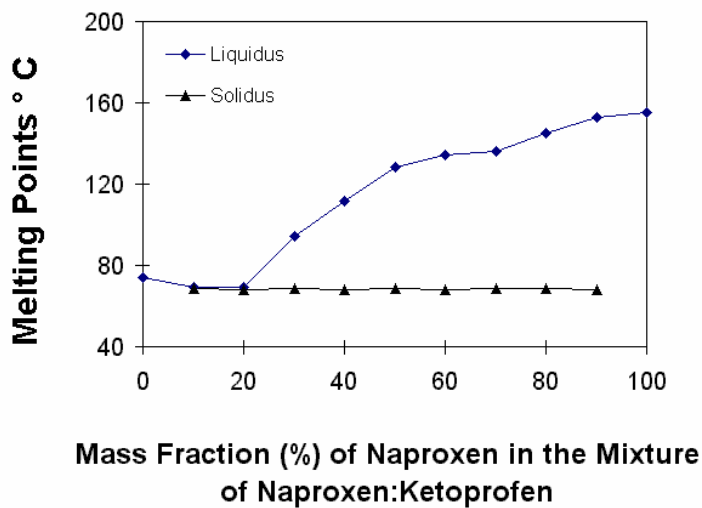
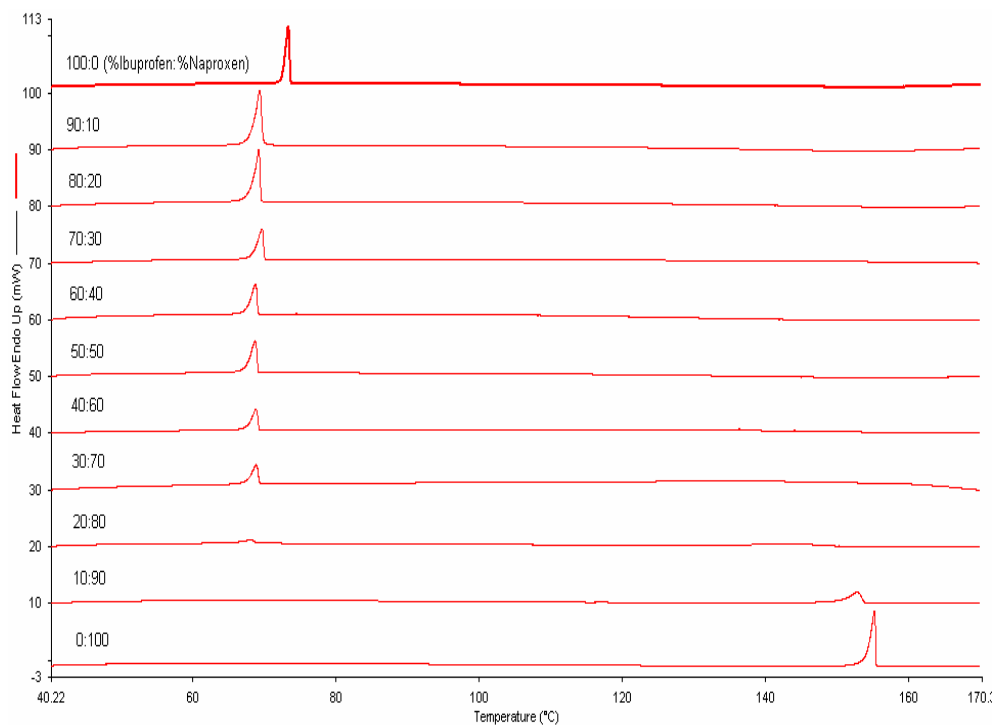
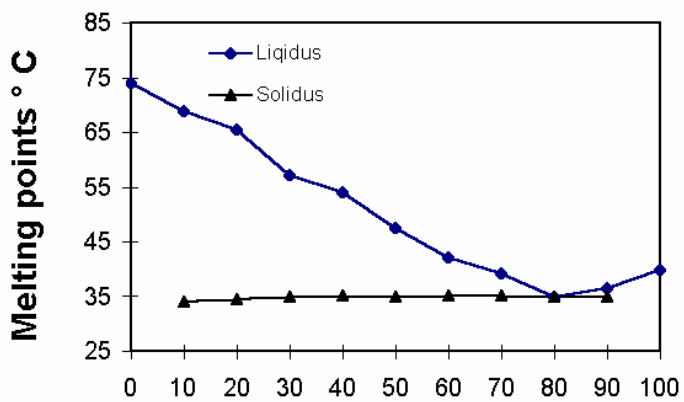
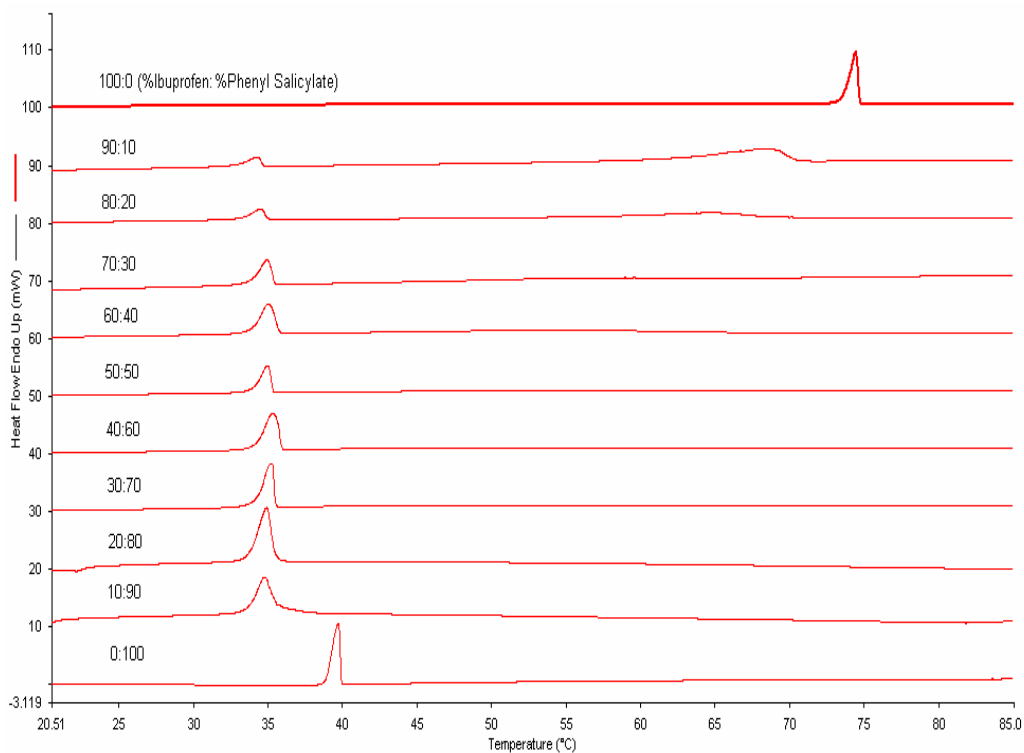


Figure 2.3. DSC phase diagram of ibuprofen and naproxen mixtures



Mass Fraction (%) of Phenyl Salicylate in Mixture of Ibuprofen and Phenyl Salicylate

Figure 2.4. DSC phase diagram of ibuprofen and phenyl salicylate mixtures

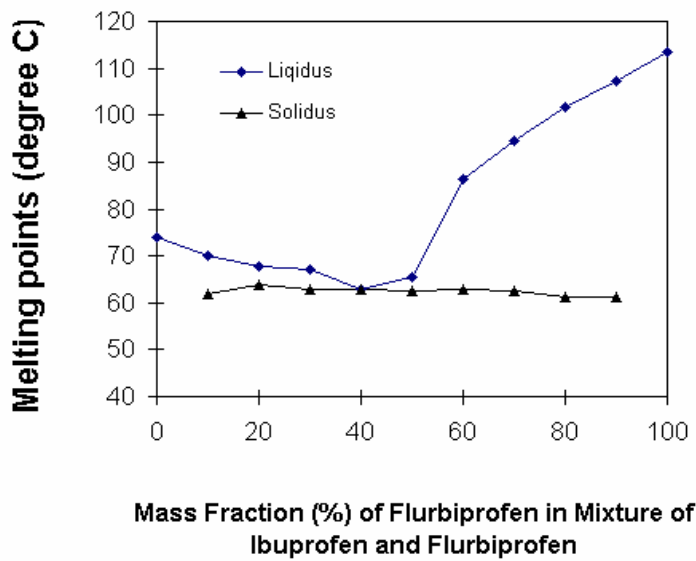
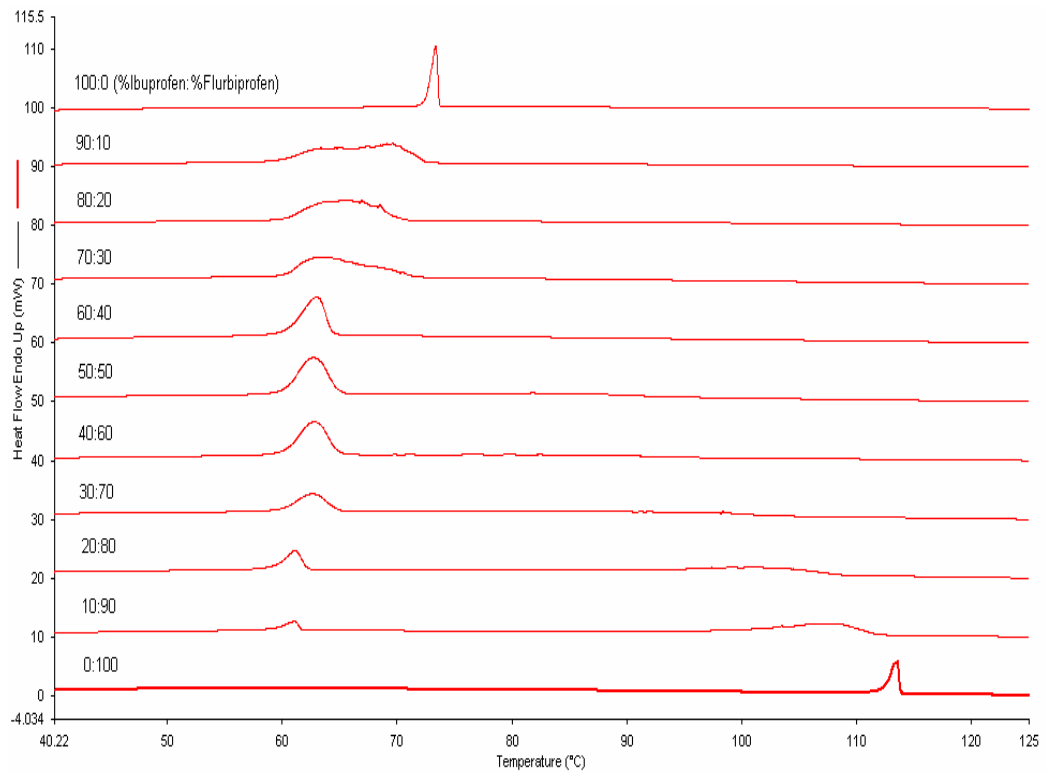


Figure 2.5. DSC phase diagram of ibuprofen and flurbiprofen mixtures

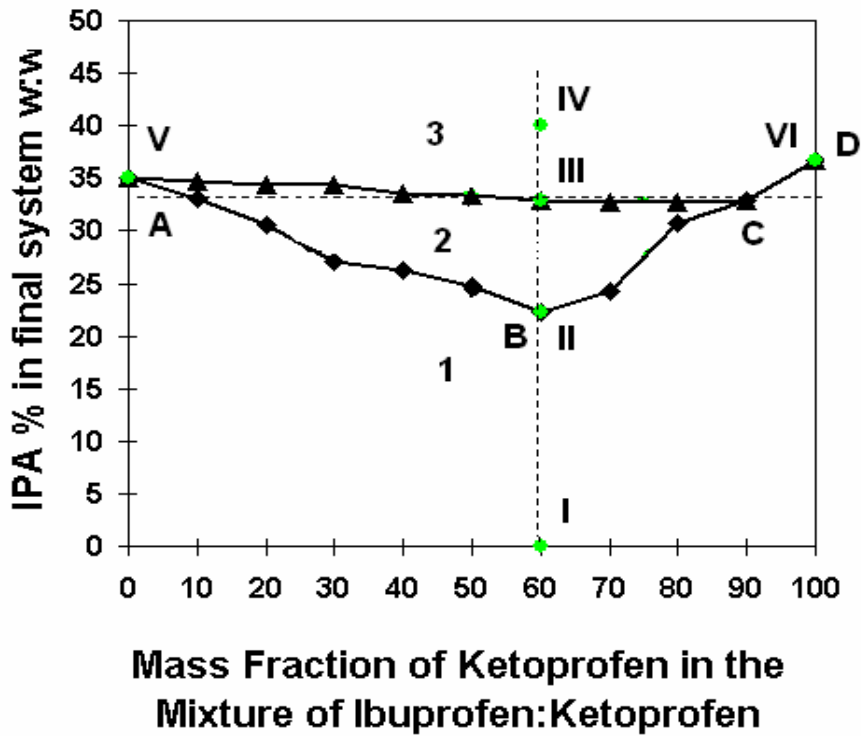


Figure 2.6. Phase diagram of ibuprofen – ketoprofen - IPA system at 25 °C and selected preparations.

1 - Solid crystals remaining 2 - Two-phase liquid system 3 - Alcoholic aqueous solution

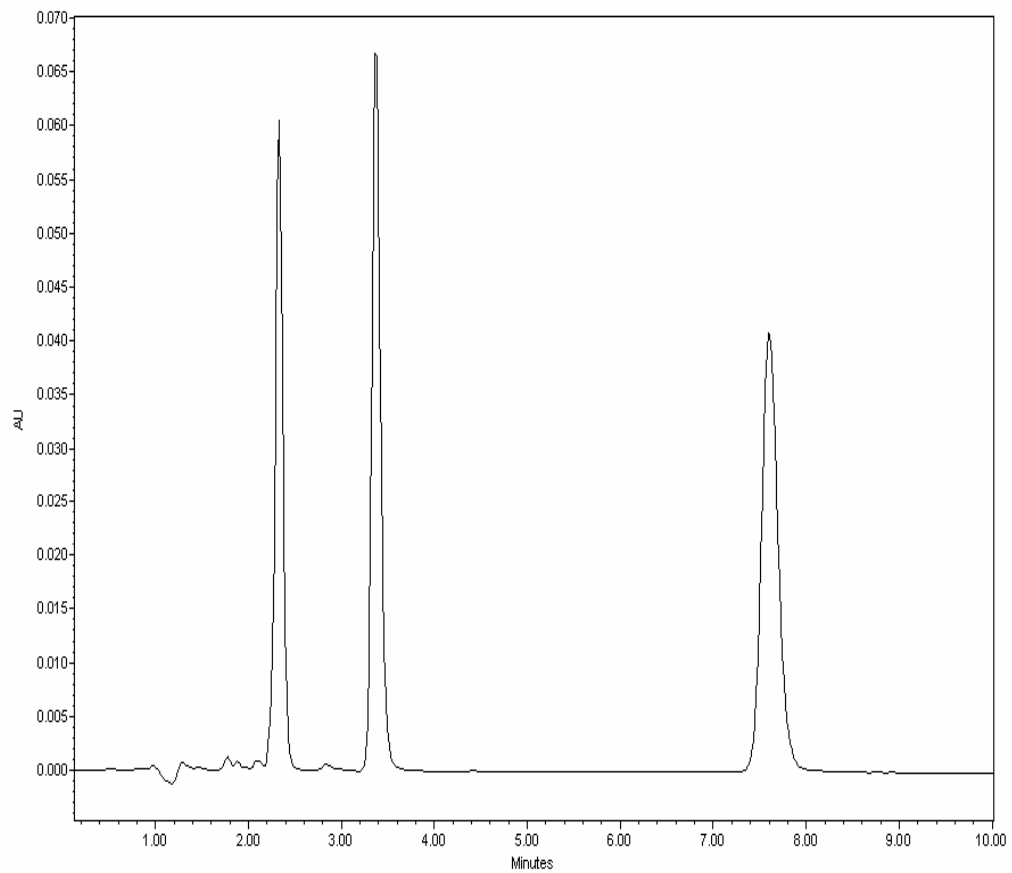


Figure 2.7. HPLC profile of ibuprofen (7.6 min), ketoprofen (3.3 min) and internal standard (2.3 min)

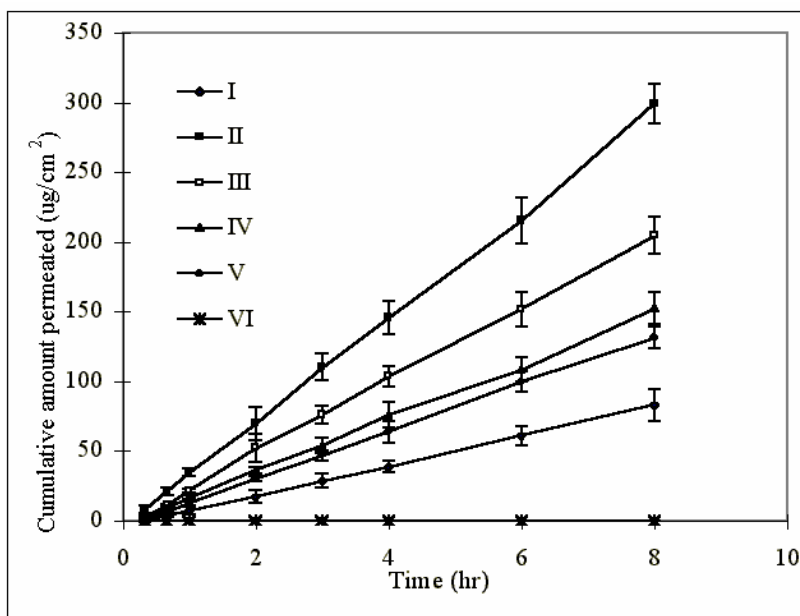


Figure 2.8. Permeation profiles of ibuprofen through shed snake skin (n = 3, error bar = SD)

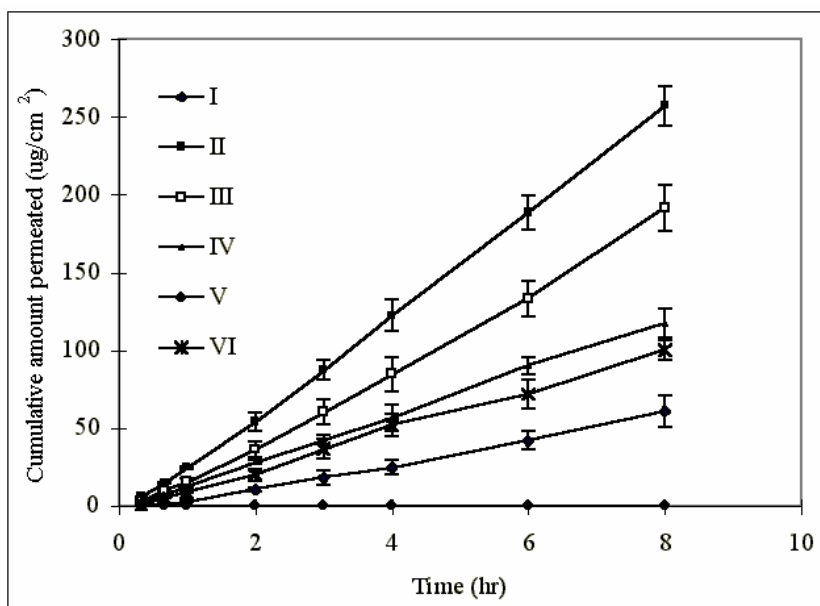


Figure 2.9. Permeation profiles of ketoprofen through shed snake skin (n = 3, error bar = SD)

CHAPTER 3

PHYSICOCHEMICAL STUDIES OF THE BINARY EUTECTIC OF IBUPROFEN AND KETOPROFEN AND MATHEMATICAL MODELS FOR ENHANCED TRANSDERMAL DELIVERY

Yuan, X., Capomacchia, A.C. To be submitted to the International Journal of

Pharmaceutics

Abstract

The thermodynamic, eutectic and crystalline properties of the mixture were investigated using differential scanning calorimetry (DSC) and X-ray powder diffractometry (XRPD). DSC studies showed that enthalpy (11.3 kJ/mol) and entropy of fusion (33.7 J/K/mol) of the binary eutectic were significantly reduced as compared to those of the individual drugs. XRPD indicated that the binary eutectic did not form a new crystalline structure. The effects of reduced melting points of the drugs on the membrane flux were predicted by two mathematical models and related thermodynamic data. The predicted values of flux of these compounds were compared with those obtained from permeation studies using shed snake skin as the model membrane. The steady state fluxes of ibuprofen and ketoprofen from different preparations of the binary eutectic mixtures were higher than those from the reference preparations of pure drugs. The theoretical models correctly predicted the increasing trend of fluxes, and the predicted values were not significantly different from the experimental result of maximum fluxes of drugs.

Keywords: Ibuprofen; Ketoprofen; Eutectic; DSC; X-ray Powder Diffraction; Enhanced membrane permeation; Transdermal drug delivery

1. Introduction

Ibuprofen and ketoprofen are among the most widely used non-steroidal anti-inflammatory drugs (NSAIDs) and have been used as topical preparations for treating rheumatoid arthritis and related diseases (Lawrence et al., 1998). In the U.S., it was estimated that these conditions afflict over 40 million patients, or about one of every six people, making it one of the most prevalent diseases in this country (Centers for Disease Control and Prevention, 2002). Oral dosage forms of NSAIDs often upset the stomach and can cause nausea and kidney toxicity. Much research has been directed toward the development of these drugs as topical formulations to overcome the adverse effects associated with oral dosing to enhance their efficacy topically (Rovensky J et al, 2001. Vaile JH, Davis P, 1998. Chlud K, 1991. Valenta C et al, 2000).

Among many factors that could affect the permeation of drugs through the skin, one particularly important factor is the intrinsic solubility of drug in skin lipids, which is also related to the physicochemical and thermodynamic properties of the drug. It has been shown that the melting points of some drugs are inversely proportional to their lipophilicity ($\log P$) and solubility in skin lipids and, thus to their transdermal flux (Calpena et al., 1994). Based on the ideal solution theory, Kasting proposed the following equation to describe the relationship between transdermal permeation and melting point of the permeant (Kasting et al., 1987), in which the ideal solubility, S_{ideal} , of a penetrant in skin lipids could be estimated as shown below:

$$S_{ideal} = \frac{\rho}{1 - \{1 - \exp[\frac{\Delta S_f}{RT}(T_m - T)]\}} \frac{M_l}{M_w} \quad (1)$$

where ρ is the density of skin lipids and M_l is their average molecular weight. M_w is the molecular weight of the permeant. T_m is the melting point in degrees Kelvin and ΔS_f is the entropy of fusion of the permeant. The S_{ideal} was then entered into a proposed model to predict the steady state flux (J_m) from its molecular weight and the melting point of the permeant:

$$\log(J_m/S_{ideal}) = \log(D_0/h) - (\beta/2.303)v \quad (2)$$

where D_0 is a parameter related to diffusion coefficient D by $D = D_0 \exp(-\beta v)$, where v is molecular van der Waals volume and β is a parameter related to the skin properties. v is the property of the permeant while D_0 and β are properties of the skin. The values of these parameters are estimated, and equation (2) is simplified as:

$$\log(J_m/S_{ideal}) = 1.80 - (0.0216/2.303) M_w \quad (3)$$

Since the ΔS_f varies slightly with the melting point, S_{ideal} increases with decreasing the melting point for any given molecular weight. It follows that there should be an increase in transdermal flux with decreasing melting point, all other factors being equal. Again based on the ideal solution theory, Touitou proposed a melting temperature-membrane transport (MTMT) concept to predict the relative transdermal fluxes with different melting points (Touitou et al., 1994). The solubility, in terms of mole fraction solute, X , of a permeant in a given solvent, was then related to the melting temperature, T_m , and the enthalpy of fusion, ΔH :

$$\ln X = -\frac{\Delta H}{R} \left(\frac{T_m - T}{T \cdot T_m} \right) \quad (4)$$

where R is the gas constant and T denotes the temperature of the solution of permeant.

All of the above equations indicate that a depression in the melting point of a permeant would increase its solubility in skin lipids and thus enhance transdermal permeation.

Therefore, if the melting point of a drug can be reduced without causing unfavorable changes to other physicochemical parameters, then transdermal flux should be increased accordingly. A method by which the melting point of a compound can be reduced is eutectic formation (Grant et al., 1982. Ford et al., 1989). By definition, a binary eutectic is a mixture of two components which do not interact with each other to form a new chemical entity, but which, at certain ratios can inhibit the crystallization process of one another resulting in a system with a lower melting point than either of the components. It has been shown that solid drugs of local anesthetics can be transformed into an oily state by depressing melting points of the compounds below ambient temperature (25 °C). In this way, the preparation provided the maximum thermodynamic activity for the drugs (Brodin et al., 1984. Adela et al., 1985).

In this study, the melting point depression and thermodynamic properties of the binary eutectic of ibuprofen and ketoprofen were investigated using differential scanning calorimetry (DSC). The relationship between crystalline structure of pure drugs and the binary eutectic was investigated using X-ray powder diffractometry (XRPD). *In vitro* diffusion was conducted to study the effects of melting point depression by eutectic formation on the percutaneous absorption, and the experimental results of the steady state fluxes were compared to those predicted by the two proposed mathematical models.

2. Materials and methods

2.1 Materials

The following chemicals were obtained from commercial sources and used as received: ibuprofen, ketoprofen (Sigma Chemical Co., St. Louis, MO), isopropyl alcohol, HPLC grade acetonitrile, monopotassium phosphate, disodium citrate, chloric acid, citric acid, disodium phosphate, dibasic sodium phosphate, phosphoric acid (J. T. Baker Chemical Co., Phillipsburg, NJ). Distilled, deionized water was prepared by the Milli Q system (Millipore Corporation, Bedford, MA). Shed snake skin was donated by the Sandy Creek Nature Center (Athens, GA).

2.2 DSC studies of binary mixture of ibuprofen and ketoprofen

Ketoprofen was mixed with ibuprofen at various weight ratios from 10:90 to 90:10 in the glass test tubes fixing the total weight at 100 mg. To achieve complete mixing, the mixtures were melted in the test tubes on the water bath. After vortexing for one minute, the melts were left in the refrigerator for three days. A spatula was used to blend the glassy melt to help intimate mixing and promote crystallization of the melts. Approximately 5.0 mg of each mixture was carefully sealed into aluminum sample pans for DSC analysis. A Perkin Elmer differential scanning calorimeter (Norwalk, CT) equipped with Perkin Elmer TAC 7/DX thermal analysis controller was used with carrier gas N₂ at a pressure of 20 *psi*. Thermograms were obtained at a heating rate of 1 °C/min

against an empty reference pan. The scanning range was between 40 and 100 °C. The integration of peak area, peak temperature, onset time, enthalpy (ΔH) and entropy (ΔS) of fusion of ibuprofen, ketoprofen and their binary eutectic were either recorded using the Pyris software package or calculated ($\Delta G = \Delta H - T\Delta S$).

2.3 XRPD studies of binary eutectic of ibuprofen and ketoprofen

Ibuprofen (400 mg) was mixed with ketoprofen (600 mg) in a test tube, and the mixture was then heated in a water bath. After melting, the mixture was vortexed for one minute. After congealing in the refrigerator for three days, the solid eutectic was crushed into fine particles by mortar and pestle and mixed well using a spatula. An appropriate amount of the powder mixture was loaded onto glass sample holder and subjected to X-ray powder diffractometry. Pure ibuprofen and ketoprofen were loaded on the glass sample holders as received without further processing. The X-ray powder diffractograms of pure ibuprofen, ketoprofen and their binary eutectic were obtained by a Scintag XDS 2000TM diffractometer (Scintag Inc., Cupertino, CA) with Co-K α radiation. The data were collected at the step scan rate of 0.06 ° min⁻¹ with a step size of 0.03 ° over a 2θ range of 2 – 50°. A synthesized XRPD pattern was generated from the original XRPD data of ibuprofen and ketoprofen by using Microsoft Excel (Office 2000, Microsoft) program.

2.4 Membrane permeation studies

The *in vitro* permeation rates of ibuprofen and ketoprofen and their binary eutectic mixture in the select preparations were determined using shed snake skin as a model membrane. A whole piece of skin was cut into small circular pieces of approximately 2.5 cm in diameter. The skin samples, which were left in the distilled water for 30 min to allow for complete hydration, were carefully mounted onto Franz diffusion cells with the stratum corneum side facing the donor compartment. The following preparations were used to compare the permeation rates: ibuprofen (40 mg), ketoprofen (60 mg) and binary eutectic mixture, which contained 40 mg of ibuprofen and 60 mg of ketoprofen, were dissolved separately in 2 ml of 50 % of IPA solution containing citrate buffer (pH 4.0) to obtain Preparations I, II and III, respectively, which were three unsaturated aqueous IPA solution with the same drug concentration. 40 mg of ibuprofen, 60 mg of ketoprofen and 100 mg of the binary eutectic mixture of these two drugs were put separately into 1 ml of citrate buffer (pH 4.0). Then minimum amounts of IPA were used to convert the solid drugs in the suspensions into liquid after vigorous vortexing and saturated aqueous IPA Preparations IV, V and VI with the maximum thermodynamic activity were obtained. Ibuprofen (40 mg), ketoprofen (60 mg) and binary eutectic mixture (100 mg) were suspended into 1.0 ml of buffer (pH 4.0) and saturated aqueous Preparations VII, VIII and IX, which also had the maximum thermodynamic activity of drugs, were obtained. Each of these preparations was applied to the skin surface and the donor compartments were covered with Parafilm® (American National Can, Neenah, WI) to avoid evaporation of the vehicle. The receptor

compartments were filled with 0.05 M phosphate buffer (pH 7.4) and were maintained at 32 °C by circulating water from a thermostat pump (Haake, Model F4391, Berlin, Germany). The receiver phase was continuously stirred at 300 rpm using a star head magnetic stirring bar. The effective diffusion area of the skin was 2.0 cm², and the volume of the receptor compartment was 6.0 cm³. Each test was replicated three times. During 8 hrs of the diffusion test, 200 µl of the receptor phase was periodically transferred into HPLC autosampler vials using a micro-syringe, and immediately replaced with fresh buffer solution. After the sample was taken, 20 µl of the internal standard (pentobarbital acid solution) and 1.0 ml of 20% ACN solution were placed into the HPLC vials and vortexed. Steady state flux, J_{ss} (µg/cm²/hr), values for ibuprofen and ketoprofen, were calculated using Fick's first law: $J_{ss} = \Delta M / S \Delta t = D \cdot K \cdot C_d / h$ where S is the effective diffusion area (cm²); $\Delta M / \Delta t$ is the amount of drug penetrating through the membrane per unit time at steady state (µg/hr); D is the diffusion coefficient (cm²/hr) or diffusivity and $D = h^2 / 6 \cdot L$; K is the partition coefficient between vehicle and skin; h is the membrane thickness (cm) and L is the lag time (hr). One-way ANOVA test was performed by the SAS statistical package to determine significant differences of J_{ss} among the test preparations.

2.5 HPLC analysis of ibuprofen and ketoprofen

The Waters HPLC systems (Waters, Milford, MA) consisting of a Model 616 solvent delivery pump, a Model 600S controller, a Model 717plus autosampler equipped with a temperature-controlled rack, a photo-diode array UV detector, and a Millennium data station was used to collect and process the data. Ibuprofen, ketoprofen and the

internal standard (pentobarbital acid) were separated on a Waters C-18 analytical column (250 × 4.6 mm I.D., 5µm, Waters, Milford, MA) at ambient temperature. The mobile phase was 50:50 (v/v) acetonitrile : phosphate buffer (0.025 M, pH 2.0). The flow rate was set at 1.0 ml/min. Absorbance was monitored at 223 nm using a photo-diode array UV detector. The automated injection volume was 20 µl for each sample. Weekly calibrations using the peak height ratios of drugs over internal standard were obtained for different concentrations from 20 ng/ml to 2 mg/ml. Separation of the peaks of ibuprofen (7.6 min), ketoprofen (3.3 min) and the internal standard (2.3 min) were achieved within a 10 min run as shown in Figure 3.6.

3. Results and discussion

3.1 DSC studies of binary eutectic of ibuprofen and ketoprofen

Differential scanning calorimetry (DSC) is widely-used to determine the thermochemical properties of unknown mixtures or poorly characterized phases. The calorimeter equipped DSC instrument can accurately measure endothermic or exothermic heat flow of the sample undergoing a phase change, as well as, heat capacity of the sample. The DSC thermograms for the mixtures of ibuprofen and ketoprofen showed significantly depressed melting points (Figure 3.1) and clearly indicated the binary eutectic formation between the two compounds. The eutectic point appeared around 61 °C, while the pure forms of ibuprofen and ketoprofen melted at 74 °C and 94 °C, respectively. The binary mixtures produced two endothermic peaks, the first one with a lower melting range of 58 – 61 °C, where the initial melting of the binary eutectic occurred. In the phase diagram, this point is called the temperature of *solidus*. The second

peak known as the temperature of *liquidus* appeared at different positions according to different weight ratios of the drugs and was wider than the first peak, as shown in Figure 3.1. The mixtures composed of ibuprofen and ketoprofen at weight ratios between 40:60 and 60:40 showed one single merged peak, which represented the eutectic melting point. When the peak of *solidus* merged with the peak of *liquidus*, the apex of the merged peak was somewhat higher than the apex of *solidus* because of merging of the two peaks and therefore up-shifting of the peak apex. Therefore, the temperature corresponding to the merged peak was a little bit higher than the temperature corresponding to the peak of *solidus*. The thermodynamic data obtained from DSC and calculation ($\Delta G = \Delta H - T\Delta S$) are presented in Table 3.1. The enthalpy and entropy of fusion values of the binary eutectic were significantly lower than those of the pure ibuprofen and ketoprofen.

Combining Equations (1) and (2) shown earlier, the following Equation (5) is obtained and the flux of a drug through the membrane can be estimated if each of the parameters is substituted in the equation:

$$\log J_m = \log(D_0/h) - (\beta/2.303)v + \log \rho - \log \left\{ 1 - \frac{M_1}{M_w} + \exp\left[\frac{\Delta S_f}{RT}(T_m - T)\right] \frac{M_1}{M_w} \right\} \quad (5)$$

Equations (1), (2) and (5) show that, with other conditions being equal, the lower the melting point (T_m), the higher the solubility (S_{ideal}) in skin lipids, and thus the higher the flux (J_m) of drug through the skin. Eutectic formation is an effective way to depress the melting point of drug without changing its chemical property, and thus can enhance its membrane transport. If the depressed melting point of drug in the eutectic, the solubility of drug in skin lipids, and the flux of drug through the skin are denoted as T_m' , S_{ideal}' and J_m' , respectively, Equation (6) can be derived from Equation (2) or (3):

$$\log(J_m'/S_{ideal}') = \log(J_m/S_{ideal}) \quad (6)$$

Thus, the increases of flux offered by the eutectic system over the individual drugs can be calculated using Equation (7):

$$\frac{J_m'}{J_m} = \frac{S_{ideal}'}{S_{ideal}} = \frac{\frac{M_w}{M_1} - 1 + \exp\left[\frac{\Delta S_f}{RT}(T_m - T)\right]}{\frac{M_w}{M_1} - 1 + \exp\left[\frac{\Delta S_f'}{RT}(T_m' - T)\right]} \quad (7)$$

It is difficult, however, to accurately measure the average molecular weight of skin lipids (M_l) due to their molecular complexity. Therefore, in this study, the average molecular weight was estimated using the percentages of different lipids and their molecular weights known for the human stratum corneum (Moghimi et al., 1999) as shown in Table 3.2. The average molecular weight thus obtained was 604.6. Equation (7) was then used to predict the changes of drug solubility in skin lipids and fluxes from the eutectic system over the individual drugs after substituting the experimental thermodynamic data and molecular weights into Equation (7). For ibuprofen, J_m'/J_m was found to be 3.64, suggesting that the flux of ibuprofen through the stratum corneum could be increased 3.64 - fold if the melting points of the drugs were depressed by eutectic formation as shown in Figure 3.1. For ketoprofen, J_m'/J_m of 3.74 was obtained, suggesting that the flux of this drug could increase by 3.74 - fold.

In addition, the changes of steady state fluxes of drugs in the eutectic system can also be estimated using Equation (4). Based on the melting temperature-membrane transport (MTMT) concept theory, if the solubility of the drug in mole fraction, and the

enthalpy of fusion in the eutectic system are denoted as X' and $\Delta H'$, respectively,

Equation (8) can be obtained from Equation (4):

$$\ln X' - \ln X = \ln \frac{X'}{X} = \frac{\Delta H}{R} \left(\frac{T_m - T}{T \cdot T_m} \right) - \frac{\Delta H'}{R} \left(\frac{T_m' - T}{T \cdot T_m'} \right) \quad (8)$$

Thus, the ratio of the flux increased can be expressed as:

$$\frac{J_m'}{J_m} = \frac{X'}{X} = \exp \left\{ \frac{1}{R} \left[\Delta H \cdot \left(\frac{1}{T} - \frac{1}{T_m} \right) - \Delta H' \cdot \left(\frac{1}{T} - \frac{1}{T_m'} \right) \right] \right\} \quad (9)$$

Equation (9) can be used to predict the ratio of drug solubility (X'/X) in skin lipids and the ratio of drug fluxes (J_m'/J_m), if relevant thermodynamic data are known. For ibuprofen, J_m'/J_m of 2.59 was obtained from the above equation after substituting the thermodynamic data obtained from the DSC studies, suggesting that its flux through the stratum corneum would be increased by 2.59 - fold. Using the same equation, J_m'/J_m of 2.78 was obtained for ketoprofen. The difference in the predicted values between Equations (7) and (9) could be attributed to the fact that the Equation (9), based on the MTMT theory, did not take into consideration of the molecular weights of the permeant (M_w) and skin lipids (M_l) as Equation (7) did.

3.2 XRPD studies of binary eutectic of ibuprofen and ketoprofen

In XRPD, the crystalline unit-cell edge length in a powdered microcrystalline sample can be determined. The tiny crystals in the sample have random orientation and, for any given set of planes, some of the tiny crystals will be oriented at the value of θ that satisfies the Bragg equation, and a Bragg reflection can be obtained from each of the planes. The X-rays reflected from a plane makes an angle 2θ with the direction of the

incident beam, so the diffraction angles are readily measured to give a distinct diffraction pattern for the crystalline substance measured. The same crystalline substance always gives the same pattern, while in a mixture of substances, each produces its own pattern independent of the others. Therefore, the X-ray diffraction pattern of a substance is like its own fingerprint. The obtained XRPD patterns of ibuprofen, ketoprofen and their binary eutectic are shown in Figures 3.2 - 3.4, respectively. If the binary eutectic of ibuprofen and ketoprofen formed a new compact structure with organized crystal lattices, the X-ray crystallography will show a distinct XRPD pattern from that of both ibuprofen and ketoprofen. If the binary eutectic is only a physical mixture without forming a new crystal structure, the XRPD pattern will be simply the addition of those of ibuprofen and ketoprofen. To achieve better resolution, Co- K_{α} radiation, rather than Cu- K_{α} radiation, was used as the energy source.

The original XRPD data of ibuprofen and ketoprofen were processed with Excel software to obtain the synthesized XRPD as shown in Figure 3.5; thus was basically the sum of the signals of ibuprofen and ketoprofen at the corresponding diffraction range. The signal intensity (CPS) was calculated as the sum of 40% of the intensity of ibuprofen and 60% of the intensity of ketoprofen, according to their weight ratio in the binary eutectic mixture. The peak around 7.5 degree in the synthesized XRPD was found to be two overlapping peaks after magnification. Therefore, the XRPD pattern of the binary eutectic is simply the addition of the diffractogram of ibuprofen to that of ketoprofen without any major proprietary peaks. In other words, in this eutectic mixture, ibuprofen molecules have only weak interaction with ketoprofen molecules without forming new crystal lattices. However, the weak forces interacting between ibuprofen and ketoprofen

interrupted the regular crystal lattices of both drugs and caused the lattices to be weaker than in crystals of the pure drugs. The decreased lattice energy of these crystals was responsible for decreased melting points of the compounds. At the proper weight ratio, the binary mixture exhibited the lowest melting point, called the eutectic point of these compounds. This phenomenon was clearly observed from the DSC thermogram shown in Figure 3.1.

3.3 Membrane permeation studies

In order to determine the effect of the melting point depressions of drugs in binary eutectics on membrane permeation, the unsaturated and saturated preparations of ibuprofen, ketoprofen and their binary eutectics were compared in permeation studies using shed snake skin as the model membrane. The permeation profiles of ibuprofen and ketoprofen are shown in Figures 3.7 and 3.8, respectively. The steady state flux and diffusivity were calculated from Fick's first law and are shown in Table 3.3.

The flux of ibuprofen from the unsaturated aqueous IPA Preparation I was 12.9 $\mu\text{g}/\text{cm}^2/\text{hr}$. The flux of ketoprofen from the unsaturated aqueous IPA Preparation II was 9.8 $\mu\text{g}/\text{cm}^2/\text{hr}$, while Preparation III, the unsaturated aqueous IPA solution of binary eutectic, gave higher fluxes of 20.0 $\mu\text{g}/\text{cm}^2/\text{hr}$ for ibuprofen and 15.1 $\mu\text{g}/\text{cm}^2/\text{hr}$ for ketoprofen. Therefore, the fluxes of ibuprofen and ketoprofen in the solution of the binary eutectic increased 1.55 and 1.54 - fold, respectively, compared with those in the solutions of pure drugs at the same donor concentration. The fluxes of ibuprofen and ketoprofen from the saturated aqueous IPA Preparations IV and V were 16.3 and 12.0

$\mu\text{g}/\text{cm}^2/\text{hr}$, respectively. Similarly, the saturated aqueous IPA Preparation VI of the binary eutectic showed higher permeation rates of both ibuprofen and ketoprofen, which were 38.8 and 33.9 $\mu\text{g}/\text{cm}^2/\text{hr}$, respectively. The fluxes of ibuprofen and ketoprofen in Preparation VI increased 2.38 and 2.83 - fold, respectively, as compared to those obtained from the saturated aqueous IPA solutions of pure drugs with the same thermodynamic activity. The fluxes of ibuprofen and ketoprofen from the saturated aqueous Preparations VII and VIII were 4.6 and 3.2 $\mu\text{g}/\text{cm}^2/\text{hr}$, respectively, while the saturated aqueous Preparation IX of the binary eutectic mixture showed higher fluxes of both ibuprofen and ketoprofen, which were 10.1 and 8.3 $\mu\text{g}/\text{cm}^2/\text{hr}$, respectively. Therefore, the fluxes of ibuprofen and ketoprofen in Preparation IX increased 2.20 and 2.59 - fold, respectively, as compared to those obtained from the saturated aqueous solution of pure drugs. The flux values, which were compared between the different preparations (I and II to III; IV and V to VI; VII and VIII to IX), were statistically different ($n = 3$, $P < 0.05$) using one-way ANOVA performed by SAS statistical package.

Based on the first proposed mathematical models as shown in Equation (7), the fluxes of ibuprofen and ketoprofen were predicted to increase by 3.64 and 3.74 - fold, respectively. However, the increases of fluxes (Table 3.4) obtained from the experiments shown above were smaller than those predicted values. In the calculation of the predicted fluxes, the known values of percentages and molecular weights of human skin lipids were substituted instead of those of snake skin. The observed difference might be attributed to difference in snake skin and human stratum corneum, although it was shown that the structure, composition, lipids content, water permeability of snake skin is similar to those of human skin, and that snake skin could be used as a good model membrane (Itoh and

Rytting, 1990. Higuchi and Konishi, 1987). Based on the second mathematical model shown in Equation (9), which was derived from the MTMT theory, the predicted increase of fluxes for ibuprofen and ketoprofen were 2.59 and 2.78 - fold, respectively. These values were very close to the experimental values obtained from the saturated preparations of the binary eutectic, which were 2.38 and 2.83 - fold for saturated IPA Preparation VI; 2.20 and 2.59 - fold for saturated aqueous Preparation IX. However, the unsaturated solutions of Preparation III with the same drug concentration as Preparation I and II showed much lower increases, which were only 1.55 and 1.54 - fold, respectively. This was due to the fact that thermodynamic activities of drugs in unsaturated Preparations I, II and III, which were unproportionally lower than those in saturated preparations. Therefore, the proposed models shown above were more applicable to predict the changes of the potential maximal flux of drug under the condition of maximum thermodynamic activity, than when the donor drug concentrations were the same. Although Equation (9) predicted the fluxes more precisely than Equation (7), both models correctly predicted the increase of fluxes of the compounds due to their reduced melting points by eutectic formation. The results obtained thus confirmed the validity of the proposed mathematical models, which demonstrated that the lower the melting point of drug, the higher the lipids solubility and thus the higher the permeation rate of the compound through the skin.

4. Conclusions

The study showed that the melting points of ibuprofen and ketoprofen were mutually depressed by eutectic formation, with reduced enthalpy and entropy of fusion of the drugs in the binary eutectic. The binary eutectic did not form a new crystalline structure as indicated in XRPD patterns. The two proposed mathematical models based on the ideal solution theory correctly predicted the increases of the steady state fluxes of these drugs as a result of melting point depression. The experimentally determined flux values confirmed the enhancement of the membrane permeation of these drugs as predicted by the models. The study suggested that the preparation based on binary eutectic could be used to develop transdermal formulations for enhanced drug delivery of ibuprofen and ketoprofen.

References

Adela, A., Nyqvist-Mayer, Brodin, A. F., Frank, S. G., 1985. Phase distribution studies on an oil-water emulsion based on eutectic mixture of lidocaine and prilocaine as the dispersed phase. *J. Pharm. Sci.* 74: 1192-1195.

Brodin, A., Nyqvist-Mayer, A., Wadsten, T., Forslund, B. and Broberg, F., 1984. Phase diagram and aqueous solubility of the lidocaine-prilocaine binary system. *J. Pharm. Sci.* 73: 481-484.

Calpena, A. C., Blanes, C., Moreno, J., Obach, R., Domenech, J., 1994. A comparative in vitro study of transdermal absorption of anti-emetics. *J. Pharm. Sci.* 83: 29-33.

Centers for Disease Control and Prevention (CDC), National Center for Chronic Disease Prevention and Health Promotion, Atlanta, GA, USA. The National Arthritis Action Plan: A Public Health Strategy (NAAP), 2002

Chlud K. Percutaneous Therapy of Painful Osteoarthritis. *Therapeutische Umschau* 48 (1): 42-45 JAN 1991

Ford, J. L., Timmins, P., 1989. *Pharmaceutical thermal analysis*. New York, John Wiley and Sons pp. 47-67.

Grant, D., Abougela, I., 1982. Physico-chemical interactions in pharmaceutical formulations. *Anal. Proc.* 19: 545-549.

Higuchi, T., Konishi, R., 1987. In vitro testing and transdermal delivery, *Therap. Res.*, (6): 280-288

Itoh, T., Rytting, J. H., 1990. Use of shed snake skin as a model membrane for in vitro percutaneous penetration studies: comparison with human skin, *Pharmaceutical Research*, (7): 1042-1047

Lawrence, R. C., Helmick, C. G., Arnett, F. C., 1998. Estimates of the Prevalence of Arthritis and Selected Musculoskeletal Disorders in the United States. *Arth. Rheum.* 41: 778-799.

Moghimi et al., 1999. Stratum corneum and barrier performance. *Percutaneous absorption.* 518-522.

Kasting, G. B., Smith, R. L., Cooper, 1987. E. R. Effects of lipid solubility and molecular size on percutaneous absorption. *Pharmacol. Skin* 1: 138-153.

Rovensky J, Micekova D, Gubzova Z, Fimmers R, Lenhard G, Vogtle-Junkert U, Schreyger F. Treatment of knee osteoarthritis with a topical non-steroidal antiinflammatory drug. Results of a randomized, double-blind, placebo-controlled study

on the efficacy and safety of a 5% ibuprofen cream. *Drugs under Experimental and Clinical Research*. 27 (5-6): 209-221 2001

Touitou, E., Chow D. D., Chaw J. R., Chiral β -blockers for transdermal delivery. *Int. J. Pharm.* 104: 19-28 1994.

Vaile JH, Davis P. Topical NSAIDs for musculoskeletal conditions - A review of the literature. *Drugs* 56 (5): 783-799 NOV 1998

Valenta C, Wanka M, Heidlas J. Evaluation of novel soya-lecithin formulations for dermal use containing ketoprofen as a model drug. *Journal of Controlled Release* 63 (1-2): 165-173 JAN 3 2000

Table 3.1. Thermodynamic data of ibuprofen, ketoprofen and their binary eutectic (n = 4)

Drug	Ibuprofen	Ketoprofen	Binary eutectic
Melting point (K)	347.6 ± 0.46	366.3 ± 0.88	335.2 ± 1.78
Enthalpy (kJ/mol)	25.3 ± 0.15	20.3 ± 0.17	11.3 ± 0.26
Entropy (J/K/mol)	72.8 ± 0.39	55.5 ± 0.48	33.7 ± 0.81

Table 3.2. Composition¹ (weight percentage) and molecular weights (MW) of human stratum corneum lipids

Constituents	Weight Percentage (%)	MW	Average MW in skin lipid
Ceramide 1	14	1011	141.5
Ceramide 2	4.3	649	27.9
Glucosylceramides	Trace	N/A	N/A
Stearic acid	1.9	284.5	5.4
Palmitic acid	7.0	256.5	18.0
Myristic acid	0.7	228.4	1.6
Oleic acid	6.3	282.5	17.8
Linoleic acid	2.4	280.5	6.7
Palmitoleic acid	0.7	254.4	1.8
Other fatty acids	< 0.1	N/A	N/A
Cholesterol	14	386.7	54.1
Cholesteryl sulphate	1.5	466.7	7.0
Sterol/wax esters	5.4	400	21.6
Di- and triglycerides ²	25	885.4	221.4
Squalene	4.8	410.7	19.7
n-Alkanes	6.1	352	21.5
Phospholipids	4.9	787	38.6
Total	100	N/A	604.6

¹ Moghimi et al., 1999

² Triolein is used to estimate di- and triglycerides.

Table 3.3. Steady state fluxes (J_{ss}) of ibuprofen and ketoprofen through the skin (n = 3)

Preparation	J_{ss} of ibuprofen ($\mu\text{g}/\text{cm}^2/\text{hr}$)	J_{ss} of ketoprofen ($\mu\text{g}/\text{cm}^2/\text{hr}$)
I	12.9	N/A
II	N/A	9.8
III	20.0	15.1
IV	16.3	N/A
V	N/A	12.0
VI	38.8	33.9
VII	4.6	N/A
VIII	N/A	3.2
IX	10.1	8.3

Table 3.4. Increases of fluxes (- fold) of ibuprofen and ketoprofen

Drug	Unsaturated IPA solution	Saturated IPA solution	Saturated aqueous solution	Theoretical (Equation 7)	Theoretical (Equation 9)
Ibuprofen	1.55	2.38	2.20	3.64	2.59
Ketoprofen	1.54	2.83	2.59	3.74	2.78

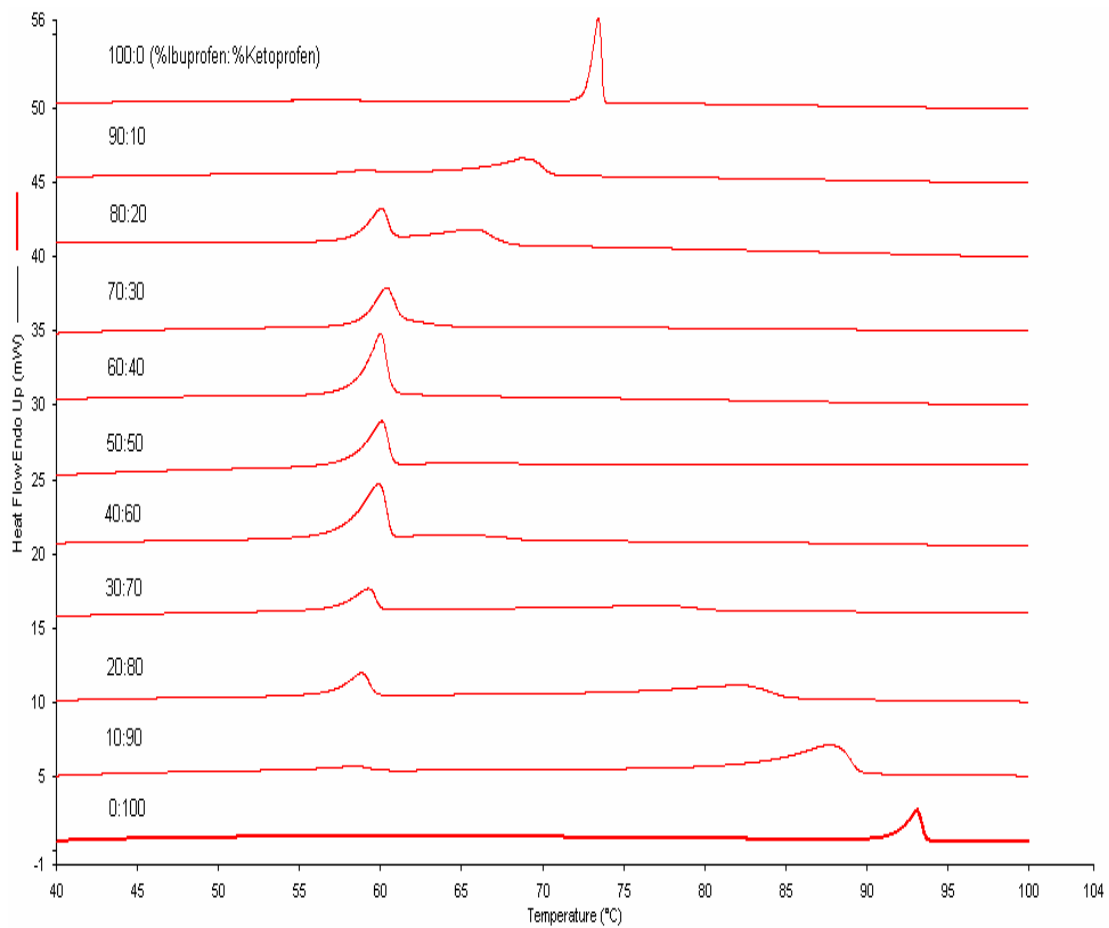


Figure 3.1. DSC diagram of binary mixtures of ibuprofen with ketoprofen

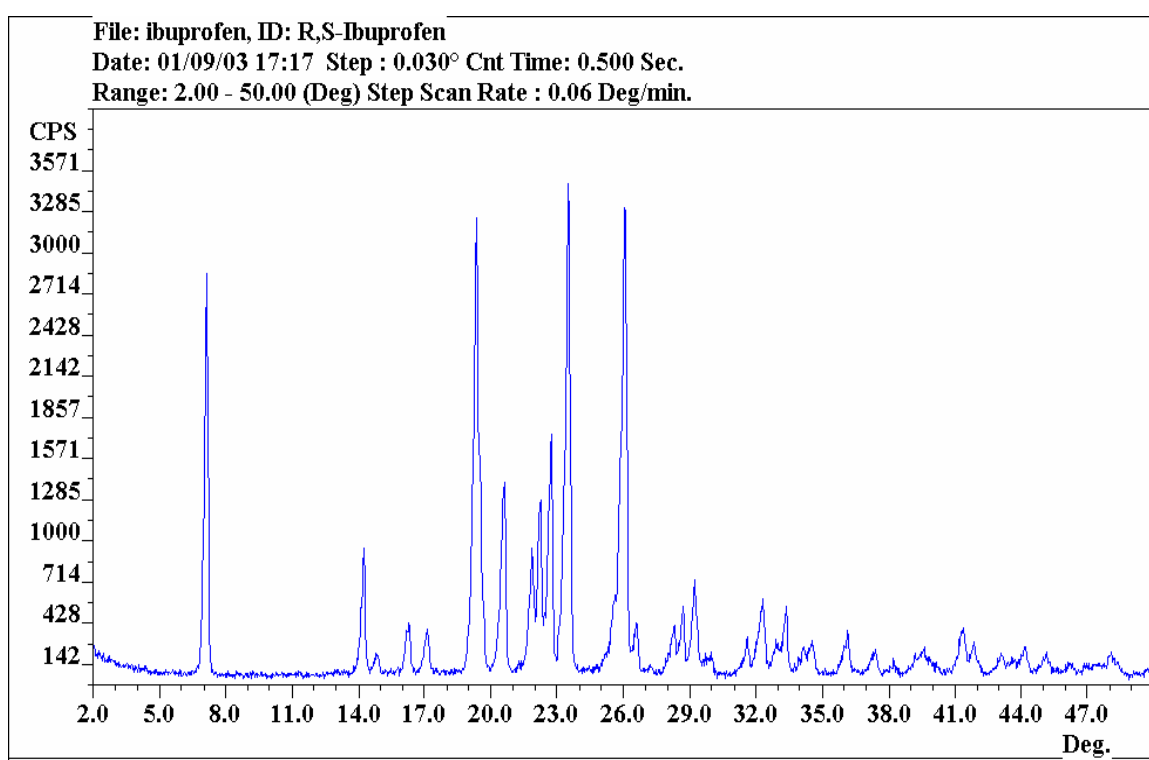


Figure 3.2. X-ray powder diffraction of pure ibuprofen

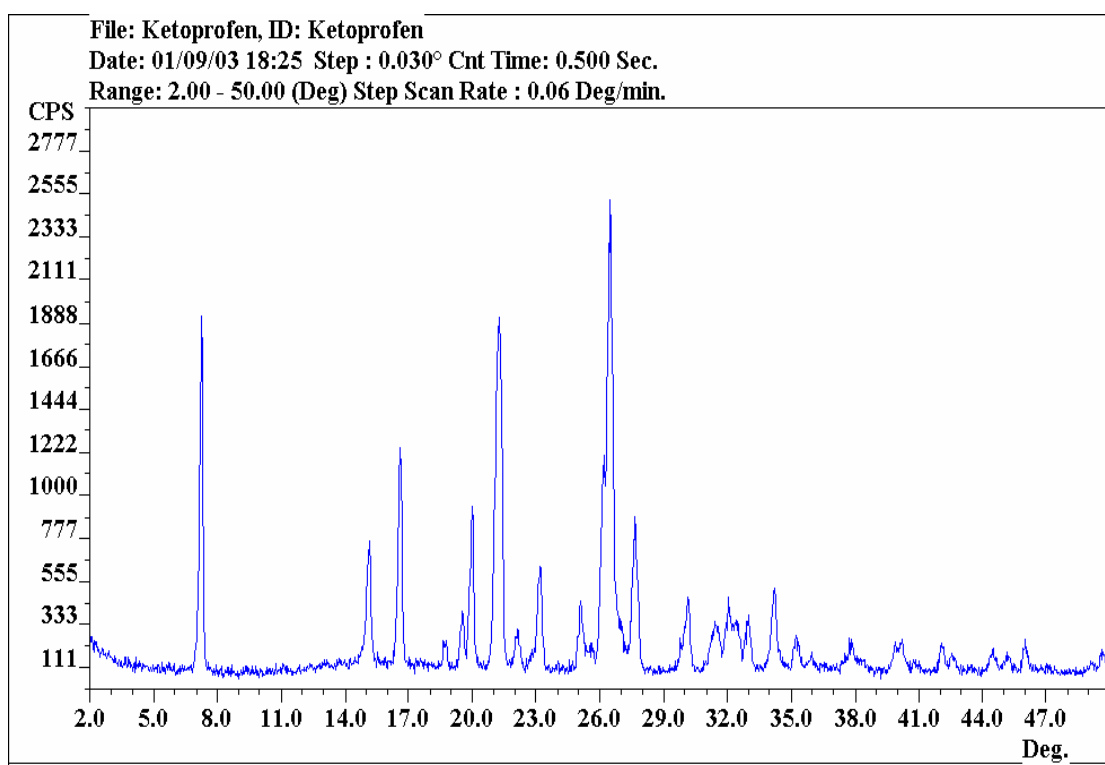


Figure 3.3. X-ray powder diffraction of pure ketoprofen

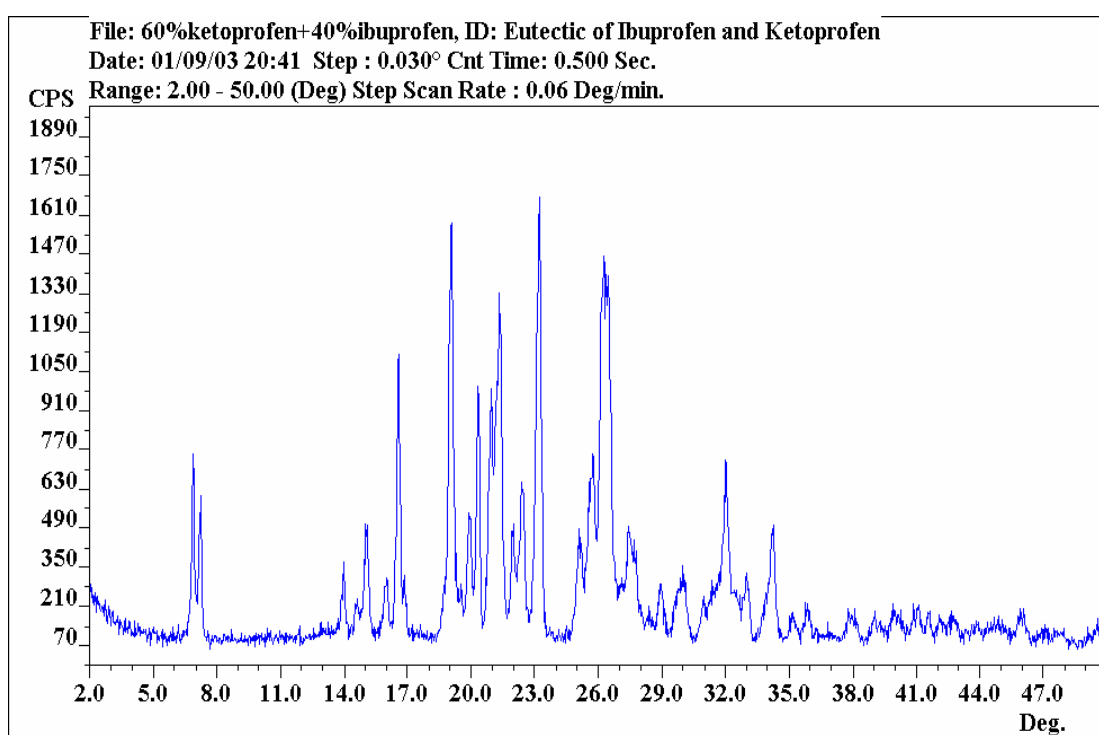


Figure 3.4. X-ray powder diffraction of the binary eutectic of ibuprofen and ketoprofen

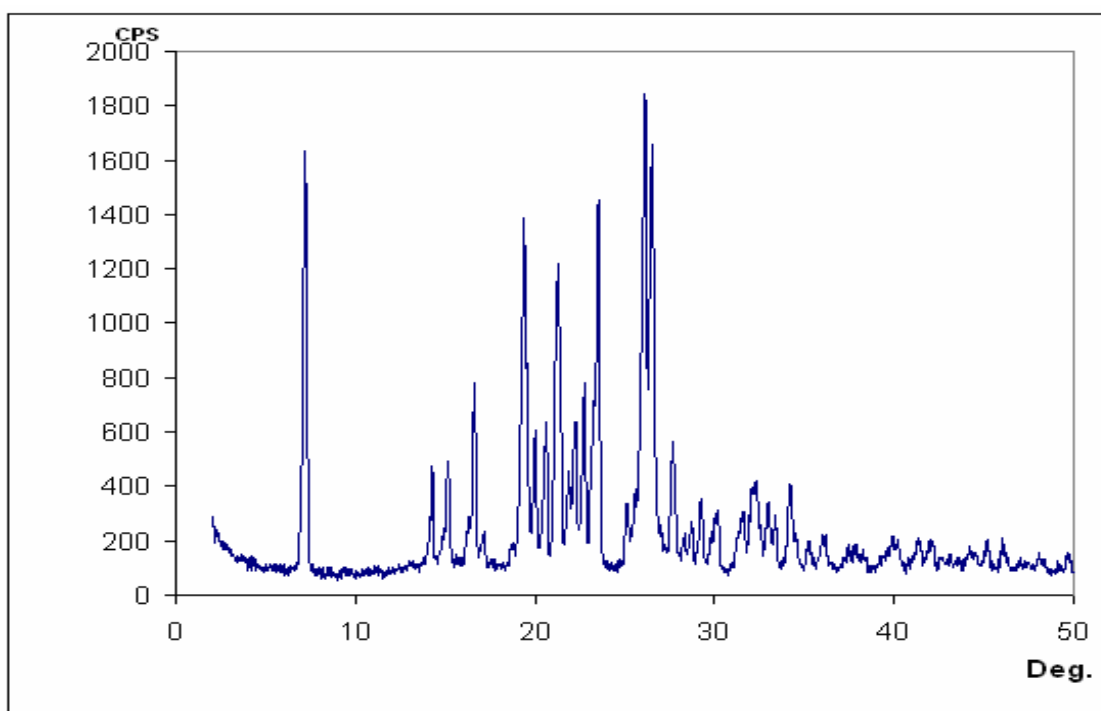


Figure 3.5. Synthesized XRPD pattern from the original XRPD data of ibuprofen (40%) and ketoprofen (60%)

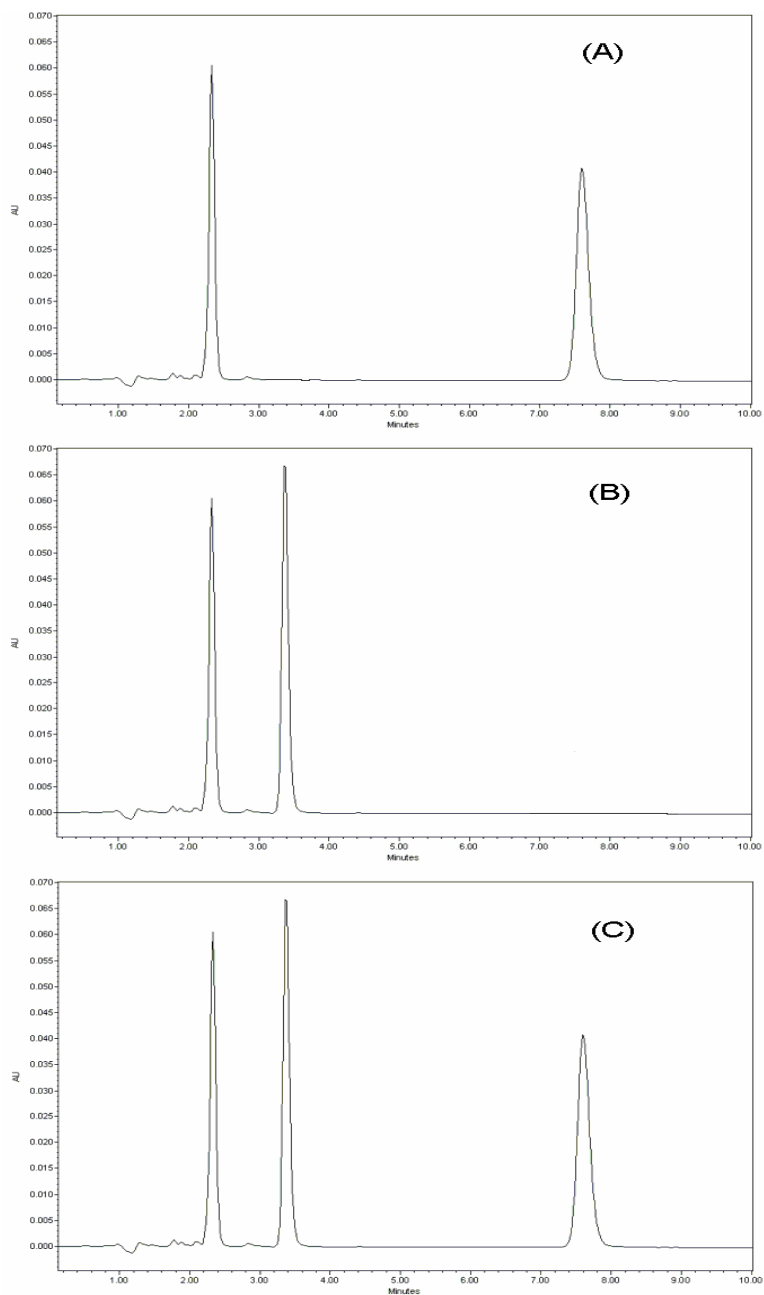


Figure 3.6. HPLC profiles (A) Ibuprofen (7.6 min) and internal standard (2.3 min); (B) Ketoprofen (3.3 min) and internal standard (2.3 min); (C) Ibuprofen, Ketoprofen and internal standard (2.3 min)

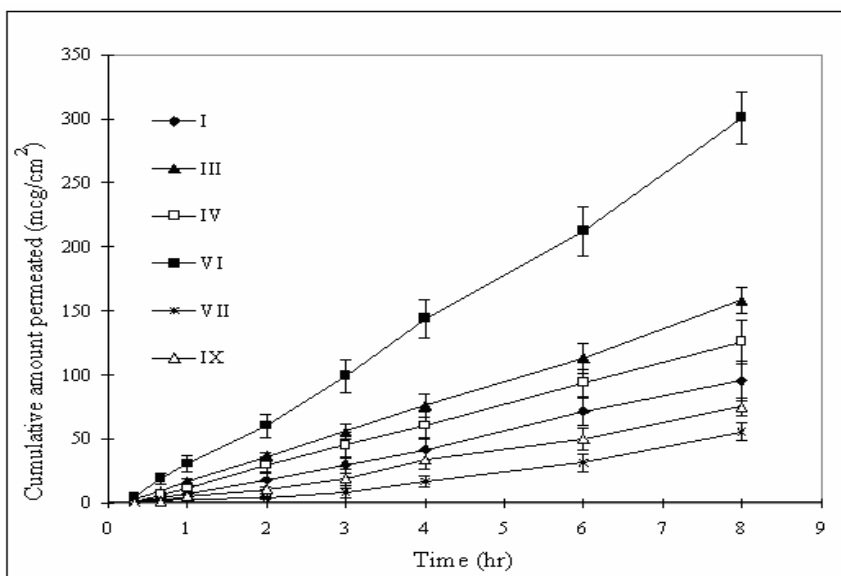


Figure 3.7. Permeation profiles of ibuprofen through shed snake skin (n = 3, error bar = SD)

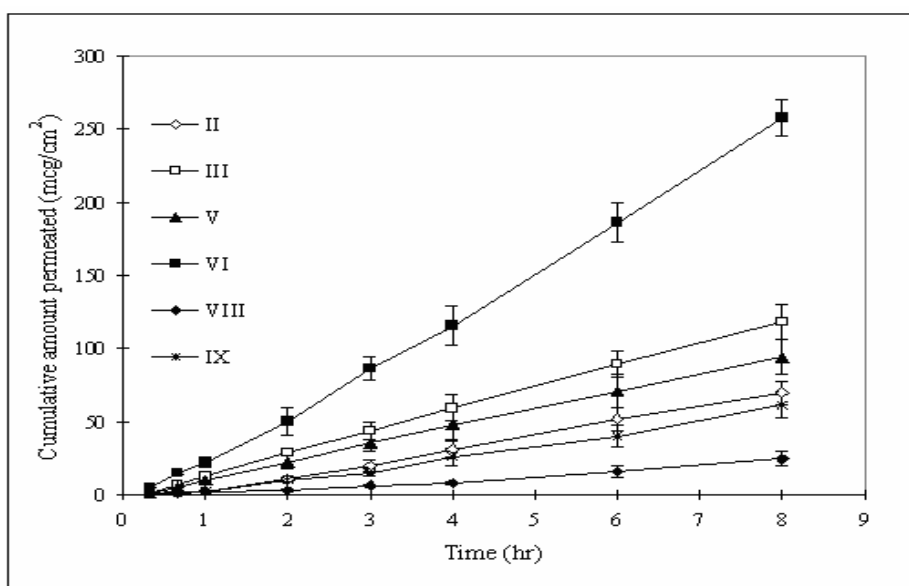


Figure 3.8. Permeation profiles of ketoprofen through shed snake skin (n = 3, error bar = SD)

CHAPTER 4

THE PERMEATION AND STABILITY OF IBUPROFEN AND KETOPROFEN IN BINARY EUTECTIC TWO-PHASE LIQUID SYSTEM

Yuan, X., Capomacchia, A.C. To be submitted to the Journal of Pharmaceutical
Development and Technology

Abstract

Ibuprofen and ketoprofen formed a binary eutectic mixture at proper molar ratios, mutually depressing their melting points. The addition of aqueous isopropyl alcohol (IPA) to the mixture formed a two-phase liquid system consisting of an aqueous phase and an oily phase. The permeation rates of ibuprofen and ketoprofen in preparation of the two-phase liquid system were compared to those in reference preparations selected from the composite phase diagram using Franz diffusion cells and shed snake skin as the model membrane. Because the high concentration of the drugs in the oily phase, the preparation of the binary eutectic two-phase liquid system showed the highest permeation rates of both ibuprofen and ketoprofen among all the test preparations. In stability studies, the two-phase system was found to be physically stable and no degradation of drugs was observed after three-month storage at different temperatures.

Keywords: Ibuprofen; Ketoprofen; Eutectic; Two-phase liquid system; Permeation; Transdermal drug delivery.

1. Introduction

Arthritis is among the most prevalent and debilitating diseases in the world. In the U.S. alone, it was estimated that arthritis and related conditions affect over 40 million Americans, or about one of every six people. By 2020, as the baby boom generation ages, an estimated 60 million Americans will be affected by arthritis (Centers for Disease Control and Prevention, 2002). Ibuprofen and ketoprofen are some of the most widely used non-steroidal anti-inflammatory drugs (NSAIDs) and have been formulated to a number of topical preparations for the treatment of rheumatoid arthritis and related diseases (Lawrence et al., 1998). Topical preparations of NSAIDs offer several advantages over oral administration, which include avoidance of hepatic first-pass metabolism, reduction in side effects of gastric irritation, better patient compliance and potentially enhanced therapeutic efficacy. One of the most important factors that could affect the efficacy of dermal drug therapy is the intrinsic solubility of the drugs in skin lipids, which is also closely related to the melting point of drugs. It was shown that the lower the melting point, the higher skin solubility, therefore, the higher membrane permeation or flux in transdermal drug delivery (Calpena et al., 1994). Previous studies have shown that some solid drugs that can be transformed into an oily state by depressing their melting points below ambient temperature (25 °C) provided the maximum thermodynamic activity in the formulation and thus higher permeation rates (Brodin et al., 1984. Adela et al., 1985). A relationship between transdermal flux and melting point of the penetrant based on the ideal solution theory was proposed by Kasting (Kasting et

al., 1987) and used to calculate the ideal solubility, S_{ideal} , of the penetrant in skin lipids as shown below:

$$S_{ideal} = \frac{\rho}{1 - \{1 - \exp[\frac{\Delta S_f}{RT}(T_m - T)]\}} \frac{M_l}{MW} \quad (1)$$

where ρ is the density of skin lipids, M_l is the average molecular weight of skin lipids, MW is the molecular weight of penetrant, T_m is the melting point in degrees Kelvin, ΔS_f ($\Delta S_f = \Delta H_f / T_m$) is the entropy of fusion of penetrant and ΔH_f is the heat of fusion.

Therefore, if one can reduce the melting point of drug without causing unfavorable changes to other physicochemical parameters, the change can possibly improve the drug solubility in skin lipids and enhance transdermal flux. One of the methods by which the melting point of compounds can be reduced is by formation of a eutectic mixture (Grant et al., 1982; Ford et al., 1989). By definition, binary eutectic is a mixture of two compounds which do not interact with each other to form a new chemical entity, but which at certain ratios inhibit the crystallization process of the other compound, resulting in a lower melting point than either of the compounds.

In a previous study (Yuan et al. 2003), the melting points of ketoprofen and several other NSAIDs were shown to be significantly depressed in the presence of ibuprofen by forming a binary eutectic mixture. It was also shown that the eutectic mixture was spontaneously converted to a two-phase liquid system consisting of an aqueous and oily phase in the presence of aqueous isopropyl alcohol (aIPA). Preliminary data showed that ibuprofen and ketoprofen in the emulsion made from a two-phase liquid system gave higher membrane permeation rates than the saturated solution of either drug. In this more thorough study, sixteen preparations were selected from the phase diagram

to perform *in vitro* diffusion tests using shed snake skin as the model membrane. The physicochemical stability and concentration of drugs in the binary eutectic two-phase liquid system at different temperatures were also studied in the hope of developing stable transdermal formulations for these drugs.

2. Materials and methods

2.1 Materials

The following chemicals were obtained from commercial suppliers and used as received: ibuprofen, ketoprofen (Sigma Chemical Co., St. Louis, MO), isopropyl alcohol (IPA), HPLC grade acetonitrile, monopotassium phosphate, disodium citrate, citric acid, disodium phosphate, dibasic sodium phosphate, phosphoric acid (J. T. Baker Chemical Co., Phillipsburg, NJ) and Cremphor (BASF corporation, Mount Oliver, NJ). Distilled, deionized water was prepared by a Milli Q system (Millipore Corporation, Bedford, MA). Shed snake skin was donated by the Sandy Creek Nature Center (Athens, GA).

2.2 Preparations used in permeation studies

A phase diagram (Figure 4.1) was constructed for the binary mixtures of ibuprofen and ketoprofen in the presence of aqueous isopropyl alcohol. Basically, appropriate amounts of ibuprofen and ketoprofen were weighed and mixed at different weight ratios from 10:90 to 90:10 in test tubes, making the total weight as 100 mg. After

mixing with one ml of citrate buffer (0.05 M, pH 4.0), the suspension was titrated with IPA using a micro-syringe and vortexed until the solid particles were completely transformed into an oily phase, which was separated from the aqueous bulk phase. A microscopic examination confirmed the complete phase transition of the compounds. After vigorous mixing on a vortex, an emulsion was formed with the internal oily phase dispersed in the external aqueous phase. When the emulsion was further titrated with IPA, the oily phase was completely solubilized to become a homogeneous aqueous alcoholic solution. Due to the higher melting point of ketoprofen, the mixtures with over 90 % ketoprofen in suspension were transformed completely to clear homogeneous solution without forming the oily phase, and thereafter the two-phase liquid system as shown in Figure 4.1. To obtain the phase diagram of the system, the volumes of IPA used to completely transform crystals into oil or clear solution and to completely dissolve the oil into aqueous alcoholic phase were plotted against the IPA percentages (w/w) in the whole system. In order to find out the best preparation which offers the highest permeation rates of drugs, sixteen preparations including the binary eutectic two-phase liquid system (Preparation 2) were chosen from the phase diagram (Figure 4.1), and 0.5% of Cremphor was added as the surfactant into each one to compare the *in vitro* diffusion fluxes of these preparations. The select preparations, which are shown in Table 4.1 and denoted in Figure 4.1, comprised the saturated or unsaturated solution, suspension and two-phase liquid system of ibuprofen and ketoprofen at different ratios.

2.3 *In vitro* permeation study

The permeation rates of ibuprofen and ketoprofen from different preparations were studied using shed snake skin as the model membrane. A whole piece of skin was cut into small circular pieces with the size of approximately 2.5 cm in diameter that fit with the Franz diffusion cells. The skin was first placed into the distilled water for 30 min to allow for complete hydration, and then carefully mounted onto the diffusion cells with the outer stratum corneum side facing the donor compartment. Each of the test preparations was poured onto the skin surface and the donor compartments were covered with parafilm (American National Can, Neenah, WI) to avoid evaporation of the solvent. The receptor compartments of diffusion cells were filled with 0.05 M phosphate buffer (pH 7.4) and were maintained at 32 °C by circulating water from a thermostat pump (Haake, Model F4391, Berlin, Germany). The receiver phase was continuously stirred at 300 rpm using a star head magnetic stirring bar. The effective diffusion area of the skin was 2.0 cm², and the volume of the receptor compartment was 6.0 ml. Each test was replicated three times. During 8 hrs of the diffusion test, 200 µl of the receptor phase was periodically drawn using a micro-syringe and immediately replaced with fresh buffer solution. 20 µl of the internal standard solution containing pentobarbital acid and 1.0 ml of 20% ACN solution were added to the autosampler vial prior to HPLC analysis. The steady state fluxes, J_{ss} (µg/cm²/hr) of ibuprofen and ketoprofen were calculated using Fick's first law: $J_{ss} = \Delta M/S\Delta t$ where S is the effective diffusion area (cm²) and $\Delta M/\Delta t$ is the amount of drug penetrating through the membrane per unit time at steady state

($\mu\text{g/hr}$). One-way ANOVA test was performed using SAS statistical package to determine significant differences of J_{ss} among the different test preparations.

2.4 Stability studies of the binary eutectic two-phase liquid system

In the phase diagram shown in Figure 4.1, the eutectic system comprising of 40% ibuprofen and 60% ketoprofen formed a two-phase liquid system consisting of an oily phase and an aqueous phase in the presence of aqueous IPA (22.2%). In order to determine the concentration of the drugs in the binary eutectic two-phase liquid system and its physical stability, eighteen binary eutectic two-phase liquid systems were prepared. For each preparation, 80 mg ibuprofen and 120 mg ketoprofen were accurately weighed and transferred into a slender 10 ml test tube. 2.0 ml of citrate buffer (0.05 M, pH 4.0) and 800 μl of IPA were added. The suspension was vortexed until the solids were completely transformed into oily phase. The samples were centrifuged at 3000 rpm for one hour to render aqueous phase and oily phase completely separated. Three preparations were sealed in the tubes and stored at 25 °C, six at 5 °C, three at - 15 °C and six at 40 °C. The samples were examined regularly by the microscope to observe any crystal formation during the storage. After three months, nine samples, three each at different temperatures (5, 25 and 40 °C), were taken and subjected to HPLC analysis using the procedures described below. 500 μl of the aqueous phase of the two-phase liquid system was removed by syringe and transferred to a 5 ml volumetric flask. 20 % acetonitrile solution was added to the flask to make up the solution to the volume and mixed well. 200 μl of the solution was placed in the HPLC vial, then 1.0 ml of 20%

acetonitrile and 20 μ l of the internal standard solution were added prior to HPLC analysis. The samples left at -15 $^{\circ}$ C were not analyzed by HPLC due to the formation of crystals during the storage. The three samples left in the refrigerator (5 $^{\circ}$ C) and in the oven (40 $^{\circ}$ C) were removed and left at the room temperature for two days to allow for re-equilibration. After centrifuging the tubes, the aqueous phase solution was removed and subjected to HPLC analysis.

2.5 HPLC analysis of ibuprofen and ketoprofen

The Waters HPLC system (Waters, Milford, MA) consisted of a Model 616 solvent delivery pump, a Model 600S controller, a Model 717plus autosampler equipped with a temperature-controlled rack, a photo-diode array UV detector, and a Millennium data station. Ibuprofen, ketoprofen and internal standard pentobarbital acid were separated on a Waters C18 analytical column (250 \times 4.6 mm I.D., 5 μ m) at ambient temperature. The mobile phase was 50:50 (v/v) acetonitrile : sodium phosphate buffer (0.025 M, pH 2.0). The flow rate was set at 1.0 ml/min. Absorbance was monitored at 223 nm using a photo-diode array UV detector. The automated injection volume was 20 μ l for each sample. Separation of drugs by HPLC was achieved within a 10 min run and the chromatogram is shown in Figure 4.3, the retention time of ibuprofen, ketoprofen and internal standard (pentobarbital acid) were 7.6, 3.3 and 2.3 min, respectively. Weekly calibrations using the peak height ratios of drugs to internal standard were obtained for different concentrations from 20 ng/ml to 2 mg/ml.

3. Results and discussion

3.1 Preparations used in permeation studies

The phase diagram (Figure 4.1) of the binary mixture of ibuprofen and ketoprofen in the presence of aIPA showed a lower curve ABCD and an upper curve ACD, which represented the complete transformation of the drug crystals into the oily phase and the complete solubilization of the oily phase into the homogeneous aqueous phase, respectively. These two curves divided the phase diagram into the three regions. The lower region under the curve ABCD shows the area where some of the crystals of either ibuprofen or ketoprofen remained in the mixture. The middle region between the curves ABCD and ACD indicates the coexistence of the oily and aqueous phases. The upper region above ACD displays the region where only the homogeneous aqueous solution is formed due to the solubilization of the oily phase. The curve ABCD, which corresponds to the volume of IPA used to obtain the two-phase liquid system, shows the same pattern as the *liquidus* curve of the melting points of different mixtures of ibuprofen with ketoprofen in differential scanning calorimetry (DSC) thermogram (Figure 4.2) obtained from previous studies (Yuan et al. 2003). The lower the melting points of the binary mixtures in the DSC thermogram, the less IPA was required to solubilize the solid drugs. This phenomenon was probably due to fact that less enthalpy of solubilization was needed to solubilize the solid drug mixtures that exhibit lower melting points.

In order to compare the binary eutectic two-phase liquid system to other preparations and find out the best preparation which offers the highest permeation rates

of ibuprofen or ketoprofen, sixteen preparations were selected from the phase diagram (Figure 4.1) based on different weight ratios of ibuprofen and ketoprofen and percentage of IPA. The permeation rates of the all the test preparations were determined using HPLC and were transformed into response surface of 3-D mesh plot. As shown in Table 4.1 and Figure 4.1, Preparations 1 - 5 have the same drug ratio of ibuprofen to ketoprofen, therefore same amounts of ibuprofen (40 mg) and ketoprofen (60 mg) were used in order to compare the fluxes from those preparations directly. Preparations 6 - 9 have different amounts of drug ratio than these in Preparations 1 - 5. Since the amount of only one drug can be fixed as the same as in Preparations 1 - 5, 60 mg of ketoprofen was used in each one of Preparations 6 - 9, while various amounts of ibuprofen were used to change the ratios. Therefore, only the fluxes of ketoprofen in Preparations 6 - 9 were compared. For Preparations 10 - 16, the same amount of ibuprofen (40 mg) was used as in Preparations 1 - 5, while different amounts of ketoprofen were used to change the drug ratios accordingly. Preparation 16 is a saturated aIPA (35.0 %) solution using the same amount of ibuprofen as in Preparations 1 - 5 and 10 - 15, while Preparation 9 is a saturated aIPA (36.6 %) solution of the same amount of ketoprofen as used in Preparations 1 - 8. Preparations 6 and 15 have different amounts of drugs but have the same drug and IPA percentage, therefore they are denoted by the same point in the phase diagram as shown in Figure 4.1. Similarly, Preparations 8 and 12 also have the same drug and IPA percentage and are denoted by the same point.

3.2 *In vitro* permeation study

In order to identify the preparation that provides the highest permeation rates of ibuprofen and ketoprofen, the *in vitro* diffusion profiles of ibuprofen and ketoprofen from the sixteen preparations were determined using shed snake skin as the model membrane. This model was used in some previous studies (Kang et al., 2000; Kang et al., 2001; Itoh and Rytting, 1990; Higuchi and Konishi, 1987). The steady state fluxes of ibuprofen and ketoprofen listed in Table 4.1 were obtained from the data shown in Figures 4.4 – 4.5. Only the fluxes of ibuprofen or ketoprofen from the preparations containing the same amount of ibuprofen (40 mg) and ketoprofen (60 mg) were calculated and used to compare with the other preparations. The results showed that Preparation 2, made from the binary eutectic two-phase liquid system with aIPA, exhibited the highest permeation rates for both ibuprofen and ketoprofen. Due to lower melting point of the binary eutectic in the system, ibuprofen and ketoprofen had higher skin lipid solubility and therefore higher fluxes of the drugs. The maximum steady state fluxes of ibuprofen and ketoprofen from Preparation 2 were $37.8 \mu\text{g}/\text{cm}^2/\text{hr}$ and $33.3 \mu\text{g}/\text{cm}^2/\text{hr}$, respectively, while those of ibuprofen and ketoprofen from the saturated aqueous solution (Preparation 1) were $11.0 \mu\text{g}/\text{cm}^2/\text{hr}$ and $8.4 \mu\text{g}/\text{cm}^2/\text{hr}$, respectively. Comparing these two preparations, increases of 3.44 and 3.96 folds were observed for ibuprofen and ketoprofen, respectively. These increases could be attributed to a high drug concentration in the oily phase and a much higher drug concentration gradient established across the membrane. Preparation 3 had the same amounts of ibuprofen and ketoprofen as in Preparation 2, but contained a higher percentage (w/w) of IPA, which decreased the concentration of the drugs in the oily

phase, therefore showing a little lower permeation rates of ibuprofen and ketoprofen, which were 34.5 and 30.3 $\mu\text{g}/\text{cm}^2/\text{hr}$, respectively. But these differences between Preparation 2 and 3 were not statistically significant, since the P-values for ibuprofen and ketoprofen were 0.0614 and 0.0744, which were larger than the generally accepted significance level (0.05). The flux of ibuprofen from Preparation 16, the saturated aIPA solution of ibuprofen, was 17.2 $\mu\text{g}/\text{cm}^2/\text{hr}$, while that of ketoprofen in saturated aIPA solution (Preparation 9) was only 13.1 $\mu\text{g}/\text{cm}^2/\text{hr}$. Therefore, the membrane transport rates of ibuprofen and ketoprofen in the preparation made from the binary eutectic two-phase liquid system increased 2.2 and 2.54 fold, respectively, as compared to those from Preparations 16 and 9. The fluxes of ibuprofen and ketoprofen in Preparation 4 were 26.0 and 25.1 $\mu\text{g}/\text{cm}^2/\text{hr}$, respectively. Preparation 2 exhibited 1.45 and 1.33 fold increases in the fluxes of ibuprofen and ketoprofen, respectively, as compared to those measured in Preparation 4. The fluxes of ibuprofen and ketoprofen in Preparation 5, an unsaturated aIPA solution of binary eutectic system, were 19.2 $\mu\text{g}/\text{cm}^2/\text{hr}$ and 15.1 $\mu\text{g}/\text{cm}^2/\text{hr}$, respectively. Preparation 2 exhibited 1.97 and 2.21 fold increases in fluxes of ibuprofen and ketoprofen, respectively, as compared to those measured from Preparation 5. Although Preparation 4 and 5 have more IPA, which is a known permeation enhancer, Preparation 2 still showed higher permeation rates because of the higher concentration and higher thermodynamic activity of the drugs in the oily phase. Since Preparation 4 had higher thermodynamic activity than Preparation 5, which is an unsaturated aIPA solution, it showed higher permeation rates of ibuprofen and ketoprofen. The flux of ketoprofen in Preparation 8 was 30.7 $\mu\text{g}/\text{cm}^2/\text{hr}$, which is lower than that measured from Preparation 2. However, the difference was not statistically significant, since the P-value of 0.0812 was

larger than the significance level. The differences of the fluxes of ibuprofen and ketoprofen between Preparation 2 and all other preparations besides Preparation 3 and 8 were found to be statistically significant ($P < 0.05$) using one-way ANOVA performed by SAS statistical package as shown in Table 4.1.

The flux values of ibuprofen and ketoprofen are transformed to response surface in 3-D mesh plots as shown in Figures 4.6 and 4.7. From the relationship shown between the response surface of the permeation rates of drugs and percentage of drugs and IPA, It is obvious that Preparation 2 showed the highest permeation rates of both drugs in the 3-D mesh plots. In addition, Preparation 2 contained less IPA than other preparations except Preparation 1, which is also desirable for a topical formulation. Therefore, it can be concluded that Preparation 2, the emulsion made from the binary eutectic two-phase liquid system with the maximum thermodynamic activity and high drug concentration in the oily phase, resulted in the highest permeation of both ibuprofen and ketoprofen and thus could to be used as the best candidate in further formulation development for transdermal delivery of these drugs.

3.3 Stability studies of the binary eutectic two-phase liquid system

The drug concentrations in the oily and aqueous phases of the binary eutectic two-phase liquid system stored three months at different temperatures (5, 25, 40 °C) were analyzed by HPLC and are shown in Table 4.2. At the ambient temperature, the concentration of ibuprofen in the aqueous phase was 0.14 mg/ml, which was 0.40 % of the total ibuprofen added. Meanwhile, the concentration of this drug in the oily phase was

as high as 317.8 mg/ml, representing 99.60 % of the total ibuprofen in the system. The concentration of ketoprofen in the aqueous phase was 5.71 mg/ml, representing 11.42 % of the total ketoprofen added. The concentration of ketoprofen in the oily phase was 425.7 mg/ml, which was 87.68 % of ketoprofen added. The concentration of ketoprofen in the aqueous phase was higher than that of ibuprofen owing to the higher aqueous solubility of ketoprofen than that of ibuprofen. The weight percentage of ibuprofen in the oily phase was 30.50 %, while that of ketoprofen was 40.81 %. Therefore, the total weight percentage of the two drugs in the oily phase was 71.31 %. The remaining 28.69 % of the oily phase could consist of IPA, since the buffer added would be excluded out of the immiscible oily phase. When the temperature increased, the aqueous solubility of ibuprofen and ketoprofen were increased, therefore the concentration of the both drugs increased in the larger aqueous phase of two-phase liquid system, and as a result the percentages of the drugs decreased in the oily phase as shown in Table 4.2. The concentration of ibuprofen in the aqueous phase increased from 0.06 mg/ml at 5 °C to 0.37 mg/ml at 40 °C, while that in the oily phase dropped from 319.3 to 316.0 mg/ml. The concentration of ketoprofen in the aqueous phase increased from 4.09 to 13.81 mg/ml, while that in the oily phase dropped from 435.8 to 355.2 mg/ml. The total drug percentage in the oily phase also dropped from 73.19 to 63.74 %.

For all of the samples except those stored at – 15 °C, the two-phase liquid system remained physically stable after three months storage, and no re-crystallization were observed in both oily and aqueous phase. For the samples stored at – 15 °C, the crystal formation occurred due to the reduced solubility of the drugs at lower temperature. For the samples stored at 5, 25 and 40 °C, no impurity peaks appeared in the HPLC

chromatograms and no extra shoulder peaks were found in the 3-D spectrum of eluted peaks scanned by the photo-diode array detector. In addition, when the samples stored at 5 and 40 °C were left at the ambient temperature to re-equilibrate for three days prior to HPLC analysis, the concentration of drugs in the two phases reversed back to these as measured earlier at room temperature (Table 4.3). Since no impurities were found in the HPLC chromatograms and the drug concentrations did not change, there was no degradation of drugs in the two-phase liquid system after being stored for three months at different temperatures. These results suggested that the binary eutectic two-phase liquid system was stable for further development of topical formulations.

4. Conclusion

The preparation of the binary eutectic two-phase liquid system significantly improved the permeation of both ibuprofen and ketoprofen across the model membrane and showed the highest permeation rates among all test preparations selected from the phase diagram. The enhanced permeation was attributed to the lower melting point of the binary eutectic, maximum thermodynamic activity and high concentration of drugs in the oily phase of two-phase liquid system. In stability studies, the two-phase liquid system was shown to be stable at different temperatures and no impurities or degradation was observed after three-month storage. These results suggested that the binary eutectic two-phase liquid system could be used to develop an optimal formulation for the enhanced transdermal delivery of ibuprofen and ketoprofen.

References

Adela, A., Nyqvist-Mayer, Brodin, A. F., Frank, S. G., 1985. Phase distribution studies on an oil-water emulsion based on eutectic mixture of lidocaine and prilocaine as the dispersed phase. *J. Pharm. Sci.* 74: 1192-1195.

Brodin, A., Nyqvist-Mayer, A., Wadsten, T., Forslund, B. and Broberg, F., 1984. Phase diagram and aqueous solubility of the lidocaine-prilocaine binary system. *J. Pharm. Sci.* 73: 481-484.

Calpena, A. C., Blanes, C., Moreno, J., Obach, R., Domenech, J., 1994. A comparative in vitro study of transdermal absorption of anti-emetics. *J. Pharm. Sci.* 83: 29-33.

Centers for Disease Control and Prevention (CDC), National Center for Chronic Disease Prevention and Health Promotion, Atlanta, GA, USA. The National Arthritis Action Plan: A Public Health Strategy (NAAP), 2002

Ford, J. L., Timmins, P., 1989. *Pharmaceutical thermal analysis*. New York, John Wiley and Sons pp. 47-67.

Grant, D., Abougela, I., 1982. Physico-chemical interactions in pharmaceutical formulations. *Anal. Proc.* 19: 545-549.

Higuchi T., Konishi, R., 1987. In vitro testing and transdermal delivery, *Therap. Res.*, (6): 280-288.

Itoh T., Rytting, J. H., 1990. Use of shed snake skin as a model membrane for in vitro percutaneous penetration studies: comparison with human skin, *Pharmaceutical Research*. (7): 1042-1047.

Kang L. S., Jun H.W., McCall J.W., 2000. Physicochemical studies of lidocaine-menthol binary systems for enhanced membrane transport, *Int. J. Pharm.* 206 (1-2): 35-42

Kang, L. S., Jun H.W., Mani N., 2001. Preparation and characterization of two-phase melt systems of lidocaine. *Int. J. Pharm.* 222 (1): 35-44.

Kasting, G. B., Smith, R. L., Cooper, 1987. E. R. Effects of lipid solubility and molecular size on percutaneous absorption. *Pharmacol. Skin* 1: 138-153.

Lawrence, R. C., Helmick, C. G., Arnett, F. C., 1998. Estimates of the prevalence of arthritis and selected musculoskeletal disorders in the United States. *Arth. Rheum.* 41: 778-799.

Yuan, X., Capomacchia, A.C., 2003. The binary eutectic of NSAIDs and two-phase liquid system for enhanced membrane permeation. In preparation to be submitted to *Journal of Pharmaceutical Development and Technology*.

Table 4.1. Composition of the select samples and fluxes ($\mu\text{g}/\text{cm}^2/\text{hr}$) of ibuprofen and ketoprofen in permeation studies ($n = 3, \alpha = 0.05$)

No.	Ibuprofen (mg)	Ketoprofen (mg)	IPA (%, w/w)	Flux of Ibuprofen	P-value ^a	Flux of Ketoprofen	P-value ^b
1	40.0	60.0	0.0	11.0	0.0001	8.4	0.0001
2	40.0	60.0	22.2	37.8	N/A	33.3	N/A
3	40.0	60.0	32.8	34.5	0.0614	30.3	0.0744
4	40.0	60.0	40.0	26.0	0.0001	25.1	0.0001
5	40.0	60.0	40.0	19.2	0.0001	15.1	0.0001
6	20.0	60.0	28.0	N/A	N/A	20.8	0.0001
7	20.0	60.0	32.5	N/A	N/A	19.7	0.0001
8	60.0	60.0	24.5	N/A	N/A	30.7	0.0812
9	0.0	60.0	36.6	0.0	0.0001	13.1	0.0001
10	40.0	13.33	28.5	28.4	0.0001	N/A	N/A
11	40.0	13.33	34.5	20.9	0.0001	N/A	N/A
12	40.0	40.0	24.5	33.9	0.0001	N/A	N/A
13	40.0	40.0	28.0	31.7	0.0001	N/A	N/A
14	40.0	40.0	33.5	22.7	0.0001	N/A	N/A
15	40.0	120.0	28.0	16.8	0.0001	N/A	N/A
16	40.0	0.0	35.0	17.2	0.0001	0.0	0.0001

^a Comparison between the flux of ibuprofen from Preparation 2 with that from other preparations

^b Comparison between the flux of ketoprofen from Preparation 2 with that from other preparations

Table 4.2. Concentrations of ibuprofen and ketoprofen in the two phases at different temperatures

	Temperature (°C)	Ibuprofen	Ketoprofen
Concentration in aqueous phase (mg/ml)	5	0.06	4.09
	25	0.14	5.71
	40	0.37	13.81
Concentration in oily phase (mg/ml)	5	319.3	435.8
	25	317.8	425.7
	40	316.03	355.23
Percentage in aqueous phase (%)	5	0.22	9.21
	25	0.40	11.42
	40	1.06	27.62
Percentage in oily phase (%)	5	99.78	90.79
	25	99.60	87.68
	40	98.04	72.38
Percentage of weight in oil (%)	5	30.95	42.24
	25	30.50	40.81
	40	30.01	33.73
Total percentage of weight in oil (%)	5	73.19	
	25	71.31	
	40	63.74	

Table 4.3. Concentrations of ibuprofen and ketoprofen in two phases of samples stored at 5 and 40 °C after re-equilibration at room temperature

	Temperature (°C)	Ibuprofen	Ketoprofen
Concentration in aqueous phase (mg/ml)	5	0.13	5.70
	40	0.14	5.72
Concentration in oily phase (mg/ml)	5	317.4	425.6
	40	318.1	425.9
Percentage in aqueous phase (%)	5	0.42	12.38
	40	0.41	12.31
Percentage in oily phase (%)	5	99.58	87.62
	40	99.59	87.69
Percentage of weight in oil (%)	5	30.57	40.99
	40	30.49	40.82
Total percentage of weight in oil (%)	5	71.31	
	40	71.56	

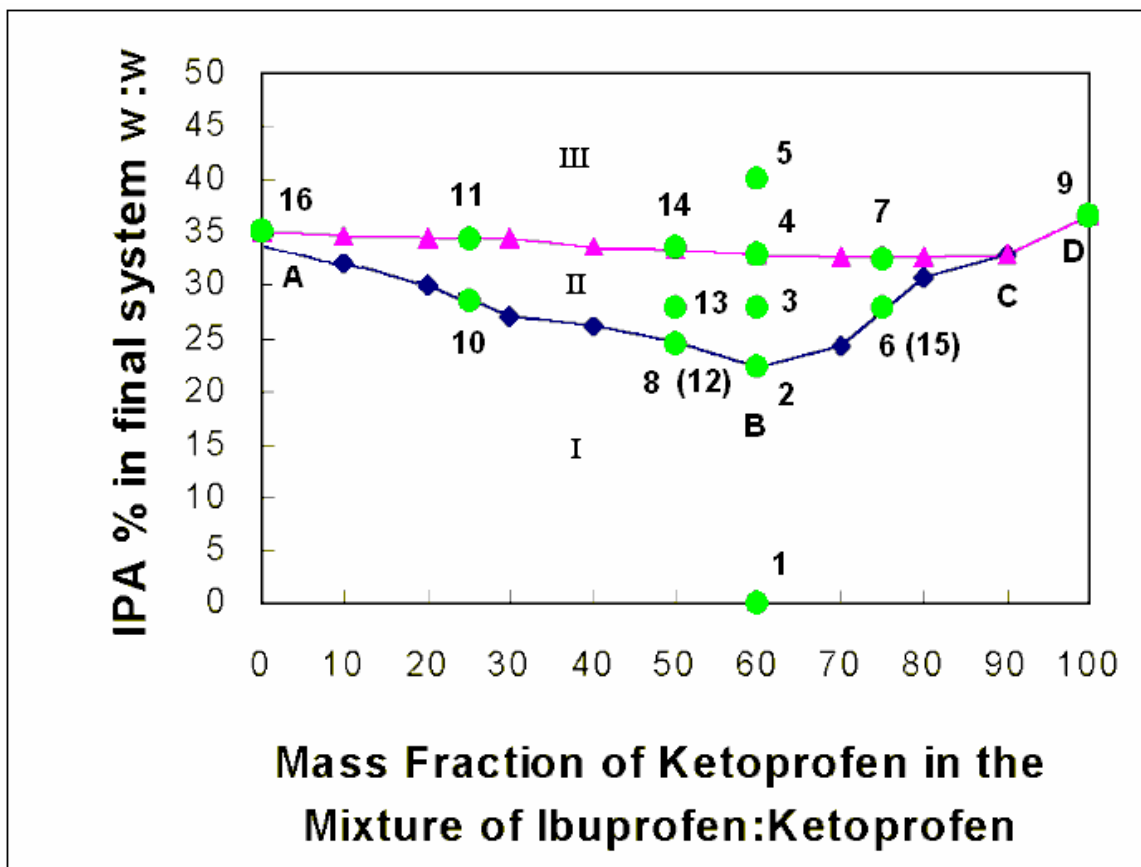


Figure 4.1. Selected preparations (1 - 16) in the phase diagram of ibuprofen-ketoprofen binary system with aqueous IPA at ambient temperature.

I. Solid crystals remaining area II. Two-phase liquid area III. Aqueous IPA solution area

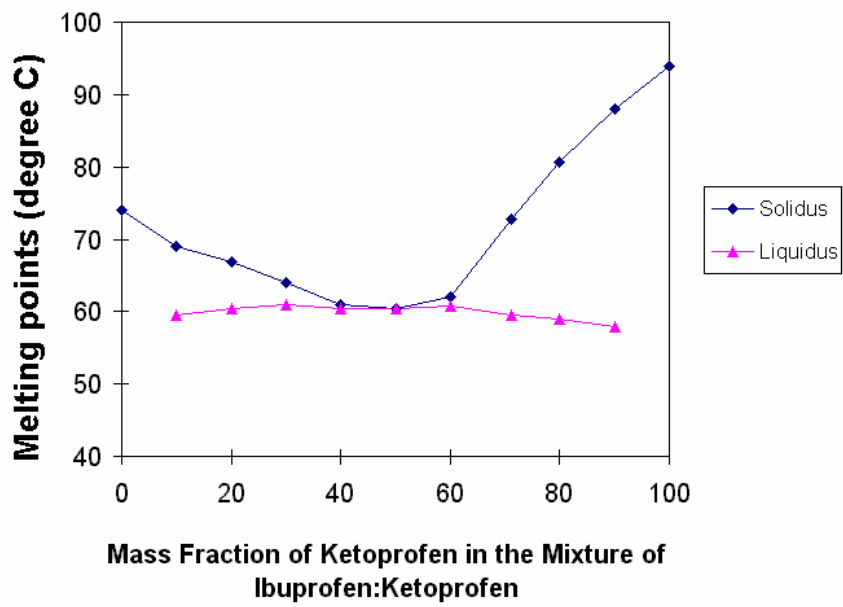


Figure 4.2. Binary phase diagram of the ibuprofen and ketoprofen mixtures

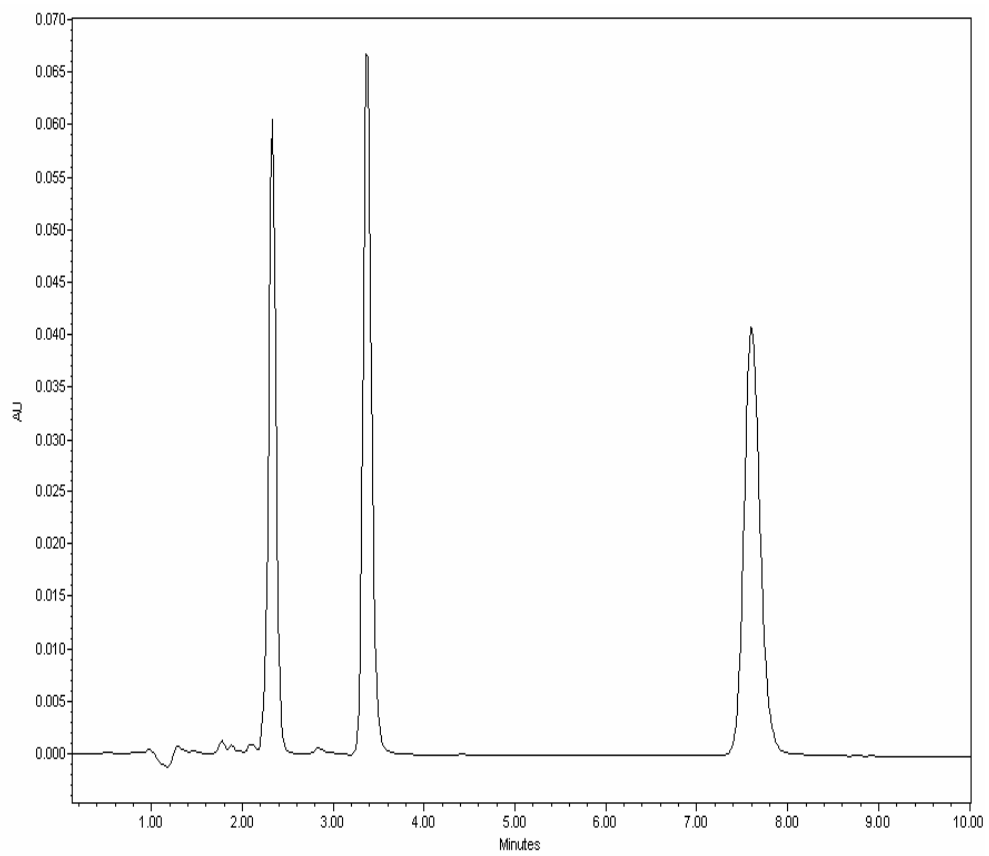


Figure 4.3. HPLC profile of ibuprofen (7.6 min), ketoprofen (3.3 min) and internal standard (2.3 min)

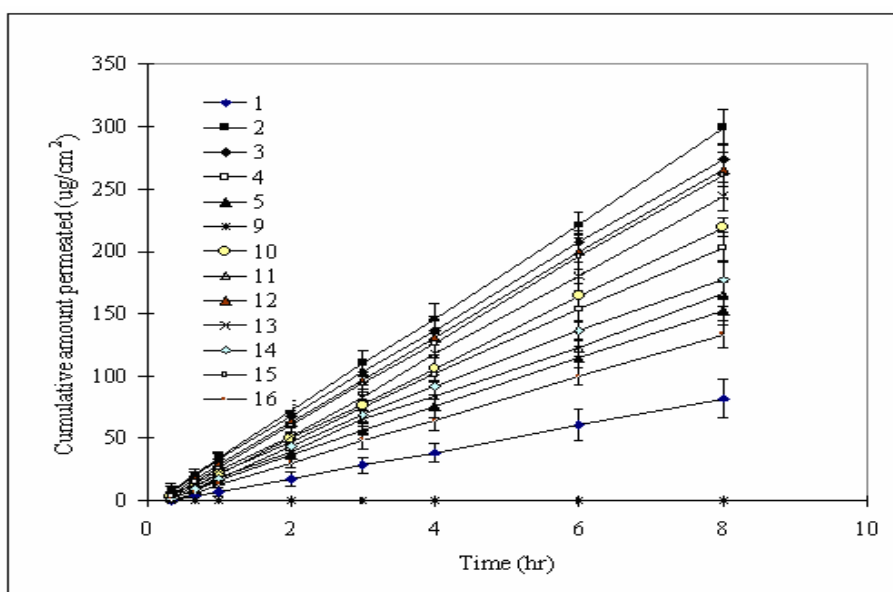


Figure 4.4. Permeation profiles of ibuprofen through snake skin (n = 3, error bar = SD)

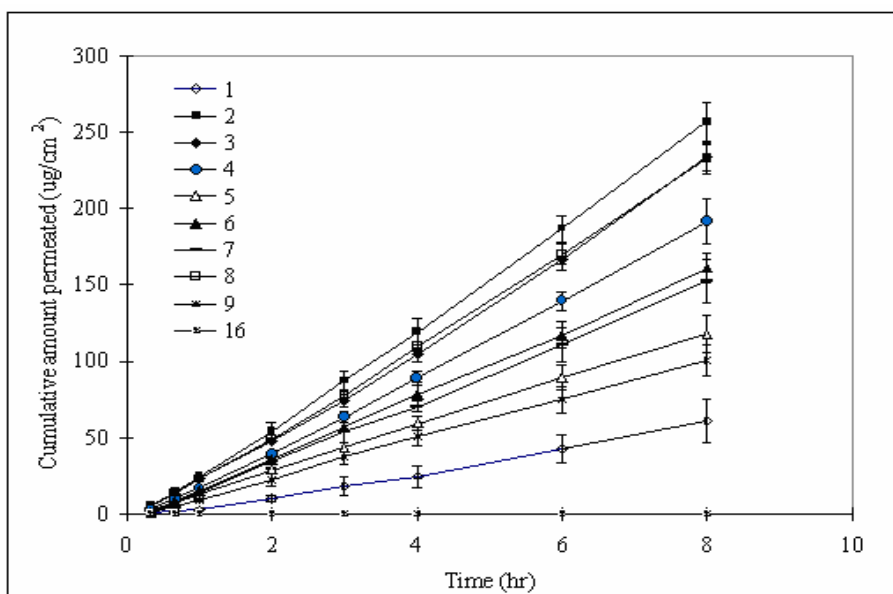


Figure 4.5. Permeation profiles of ketoprofen through snake skin (n = 3, error bar = SD)

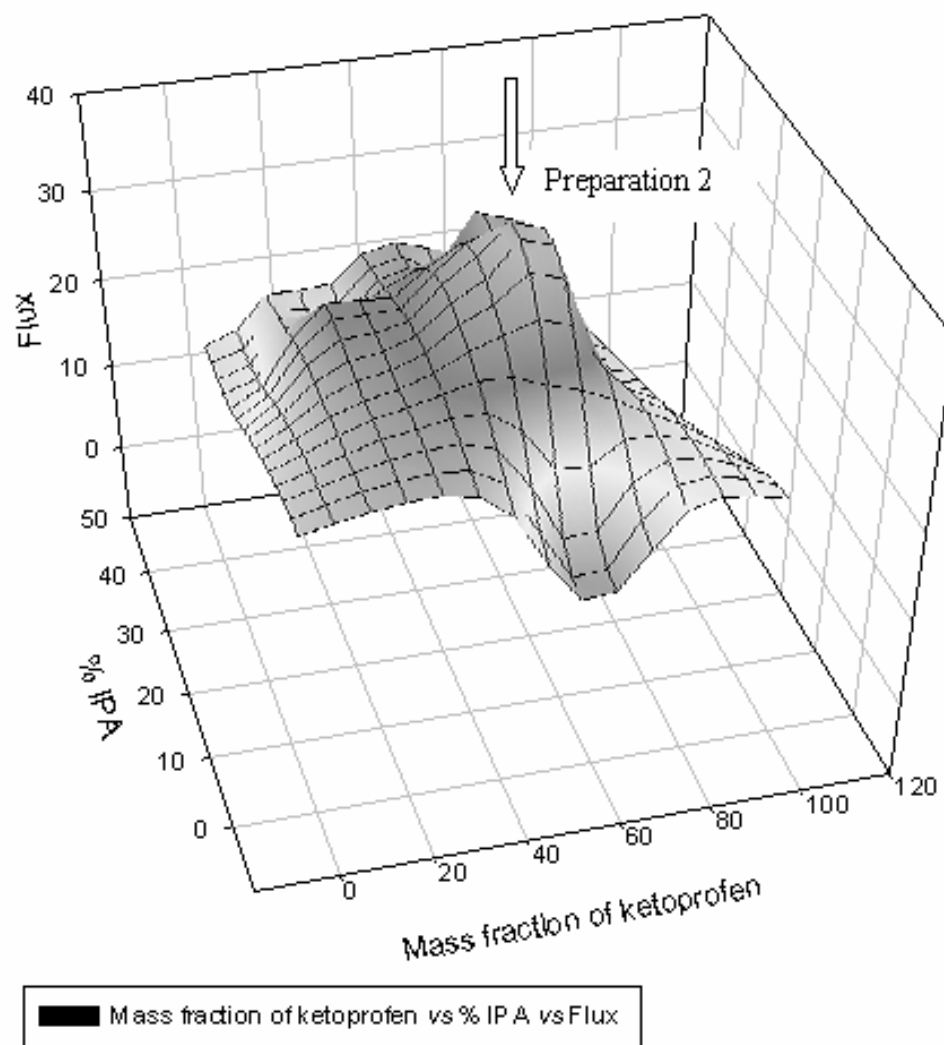


Figure 4.6. 3-D mesh plot of permeation profiles of ibuprofen through snake skin

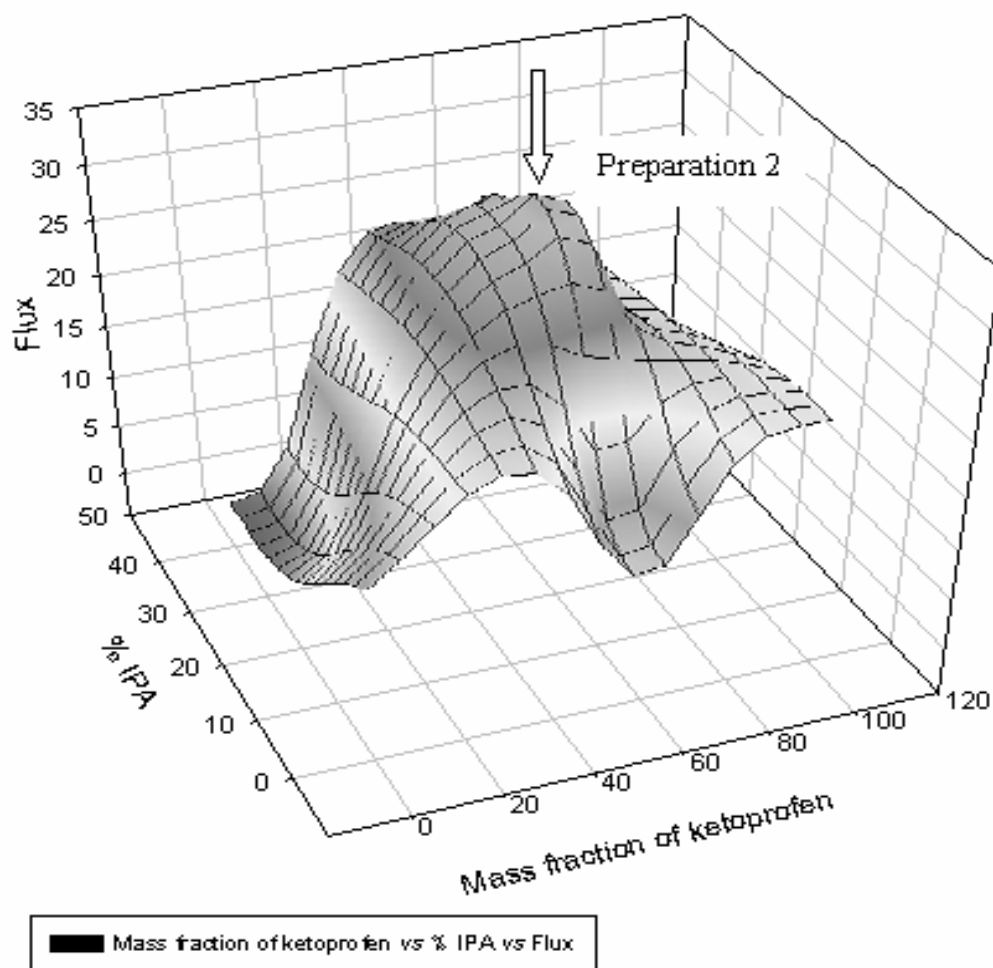


Figure 4.7. 3-D mesh plot of permeation profiles of ketoprofen through snake skin

CHAPTER 5

PHYSICOCHEMICAL STUDIES OF ENANTIOMERS, RACEMATE AND EUTECTIC OF IBUPROFEN FOR ENHANCED TRANSDERMAL DELIVERY

Yuan, X., Capomacchia, A.C. To be submitted to the Journal of Pharmaceutical Sciences

Abstract

Chiral ibuprofen has enantiomers and eutectics with lower melting points. The thermodynamic properties and crystalline structures of enantiomer, eutectic and racemate of ibuprofen were investigated by differential scanning calorimetry (DSC) and X-ray powder diffractometry (XRPD). The effect of melting point of drug on the permeation rates of percutaneous absorption was evaluated by two mathematical models and both models predicted the increases of ibuprofen flux. Enantiomer and eutectic of ibuprofen formed a two-phase liquid system containing an aqueous phase and an oily phase in presence of aqueous isopropyl alcohol. Different preparations of racemate, enantiomer and eutectic of ibuprofen were selected from the composite phase diagram to perform *in vitro* diffusion studies using shed snake skin as the model membrane. The preparation of the two-phase liquid system of eutectic showed the highest permeation rates among all the test preparations with 2.21 - fold increase in the flux as compared to the saturated aqueous IPA solution of racemic ibuprofen. The experimental results confirmed that these models could be employed to predict the maximum flux changes based on the thermodynamic data. The study also suggested that the eutectic or S-enantiomer of ibuprofen could be used to develop formulations for enhanced transdermal delivery of this drug.

Keywords: Ibuprofen; Racemic; Racemate; Enantiomer; Eutectic; DSC; X-ray powder diffraction; Enhanced transdermal drug delivery

1. Introduction

Chirality of drugs is a very common phenomenon and more than 50% of marketed drugs are chiral compounds (1, 2). Over the last twenty years, it has been recognized that the stereochemistry of chiral drugs affects their pharmacological, pharmacokinetic and toxicological actions (3). In fact, chirality is a ubiquitous and fundamental characteristic of biological systems (4, 5). The chiral enantiomers share essentially the same physicochemical properties, including refractive index, melting points, boiling points, and solubility. However, the three dimensional structural differences between the enantiomers can lead to significant biochemical differences (6 - 8). For example, permeation of different chiral enantiomers can influence the pharmacological activity of the transdermal drug delivery system.

For a chiral drug, it is important to assess the physicochemical properties and membrane permeation characteristics of its enantiomers, racemate and even mixtures of enantiomers in developing a more effective transdermal drug delivery system. The stratum corneum, the rate-limiting barrier to percutaneous absorption, is made up of several components, e.g., keratin, ceramides and fatty acids. Differential binding of enantiomers to keratin or interactions with ceramide may give rise to differences in the permeation profiles of the enantiomers (9). These components may serve as potential sources of chiral discrimination that could result in differential permeation rates, depending upon the stereochemistry of the penetrant molecule. Stereoselective processes were observed within the viable epidermis in contact dermatitis (10, 11) and with skin metabolism (12). Enantiomeric difference on the permeation of R-(-)- and S-(+)-

propranolol through rat skin was reported (13). However, no stereoselective process was observed after topical administration of racemic ibuprofen (18), which indicated that R-(-)-ibuprofen behaved the same way as S-(+)-ibuprofen (dexibuprofen) did in the percutaneous absorption. Apart from these intrinsic factors resulting from the components of the skin, the following extrinsic factors were also implicated in the percutaneous permeation across the skin: differences in the physicochemical properties between enantiomers and racemate (14); the presence of stereoselective retardants in the donor vehicle (15); chiral permeation enhancers; and differences in the hydrolysis rates of prodrugs of the enantiomers in epidermis / dermis (16).

Racemic species can be homochiral (enantiomorphous crystals), made up of molecules of the same handedness, or heterochiral (racemic crystals), consisting of an ordered array of both right- and left-handed molecules (1, 20). Random packing of the enantiomers will result in a solid solution. There are three types of crystalline racemates: (1) conglomerate, (2) racemic compound, and (3) pseudoracemate or solid solution. Conglomerate is an equimolar mixture of crystalline R- and S- enantiomers that are mechanically separable. This mixture melts as if it were a pure substance and will exhibit a eutectic in its melting point phase diagram. The second type of racemate is a racemic compound, which is also called "true racemate", is a crystal form in which two enantiomers coexist in the same unit cell. This is the most commonly encountered type of racemate and the Gibbs free energy of formation of this thermodynamically favored process is always negative. The third type of racemate is a "pseudoracemate", formed when two enantiomers form a solid solution or mixed crystal (21).

One of the major differences in physicochemical properties among enantiomers, racemate and binary mixtures of chiral enantiomers is different melting points, which will influence their solubility in the skin lipids, and therefore resulting in different permeation rates. Ibuprofen, the model racemic drug, is a routinely used non-steroidal anti-inflammatory drug (NSAID) in the racemic form. It has been found that only S-(+)-enantiomer is responsible for inhibition of prostaglandin synthetase (17), however, R-(-)-ibuprofen is converted to S-(+)-ibuprofen in the body (17). Solubility in aqueous HCl/KCl buffer solution was in the order eutectic ibuprofen > R- or S-ibuprofen > racemic ibuprofen with the eutectic having more than twice the solubility of the racemate (23, 25). The hydroscopicity of S-ibuprofen is ten times more than that of racemate (26) and the density of S-ibuprofen (1.098 g/cm^3) is lower than that of the racemic ibuprofen (1.110 g/cm^3) (27). Melting point and solubility are among the most important factors that affect transdermal delivery of the drug, which offers a therapeutic advantage as well as improved patient compliance in treating arthritis and related conditions. In this study, thermodynamic and physicochemical properties of S-(+)-ibuprofen, racemate and eutectic of ibuprofen were investigated and *in vitro* diffusion was performed to select the best candidate for the enhanced transdermal delivery of ibuprofen.

2. Materials and methods

2.1 Materials

The following chemicals were obtained from commercial suppliers and used as received: S-(+)-ibuprofen, racemic ibuprofen (Sigma Chemical Co., St. Louis, MO), isopropyl alcohol (IPA), HPLC grade acetonitrile, monopotassium phosphate, disodium citrate, hydrochloric acid, citric acid, disodium phosphate, dibasic sodium phosphate, phosphoric acid (J. T. Baker Chemical Co., Phillipsburg, NJ). Distilled, deionized water was prepared by Milli Q system (Millipore Corporation, Bedford, MA). Shed snake skin was donated by the Sandy Creek Nature Center (Athens, GA).

2.2 DSC studies of enantiomers and eutectic of chiral ibuprofen

An appropriate amount of S-ibuprofen was mixed with racemic ibuprofen in glass test tubes with the final total weight of 100 mg; molar ratios of S-ibuprofen ranged from 50 – 100 %. In order to achieve homogenous mixing, the mixtures were melted in the tube on the water bath and the melts were vortexed. Then the melts were annealed in the refrigerator (- 5 °C) for three days. Approximately 5.0 mg of each mixture was carefully sealed into an aluminum DSC sample pan with Perkin Elmer sample pan sealer for thermal analysis and was accurately weighed. A Perkin Elmer Differential Scanning Calorimeter (Norwalk, CT) equipped with a Perkin Elmer TAC 7/DX thermal analysis controller was calibrated with indium and used with carrier gas N₂ at pressure of 20 *psi*.

Thermograms were obtained at a heating rate of 1 °C/min against an empty reference pan. The scanning temperature ranges were set from 30 to 80 °C. The integration of peak area, peak temperature, onset time and enthalpy of fusion were obtained from Perkin Elmer Pyris series software for Windows (Version 3.81) or calculation ($\Delta G = \Delta H - T\Delta S$). Peak temperature from the melting endotherms were plotted versus the enantiomeric composition to give the binary phase diagram.

2.3 XRPD studies of enantiomers and eutectic of chiral ibuprofen

S-ibuprofen (344 mg) was mixed with racemic ibuprofen (56 mg) in a test tube, then the mixture, in which contained 93 % of S-ibuprofen, was heated in a water bath. After melting, the mixture was thoroughly mixed by vortexing for one minute. After congealing in the refrigerator for three days, the solid eutectic was crushed into fine particles by mortar and pestle and mixed well by spatula. An appropriate amount of the powder was loaded onto a glass sample holder and subjected to the X-ray powder diffractometry (XRPD). The pure S-ibuprofen and racemic ibuprofen were loaded on glass sample holders as received without further processing. The X-ray powder diffractograms of the pure S-enantiomer, racemate and the eutectic of ibuprofen were obtained by a Scintag XDS 2000 TM diffractometer (Scintag Inc., Cupertino, CA) with Co-K_α radiation. The data were collected at the step scan rate of 0.06 ° min⁻¹ with a step size 0.03 ° over a 2θ range of 2 to 50°.

2.4 Composite phase diagram of chiral ibuprofen in the presence of aqueous IPA

Different ratios of enantiomers of ibuprofen were used to prepare a phase diagram in the presence of aqueous isopropyl alcohol (IPA). IPA was used as the vehicle because of its miscibility with water, common use in cosmetics and proven safety as a pharmaceutical excipient and its permeation enhancing effect in topical products. Appropriate amounts of S-ibuprofen were weighed to mix with racemic ibuprofen at different molar ratios from 50 to 100 % of S-ibuprofen in the test tubes, fixing the final total weight at 100 mg. One ml citrate buffer (0.05 M, pH 4.0) was added, and IPA was used to titrate the suspension using a micro-syringe. The suspension was vortexed until the solid mixture was transformed completely into an oily liquid phase, which was separated out from the bulk aqueous phase and formed a two-phase liquid system. A microscope was used to observe complete transformation of the crystals into an oily state. After vigorous vortexing, a new emulsion was obtained with the internal oily phase dispersed in the external aqueous phase without any remaining crystals in either of the phases. When the emulsion was further titrated with IPA, a clear solution was finally obtained. To make the composite phase diagram of the system, the volumes of IPA used to completely transform crystals into oil or clear solution and to completely dissolve the oil into aqueous alcoholic phase were plotted against the IPA percentages (w/w) in the whole system.

The total amounts of ibuprofen enantiomers in the aqueous and oily phases of the two-phase liquid system formed by the titration with IPA were determined by HPLC. According to the compositions shown in Table 5.2, the appropriate amounts of S-

ibuprofen and racemic ibuprofen were put into a slender glass test tube, followed by addition of 1.0 ml of citrate buffer (0.05M, pH 4.0) and an appropriate amount of IPA using a micro-syringe. The suspension was vortexed until the solid mixture was completely transformed into an oily state. The tube was then centrifuged (3000 rpm) for an hour to completely separate the two phases. Five hundred μl of the aqueous phase was carefully transferred into a 5 ml volumetric flask, and 20 % acetonitrile in water was added to make up the sample solution to the volume. Two hundred μl of this solution was placed in an HPLC autosampler vial, then 1.0 ml of a 20% acetonitrile solution and 20 μl of the internal standard solution of ketoprofen were added and mixed well prior to HPLC analysis. Preparation IV did not form an obvious two-phase liquid system and therefore was not analyzed.

2.5 In vitro diffusion studies

The permeation rates of ibuprofen and ketoprofen in the selected preparations from the phase diagram were determined using Franz diffusion cells and shed snake skin as a model membrane. A large whole piece of the skin was cut into small circular pieces of the size that fitted to the diffusion cells. The skins, which were left in distilled water for 30 min to allow for complete hydration, was mounted onto Franz diffusion cells with the stratum corneum side facing the donor compartment. Seven preparations with the compositions shown in Table 5.2 were selected from the phase diagram for the permeation studies. Preparations I, II, III and IV were aqueous IPA solutions at the same total ibuprofen concentration, but with different enantiomeric ratios. Preparations V, VI

and VII were saturated aqueous IPA preparations of two-phase liquid systems containing an internal oily phase and external aqueous phase. The preparations were poured into the Franz diffusion cells above the stratum corneum, and the donor compartments were covered with Parafilm ® (American National Can, Neenah, WI) to avoid the loss of solvent by evaporation. The receptor compartments of the diffusion cells (Dayton Electric Mfg. Co., Chicago, IL) were filled with 0.05 M phosphate buffer (pH 7.4) and were maintained at 32 ± 1 °C by circulating water from a thermostat pump (Haake, Model F4391, Berlin, Germany). The receiver phase was continuously stirred at 300 rpm using a star head magnetic stirring bar. The effective diffusion area of the skin was 2.0 cm^2 , and the volume of the receptor compartment was 6.0 cm^3 . Each test was replicated three times. During the 8 hrs of the diffusion testing, 200 µl aliquots of the receptor phase were periodically removed into HPLC autosampler vials using a micro-syringe and immediately replaced with fresh buffer solution. Then, 20 µl of the internal standard solution and 1.0 ml of 20% acetonitrile in water were added into each vial. The vials were capped and vortexed briefly prior to HPLC analysis. The steady state flux, J_{ss} ($\mu\text{g}/\text{cm}^2/\text{hr}$) of ibuprofen and ketoprofen was calculated using Fick's first law:

$$J_{ss} = \Delta M/S \cdot \Delta t = P \cdot C_d = D \cdot K \cdot C_d/h \quad (1)$$

$$D = h^2 / 6 \cdot L \quad (2)$$

where S is the effective diffusion area (cm^2) and $\Delta M/\Delta t$ is the amount of drug penetrating through the membrane per unit time at steady state ($\mu\text{g}/\text{hr}$); P is the permeability coefficient (cm/hr); C_d is the drug concentration in donor phase ($\mu\text{g}/\text{ml}$); D is the diffusion coefficient (cm^2/hr); K is the partition coefficient between vehicle and skin; h is the membrane thickness (cm); and L is the lag time (hr). One-way ANOVA was

performed using SAS statistical package (SAS Institute Inc., Cary, NC) to determine significant differences among the J_{ss} values found for different preparations.

2.6 HPLC analysis of ibuprofen

The HPLC system consisted of a Model 616 solvent delivery pump (Waters, Milford, MA), a waters Model 600S controller, a Model 717plus autosampler equipped with a temperature-controlled rack (Waters), a Waters photo-diode array UV detector. A Waters Millennium data station was used to collect and process the data. Ibuprofen and internal standard ketoprofen were separated on a Waters C18 analytical column (250 × 4.6 mm I.D., 5 μ m, Waters, Milford, MA) at ambient temperature. The mobile phase was 50:50 (v/v) acetonitrile : phosphate buffer (0.025 M, pH 2.0). The flow rate was set at 1.0 ml/min. Absorbance was monitored at 223 nm using a photo-diode array UV detector. The injection volume was 20 μ l for each sample. Good separations of the peaks of ibuprofen (7.6 min), and internal standard of ketoprofen (3.3 min) were achieved within 10 min run as shown in Figure 5.7. Weekly calibrations using the peak height ratios of drug to internal standard were obtained for different linear ranges from 20 ng/ml to 2 mg/ml.

3. Results and discussion

3.1 DSC studies of enantiomers and eutectic of chiral ibuprofen

The DSC thermograms for the mixtures of two enantiomers of ibuprofen at different ratios are shown in Figures 5.1 – 5.3. The melting points, enthalpy and entropy of enantiomer, racemate and eutectic of ibuprofen were calculated using the Pyris software and data are shown in Table 5.1. The binary phase diagram was also plotted as shown in Figure 5.4 and the results clearly indicated that the melting point of racemic ibuprofen was significantly higher than that of the enantiomer and the eutectic of ibuprofen. In addition, the enthalpy (26.2 ± 0.3 kJ/mol) and entropy of fusion (75.2 ± 0.8 J/mol/K) of the racemate were higher than those of the enantiomers and the eutectic; while the enthalpy (18.3 ± 0.2 kJ/mol) and entropy of fusion (56.4 ± 0.6 J/mol/K) of S-enantiomer were slightly higher than those of the eutectic, which were 17.8 ± 0.2 kJ/mol and 54.8 ± 0.6 J/mol/K, respectively. The phase diagram (Figure 5.4) of the enantiomers of ibuprofen suggest that ibuprofen is a racemic compound or a true racemate, since it had two eutectic points near the pure enantiomers, which are characteristic in a typical phase diagram of a racemic compound. However, there are several different and conflicting reports about the ratio of the eutectic of two ibuprofen enantiomers, which might be due to the complexity of the DSC thermograms of mixtures of ibuprofen enantiomers. Dwivedi reported 0.18 mole fraction of S-ibuprofen to form eutectic (23); Romero reported 0.10 mole fraction (24) while Burger reported 0.07 mole fraction of S-ibuprofen and calculated 0.06 theoretically (25). In this study, it was found that 0.07 or

0.93 mole fraction of ibuprofen enantiomers formed the eutectic as shown in Figure 5.4 and therefore confirmed Burger's work.

In the phase diagram shown in Figure 5.4, the lower *solidus* curve is a line that indicates the temperature at which the system became completely solid on cooling or at which melting began on heating under equilibrium conditions; while the upper *liquidus* curve is a line on this binary phase diagram that indicates the temperature at which solidification began on cooling or at which melting was completed on heating under equilibrium conditions. The portion of the *liquidus* curve on a binary of racemic compound between the eutectic and the pure enantiomers is predicted by the simplified Schroeder-Van Laar equation (3):

$$\ln(X_A) = \left[\frac{\Delta H_A^f}{R} \right] \cdot \left[\frac{1}{T_A^f} - \frac{1}{T^f} \right] \quad (3)$$

And the *liquidus* curve between the two eutectic points or in the dystectic region was predicted by the Prigogine-Defay equation (4):

$$\ln[4X_A(1 - X_A)] = \left[\frac{2\Delta H_R^f}{R} \right] \cdot \left[\frac{1}{T_A^f} - \frac{1}{T^f} \right] \quad (4)$$

Where X represents the mole fractions of the enantiomeric composition. ΔH is the enthalpy of fusion of the enantiomers, R is the gas constant (8.345 J/mol/K) and T is the temperature. Subscripts R and A denote the values of racemic compound and pure enantiomers, respectively, and superscript f denotes the value at the final melting temperatures. As shown in Figure 5.4, the data points were in good accordance with the simulated curves calculated from the above two equations. However, some smaller peaks were observed ahead of the major peaks corresponding to the melting of the eutectic as shown in Figure 5.3. It was ascribed to an unstable phase, which originated from the

contacted S- enantiomer and racemic ibuprofen instead of the eutectic (25). While the unstable melted inhomogeneously, the stable eutectic originated from it. A corresponding unstable phase of S- enantiomer or pure racemic ibuprofen was not found.

Eutectic points were taken as the points of intersection of the curve obtained by equations (3) and (4). For ibuprofen, the racemic ibuprofen has a higher melting point than that of the pure enantiomers, and the following equations can be used to calculate the related thermodynamic parameters (22):

$$\Delta H_{T_A^f}^R = \Delta H_A^f - \Delta H_R^f + \Delta C_{P_R} (T_R^f - T_A^f) \quad (5)$$

$$\Delta S_{T_A^f}^R = \Delta S_A^f - \Delta S_R^f + R \cdot \ln(2) + \Delta C_{P_R} \cdot \ln\left(\frac{T_R^f}{T_A^f}\right) \quad (6)$$

$$\Delta G_{T_A^f}^R = \Delta H_A^f \cdot \left(\frac{T_A^f}{T_R^f} - 1\right) - T_A^f \cdot R \cdot \ln(2) + \Delta C_{P_R} \cdot [T_R^f - T_A^f - T_A^f \cdot \ln\left(\frac{T_R^f}{T_A^f}\right)] \quad (7)$$

where ΔH^R , ΔS^R and ΔG^R are enthalpy, entropy, and free energy changes, respectively, associated with the formation of a racemic compound. The subscript, T_A^f , indicates that these values are calculated at the absolute melting temperature of the enantiomers. ΔH_A^f is the enthalpy of fusion of the enantiomers, and ΔC_{P_R} is the difference between the heat capacities of the solid and super cooled liquid of the racemic compound. The contribution of the term containing the heat capacities in Equation (7) is always insignificant and negligible. However, the contribution of the heat capacities term in Equation (5) and (6) cannot be neglected (23). ΔG reflects the tendency to form a racemic compound or the stability difference between a racemic compound and the corresponding conglomerate of

enantiomers (20). ΔC_{P_R} was determined to be 52 J/mol/K, and ΔH^R , ΔS^R and ΔG^R were calculated as -6.66 kJ/mol, -9.33 J/K/mol and -3.62 kJ/mol, respectively. A negative enthalpy indicates a liberation of energy during formation of racemic ibuprofen from enantiomers. Negative Gibbs free energy indicates that the process was thermodynamically favored and the contribution from the entropy of mixing in the liquid state to the free energy of formation is the driving force for the process (28). These results also suggest that racemic ibuprofen was a racemic compound rather than a racemic mixture.

A previous study (19) showed that eutectic formation was an effective way to lower the melting point of drug without modifying its chemical structure, and thus can enhance its percutaneous absorption. With other conditions being equal, the lower the melting point (T_m) of drug, the higher the solubility (S_{ideal}) of drug in the skin lipids, and thus the higher the flux (J_m) of drug through the skin. If the depressed melting point of drug in the eutectic or mixtures is denoted as T_m' , the solubility of drug in the skin lipids is denoted as S_{ideal}' , and the flux of drug through the skin is denoted as J_m' , Thus, the folds of flux offered by the eutectic system over that by pure drugs can be calculated using Equation (8):

$$\frac{J_m'}{J_m} = \frac{S_{ideal}'}{S_{ideal}} = \frac{\frac{M_w}{M_1} - 1 + \exp\left[\frac{\Delta S_f}{RT}(T_m - T)\right]}{\frac{M_w}{M_1} - 1 + \exp\left[\frac{\Delta S_f'}{RT}(T_m' - T)\right]} \quad (8)$$

In a previous study (19), an estimation of the average molecular weight of skin lipids was calculated from the percentages of different lipids in the skin stratum corneum and the final estimated molecular weight of skin lipids was 604.6. Equation (8) can be used to predict the changes of skin solubility and flux when experimental thermodynamic data and molecular weights are substituted in. For S-ibuprofen, $J_m'/J_m = 3.20$, which means the flux of ibuprofen through the stratum corneum layer will increase 3.20 - fold as predicted by this model. For the eutectic of two enantiomers, $J_m'/J_m = 3.67$, which means the flux of this drug through the layer will increase 3.67 - fold.

Based on the MTMT theory (14,19), if the mole fraction of the drug in the eutectic in the solute and enthalpy of fusion is denoted as X' and $\Delta H'$, respectively, the following Equation (9) can be obtained, and the ratios of the increased flux can be expressed as:

$$\frac{J_m'}{J_m} = \frac{X'}{X} = \exp\left\{\frac{1}{R}\left[\Delta H \cdot \left(\frac{1}{T} - \frac{1}{T_m}\right) - \Delta H' \cdot \left(\frac{1}{T} - \frac{1}{T_m'}\right)\right]\right\}$$

Equation (9) can also be used to predict the skin solubility and flux if the thermodynamic data are known. For S-ibuprofen, J_m'/J_m of 2.52 suggests that the flux of the drug through the stratum corneum will increase 2.52 - fold. Similarly, J_m'/J_m of 2.74 was obtained for the eutectic of enantiomers. The difference in the predicted values could be attributed to the fact that the MTMT theory does not incorporate the molecular weights of permeant and skin lipid into the equations of the proposed model.

3.2 XRPD studies of enantiomers and eutectic of chiral ibuprofen

In XRPD, the diffraction occurs when X-rays radiation enters a crystalline substance and is scattered. The direction and intensity of the scattered or diffracted beams depends on the orientation of the crystal lattice with respect to the incident beam. Any face of a crystal lattice consisting of parallel rows of atoms separated by a unique distance (d-spacing), which is capable of diffracting X-rays. The diffractometer utilizes a powdered sample, a goniometer, and a fixed-position detector to measure the diffraction patterns. The powdered sample provides all possible orientations of the crystal lattice, the goniometer provides a variety of angles of incidence, and the detector measures the intensity of the diffracted beam. The resulting analysis is described graphically as a set of peaks with % intensity on the Y-axis and goniometer angle on the X-axis. The exact angle and intensity of a set of peaks is unique to the crystal structure being examined. The same substance always gives the same pattern; while in a mixture of substances, each produces its pattern independently of the others. Therefore, the X-ray diffraction pattern of a substance is like a fingerprint of the substance. The obtained XRPD patterns of racemic ibuprofen, S-ibuprofen and the binary eutectic are shown in Figures 5.6. The enantiomers are mirror images of one another with the same crystalline structures and will show the same X-ray powder diffraction pattern. However, if the racemic ibuprofen formed a racemic compound with new crystal lattices, it will show a distinct XRPD pattern from that of pure enantiomers of ibuprofen. It was found that XRPD pattern of racemic ibuprofen (Figure 5.6) was different from that of S-ibuprofen. Therefore, combining the information obtained from DSC, which showed two characteristic eutectic

points in the phase diagram and negative Gibbs free energy, XRPD studies further confirmed that racemic ibuprofen was a racemic compound capable of existing as a separate phase in the solid state independent of its constituent enantiomers. It was reported that both the racemic ibuprofen and S-ibuprofen crystal unit cells include four molecules, but crystallize in the $P2_{1/c}$ and $P2_1$ space groups, respectively (24). Thus the intermolecular forces are different in each crystal, racemic ibuprofen has stronger crystalline structure and higher lattice energy than those of pure enantiomers, and as a result it shows higher melting point and lower solubility in aqueous media. It is obvious that the XRPD pattern of the eutectic was similar to that of S-ibuprofen without showing any major proprietary peaks. The only difference was the intensity of some peaks, which might be attributed to the existence of some crystals of ibuprofen racemate. Therefore, the eutectic of ibuprofen was most likely a solid solution composing of continuously mixed crystals of enantiomers and racemate without forming a totally new or unique crystal lattice. However, there were some weak forces interacting between R- and S-ibuprofen molecules and interrupting the regular crystalline structures of the either racemate or enantiomers and thus weakened the lattices in both crystalline structures. As a consequence the decreased lattice energy caused reduced melting points of the enantiomer mixtures and gave the lowest melting point (eutectic point) at certain ratios, which is 93 % mole fraction of R- or S-ibuprofen enantiomers.

3.3 Composite Phase diagram of chiral ibuprofen in the presence of aqueous IPA

In order to prepare a topical formulation optimized for best permeation, the solid crystals of drug must be in a liquid state. It was found that the solid crystals of ibuprofen

at certain enantiomeric ratios could transform into an oily state at the ambient temperature in the presence of aqueous IPA and formed a two-phase liquid system. The composite phase diagram (Figure 5.5) showed a lower curve and an upper curve, which represented the complete transformation of the drug crystals into the oily phase and the complete solubilization of the oily phase into the homogeneous aqueous phase, respectively. The region under the lower curve shows the area where some of the ibuprofen crystals remain. The middle region between two curves indicates the coexistence of the oily and aqueous phases. The region above the upper curve displays the region where only the homogeneous aqueous phase is formed. The lower curve, which corresponds to the volume of IPA used to obtain the two-phase liquid system, has a shape similar to the *liquidus* curve of the melting points of different mixtures of ibuprofen enantiomers. The possible explanation for this phenomenon is that the lower the melting points of the mixtures of two enantiomers, the less energy or enthalpy is required to break down the more fragile lattice, and thereby the less IPA is needed to solubilize the drug crystals. Enantiomers of ibuprofen have lower melting point (51.3 °C) and ΔS_f (56.4 J/mol/K) than racemic ibuprofen, and the eutectic of ibuprofen has even lower melting point (47.9 °C) and ΔS_f (54.8 J/mol/K), as shown in Table 5.1. Therefore, enantiomers and eutectic of ibuprofen have higher solubility in aqueous media than racemic ibuprofen.

The analytical data in Table 5.3 showed that in the two-phase liquid system, the majority of ibuprofen (79.0 – 86.5 %) was present in the oily phase rather than in the aqueous phase of the system. It is clear that no common pharmaceutical oils available could dissolve drugs at such high concentrations. Therefore, the drugs in the oily phase

should provide the maximum thermodynamic activity, due to saturated drug concentration in the oily phase, and a high concentration gradient across the stratum corneum layer when the oily phase is applied on the skin surface. This condition creates a strong driving force for the compounds to move through the membrane and give enhanced percutaneous absorption (19). In addition, IPA has been shown to enhance the dermal permeation of many compounds. The majority of the remaining oily phase was probably composed of IPA, since the added buffer could not be dissolved in the lipophilic oily phase.

3.4 In vitro diffusion studies

In order to compare the permeation rates of enantiomer, racemate and eutectic of ibuprofen, seven preparations were selected from the phase diagram (Figure 5.5) and used for *in vitro* diffusion studies using shed snake skin as the model membrane. Preparations I, II, III and IV were aqueous IPA solutions with the same total ibuprofen concentration, but with 100 %, 93 %, 70 % and 50% molar ratios of S-ibuprofen, respectively. Preparation V, VI and VII were preparation of the two-phase liquid system with 100 %, 93 % and 70 % molar ratios of S-ibuprofen, respectively. The samples from the receiver compartment were removed periodically by a micro-syringe and subjected to HPLC analysis. The column used was not chiral selective, the peak of ibuprofen in a diagram represented the elution of both R- and S- ibuprofen, and the concentration calculated was the combined concentration of the two ibuprofen enantiomers. According to a previous study (18), the skin did not show enantioselective permeation of chiral

ibuprofen, therefore, the permeation rates of R- and S- enantiomers were assumed to be the same in this study.

The permeation profiles of ibuprofen are shown in Figures 5.8 and 5.9. The steady state flux was calculated from the Fick's first law and linear regression analysis of the steady state portion of the plot and the results are shown in Table 5.3. For donor preparations with the same drug concentration, Preparation II showed the highest permeation rates ($28.9 \mu\text{g}/\text{cm}^2/\text{hr}$) among them, which was due to the lowest melting point and highest solubility of the eutectic of ibuprofen. In comparison with the flux of ibuprofen ($15.7 \mu\text{g}/\text{cm}^2/\text{hr}$) in the solution of racemic ibuprofen (IV), Preparation II increased the flux value by 1.84 – fold. Preparation III had a lower flux value ($21.3 \mu\text{g}/\text{cm}^2/\text{hr}$) than the solutions of pure enantiomer (I) and eutectic (II), but had higher flux than the solution of racemic ibuprofen (IV). The differences of fluxes of ibuprofen in the above four donor preparations with the same concentration were statistically different ($P < 0.05$), using one-way ANOVA. Preparation II made from the two-phase liquid system of eutectic ibuprofen gave the highest flux ($34.7 \mu\text{g}/\text{cm}^2/\text{hr}$) among all the saturated preparations, The fluxes of ibuprofen in Preparation VII, which had only S-ibuprofen, showed lower permeation rate, which was $31.9 \mu\text{g}/\text{cm}^2/\text{hr}$. Preparation V, based on the two-phase liquid system of 70 % S-ibuprofen with higher melting point, gave a lower flux of $22.8 \mu\text{g}/\text{cm}^2/\text{hr}$. The differences of fluxes of ibuprofen in the above saturated preparations were statistically different ($P < 0.05$) using one-way ANOVA performed by SAS statistical package.

Based on Equation (8) shown earlier, the fluxes of ibuprofen in enantiomer and eutectic were predicted to increase by 3.2- and 3.67- fold, respectively, compared to that

obtained from the racemic ibuprofen. The fluxes in the preparations of the enantiomer (I) and the eutectic (II) with the same drug concentration showed 1.67- and 1.84- fold increases, respectively, while the fluxes in the saturated preparations of enantiomer (VII) and eutectic (VI) demonstrated 2.03 - and 2.21 - fold increases, respectively. The experimental values from the saturated solution were closer to the predicted values, although both were smaller. Based on Equation (9) derived from the MTMT theory, the predicted increase of fluxes for the enantiomer and eutectic of ibuprofen were 2.52 and 2.74 - fold, respectively. These values were closer to the experimental values obtained from the saturated preparations of the eutectic ibuprofen. Therefore, the proposed mathematical models predicted more precisely the maximal fluxes for the saturated preparations with the potential maximum thermodynamic activity, than for the preparations with the same drug concentration. The results also validated the rationale of the proposed mathematical models: the lower the melting points of drug, the higher the skin lipid solubility and thus the higher permeation rate of the compound through the skin.

4. Conclusions

The pure enantiomers and eutectic of ibuprofen have lower melting points than racemic ibuprofen, therefore have higher solubility in the skin lipids and higher percutaneous absorption. The increasing trend of the drug flux as a result of lower melting point was predicted by two mathematical models and was validated by the results of *in vitro* diffusion studies. The preparation of S-enantiomer and eutectic of ibuprofen

offers the enhanced permeation of ibuprofen and can be further developed into transdermal formulations. Same methodology can be applied to other chiral drugs, which has a lower eutectic point than its racemate and enantiomers, to obtain enhanced transdermal delivery of the drugs without modifying their chemical structures or incorporating chemical enhancers into formulations.

References

1. Li, Z.J. and Grant, D. J. W., Relationship between physical properties and crystal structures of chiral drugs, *J. Pharm. Sci.*, 86, 1073. 1997.
2. Millership, J.S. and Fitzpatrick, A., Commonly used chiral drugs: A survey, *Chirality*, 5, 573, 1993.
3. Nation, R. L., Chirality in new drug development – Clinical pharmacokinetic considerations, *Clin. Pharmacokinet.*, 27, 249, 1994.
4. Popa R., A sequential scenario for the origin of biological chirality. *J. Mol. Evol.*, 44, 121, 1997.
5. Liu, W. M., Remarks on origins of biomolecular asymmetry, *Orig. Life*, 12, 205, 1982.
6. Coutts, R.T. and Baker, G. B., Implications of chirality and geometric isomerism in some psychoactive drugs and their metabolites, *Chirality*, 1, 99, 1989.
7. Hutt, A.J. and Tan, S.C., Drug chirality and its clinical significance, *Drugs*, 52, 1, 1996.

8. Chrom, W.R., Effects of chirality on pharmacokinetics and pharmacodynamics, *Am. J. Hosp. Pharm.*, 49, S9, 1992.
9. Heard, C.M. and Brain, K.R., Does solute stereochemistry influence percutaneous penetration?, *Chirality*, 7, 305, 1995.
10. Bebezra, C., Stampf, J., Brbier, P., and Ducombs, G., Enantiospecificity in allergic contact dermatitis, *Contact Dermatitis*, 13, 110, 1985.
11. Papageorgiou, C., Stampf, J.L., and Benezra, C., Allergic contact dermatitis to tulips: An example of enantiospecificity, *Arch. Dermatol. Res.*, 280, 5, 1988.
12. Weston, A., Hodgson, R.M., Hewer, A.J., Kuroda, R., and Grover, P.L., Comparative studies of the metabolic activation of chrysene in rodent and human skin., *Chem. Biol. Interact.*, 54 (2), 223, 1985.
13. Miyazaki, K., Kaiho, F., Inagaki, A., Dohi, M., Hazemoto, N., Haga, M., Hara, H., and Kato, Y., Eanantiomeric difference in percutaneous penetration of propranolol through rat excised skin., *Chem. Pharm. Bull.*, 40, 1075, 1992.
14. Touitou, E., Chow, D. D., and Lawter, J.R., Chiral β -blockers for transdermal delivery, *Int. J. Pharm.*, 104, 19, 1994.

15. Heard, C.M., and Suedee, R., Stereoselective adsorption and trans-membrane transfer of propranolol enantiomers using cellulose derivatives. *Int. J. Pharm.*, 139, 15, 1996.
16. Zahir, A., Kunta, J. R., Khan, M.A., and Reddy, I.K., Effect of menthol on permeability of optically active and racemic propranolol across guinea pig skin, *Drug. Dev. Ind. Pharm.*, 24, 77, 1998.
17. Adams, S.S., Bresloff, P., Mason, C.G. (1976) Pharmacological differences between the optical isomers of ibuprofen: evidence for metabolic of the (-)-isomer. *J. Pharm. Pharmacol.* 28; 256-257.
18. J.S. Millership and P.S. Collier. Topical Administration of Racemic Ibuprofen. *Chirality* 9:313-316. 1997.
19. X. Yuan, A.C. Capomacchia. The physicochemical studies of binary eutectic of ibuprofen and ketoprofen and mathematical models for enhanced transdermal delivery. In preparation to be submitted to *International Journal of Pharmaceutics*. 2003.
20. Collet, A., Ziminiski, L., Garcia, C., and Vigne-Maeder, F., Chiral discrimination in crystalline enantiomers systems: Fact, interpretations, and speculations, in *NATO ASI Series – Supramolecular Stereochemistry*, Siegel, J.S., Ed., The Netherlands, Kluwer Academic, 1995, 91.

21. Roozeboon, H.W. B., *Phys. Chem.*, 28, 494, 1899.

22. Leclercq, M., Collet, A., and Jacques, J., Study of mixtures of optical antipodes-XII, *Tetrahedron*, 32, 821, 1976.

23. Dwivedi, S.K., Sattari, S., Jamali, F., and Mitchell, A.G., Ibuprofen racemate and enantiomers: Phase diagram, solubility and thermodynamic studies, *Int. J. Pharm.*, 87, 95, 1992.

24. Romero, A. J., Rhodes, C. T., Stereochemical aspects of the molecular pharmaceutics of ibuprofen. *J. Pharma. Pharmacol.*, 45, 258-262, 1993.

25. Artur Burger, Kurt T. Koller, Wiltrud M. Schiermeier. RS-Ibuprofen and S-Ibuprofen (Dexibuprofen) – Binary System and Unusual Solubility Behaviour . *Eur. J. Pharm. Biopharm.* 43(2) 142-147, 1996.

26. A.J. Romero and C.T. Rhodes. Approaches to Stereospecific Preformulation of Ibuprofen. *Drug Development and Industrial Pharmacy*, 17(5), 777-792, 1991.

27. Leising G, Resel R, Stelzer F, Tasch S, Lanziner A and Hantich G. Physical Aspects of Dexibuprofen and Racemic Ibuprofen. *Journal of Clinical Pharmacology*, 36(12):S3-S6 Suppl. S 1996

28. Z Jane Li, Mark T. Zell, Eric J. Munson, David J. W. Grant. Charaterization of Racemic Species of Chiral Drugs Using Thermal Analysis, Thermodynamic Calculation, and Structural Studies. *Journal of Pharmaceutical Sciences*. 88(3), 337-346, 1999

Table 5.1. Thermodynamic data of enantiomers and eutectic of ibuprofen (n = 4)

	R,S-ibuprofen	R-ibuprofen	S-ibuprofen	Eutectic
Melting point (°C)	75.1	51.3	51.3	47.9
Enthalpy (kJ/mol)	26.2 ± 0.3	18.1 ± 0.3	18.3 ± 0.2	17.8 ± 0.2
Entropy (J/mol/K)	75.2 ± 0.8	56.1 ± 0.7	56.4 ± 0.6	54.8 ± 0.6

Table 5.2. Compositions of select preparations of ibuprofen enantiomers

Preparation	Mole fraction of S-ibuprofen		R,S-ibuprofen	Buffer	IPA	Percentage
	S-ibuprofen (%)	(mg)	(mg)	(ml)	(%, w/w)	(%) ^a
I	100	100.0	0.0	1.0	35.5	N/A
II	93	86.0	14.0	1.0	35.5	N/A
III	70	40.0	60.0	1.0	35.5	N/A
IV	50	0.0	100.0	1.0	35.5	N/A
V	70	40.0	60.0	1.0	24.1	79.0 ± 1.9
VI	93	86.0	14.0	1.0	15.7	86.5 ± 1.5
VII	100	100.0	0.0	1.0	16.9	84.3 ± 1.1

^a Total percentage of R- and S- ibuprofen in the oily phase (%)

Table 5.3. Steady state flux (J_{ss}) of ibuprofen through snake skin from select preparations
(n = 3)

Preparation	J_{ss} ($\mu\text{g}/\text{cm}^2/\text{hr}$) ^a
I	26.2
II	28.9
III	21.3
IV	15.7
V	22.8
VI	34.7
VII	31.9

^a Total flux of R- and S- ibuprofen

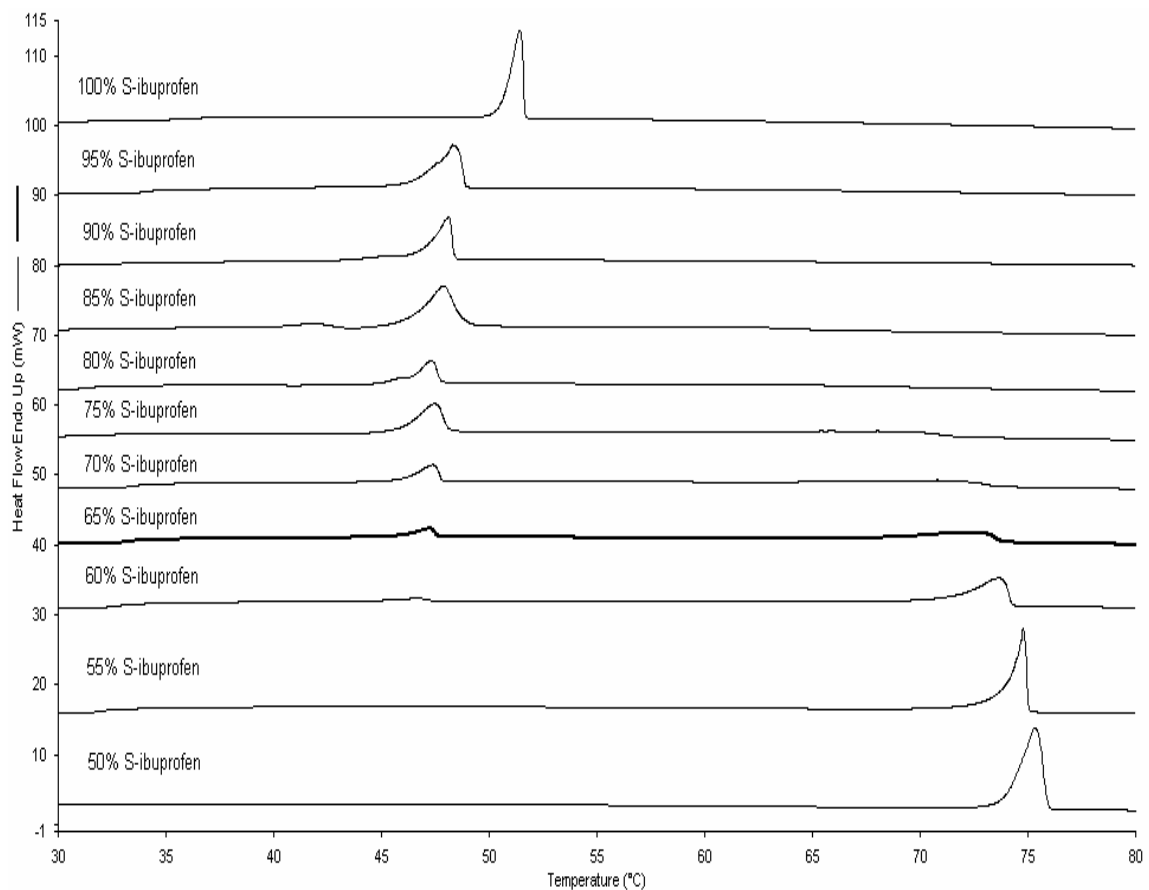


Figure 5.1. The DSC thermograms of mixtures of enantiomers of ibuprofen with S-ibuprofen ranging from 50 – 100 %

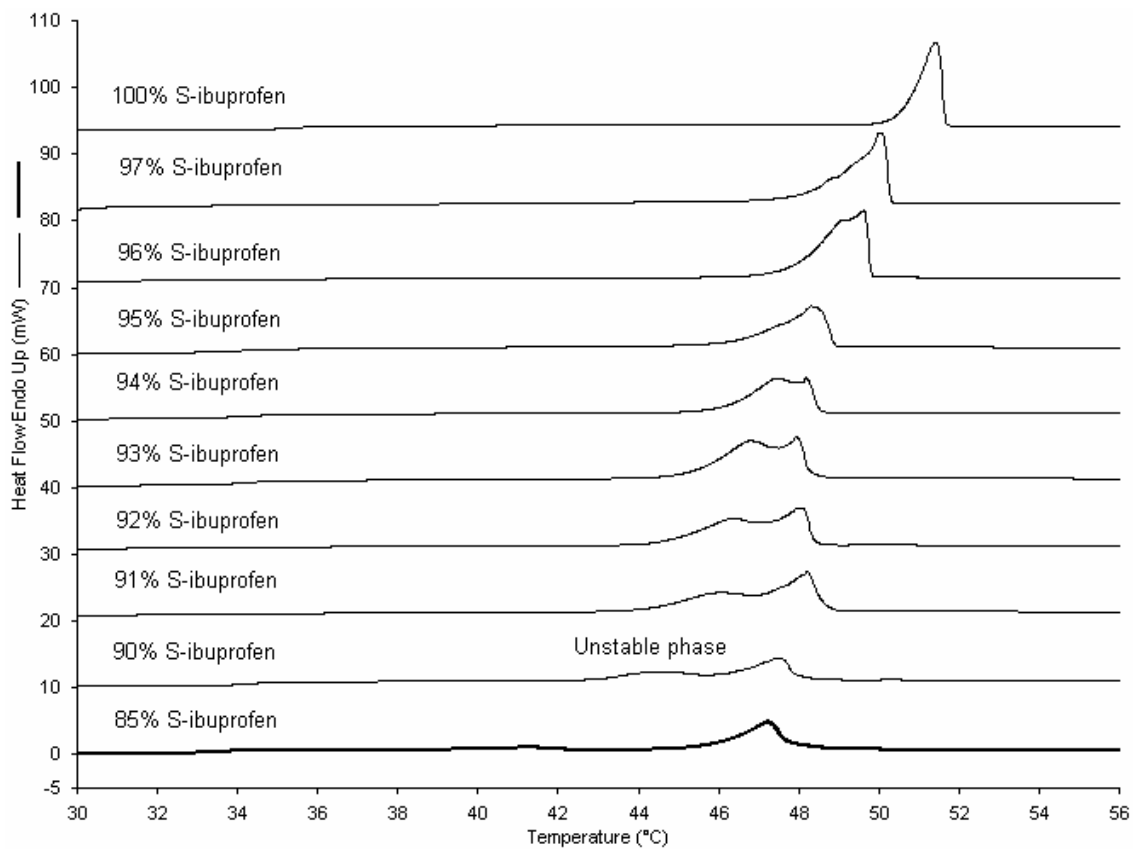


Figure 5.2. The DSC thermograms of mixtures of enantiomers of ibuprofen with S-ibuprofen ranging from 85 – 100 %

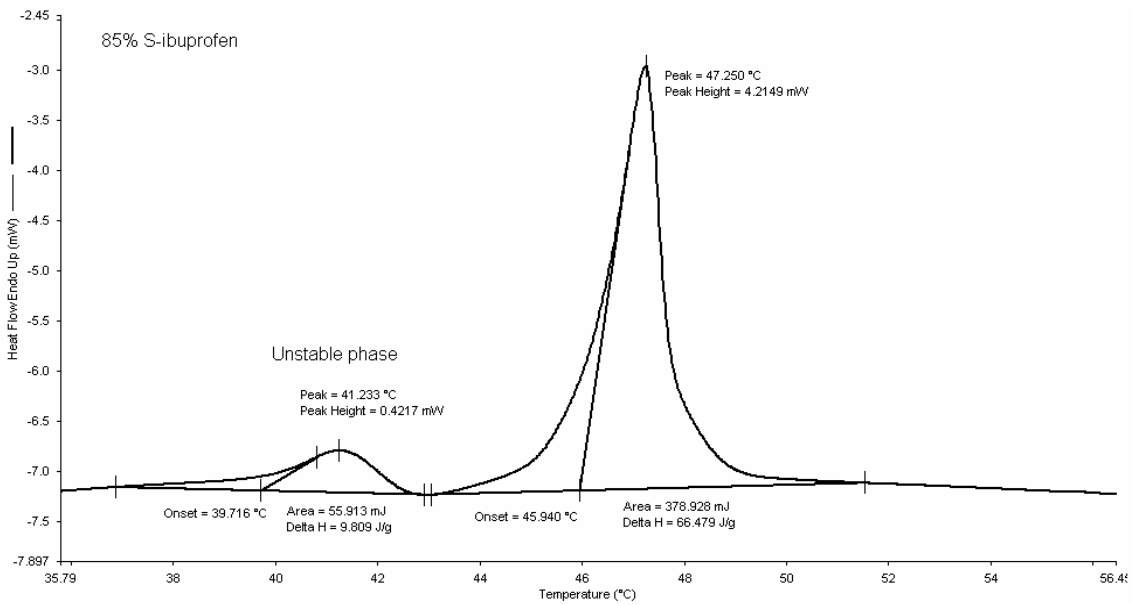
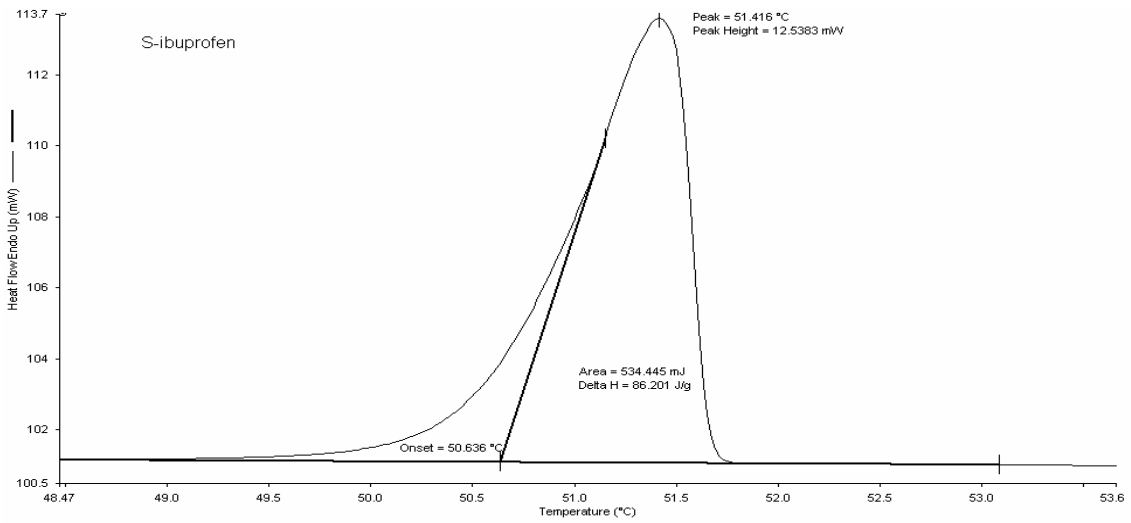


Figure 5.3. DSC thermograms of (a) S-ibuprofen and (b) 85% S-ibuprofen with a small peak showing the unstable phase

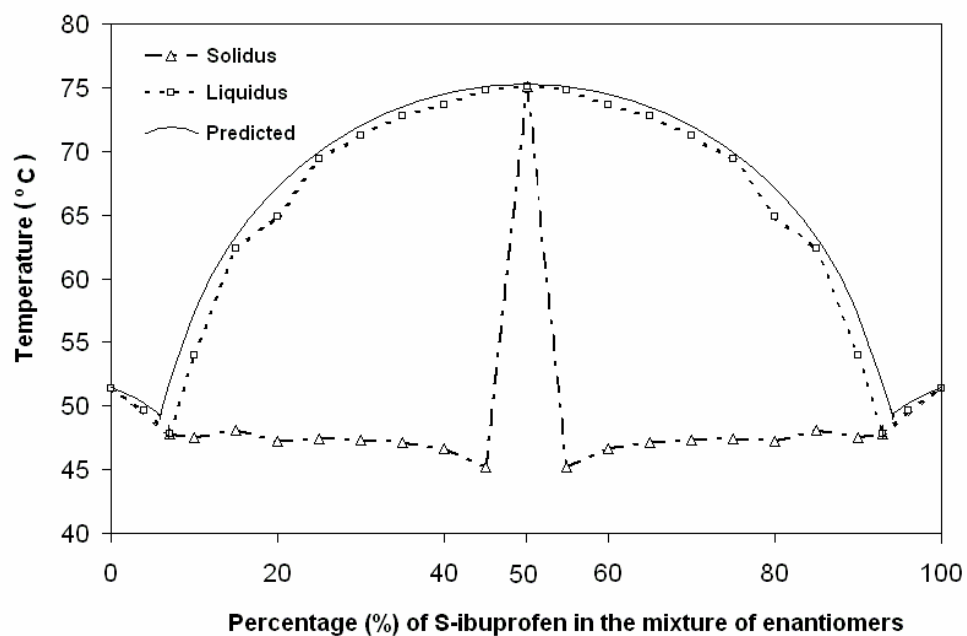


Figure 5.4. Phase diagram obtained from DSC and predicted by the models (the melting points of 0 – 50 % of S-ibuprofen are represented by using the data obtained from 50 – 100 % of S-ibuprofen).

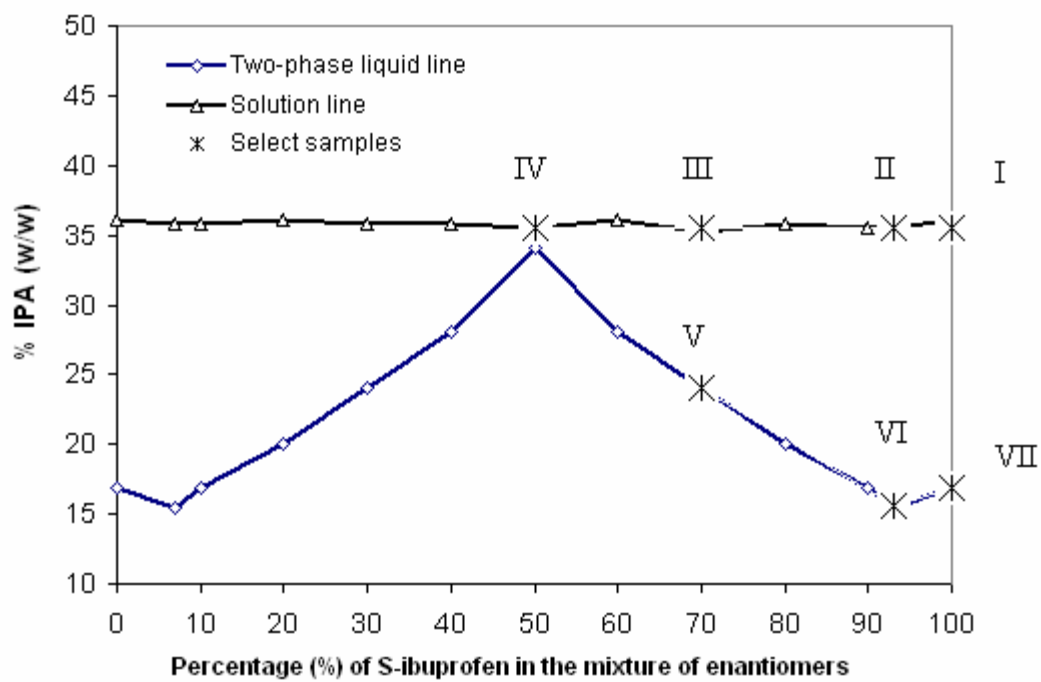


Figure 5.5. Phase diagram of enantiomers of ibuprofen in the presence of aqueous IPA

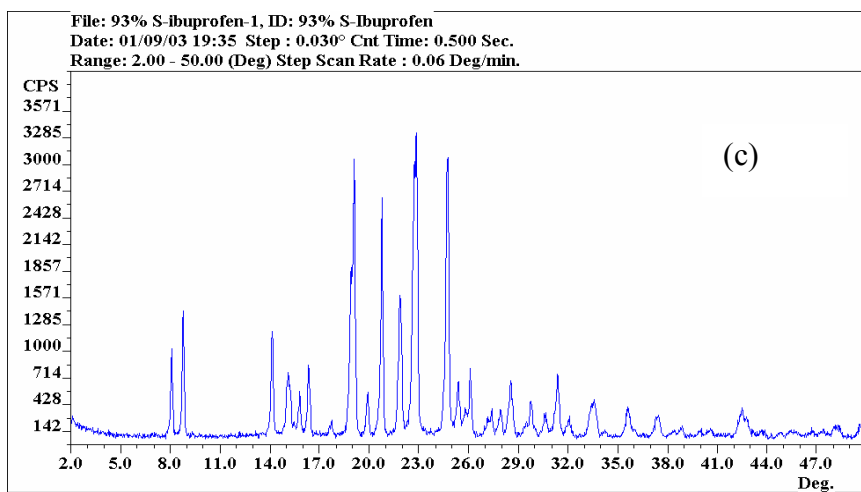
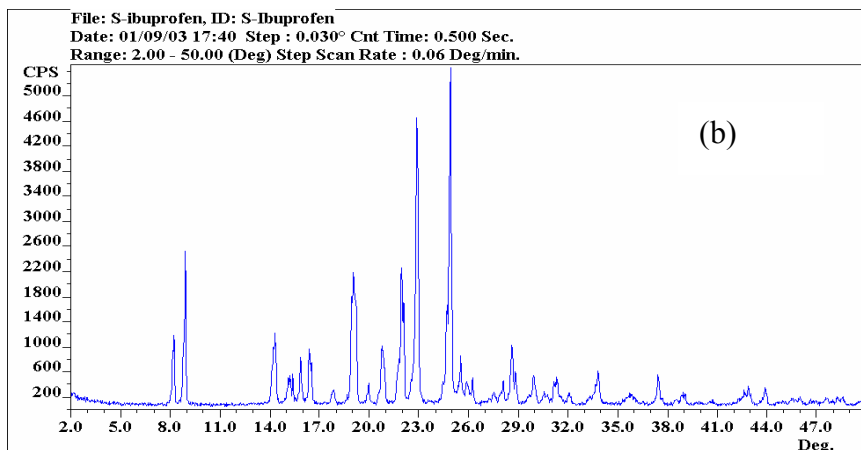
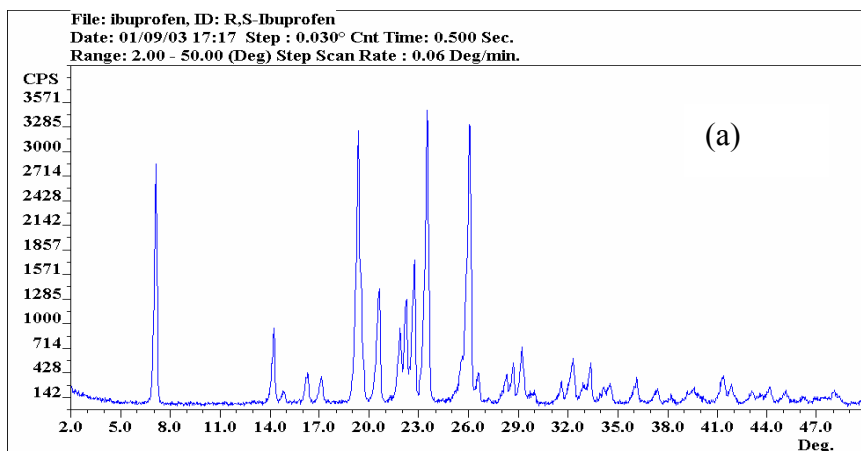


Figure 5.6. XRPD of (a): pure R,S-ibuprofen; (b): S-ibuprofen; and (c): the eutectic of enantiomers (93% S-ibuprofen)

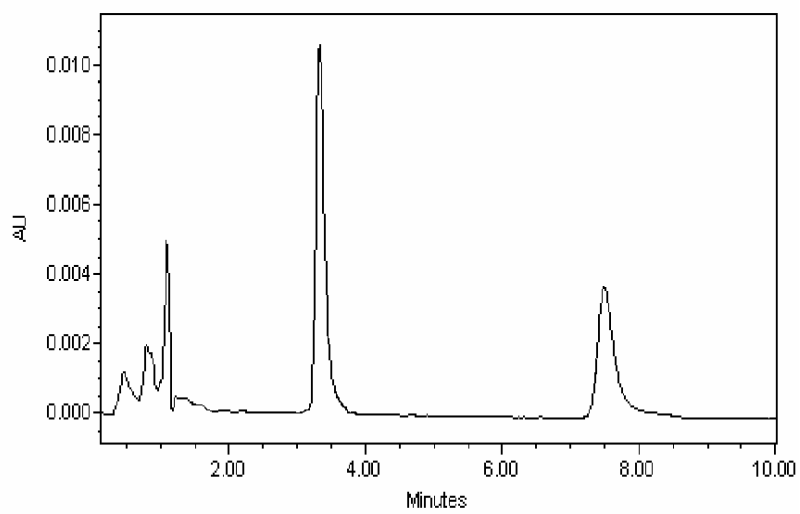


Figure 5.7. HPLC profile of separation of ibuprofen (7.6 min) and ketoprofen (3.3 min) in diffusion samples

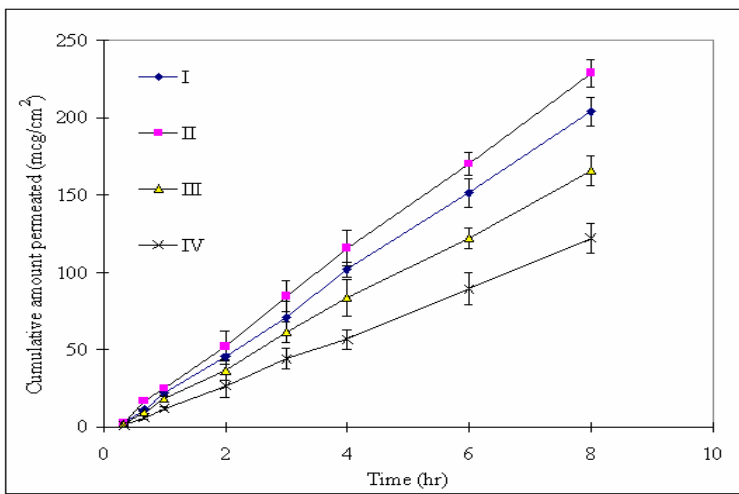


Figure 5.8. The permeation profile of ibuprofen through the shed snake skin from preparations at the same concentration

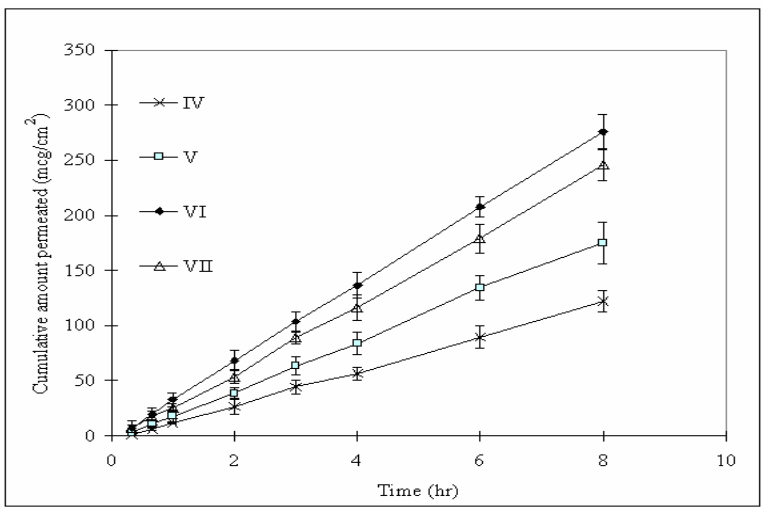


Figure 5.9. The permeation profile of ibuprofen through the shed snake skin from saturated preparations

CHAPTER 6

THE FORMULATION OF AND DRUG RELEASE FROM EMULSION, CREAM AND GEL OF THE BINARY EUTECTIC OF IBUPROFEN AND KETOPROFEN

Yuan, X., Capomacchia, A.C. To be submitted to the Journal of Drug Development and Industrial Pharmacy

Abstract

Ibuprofen and ketoprofen form a binary eutectic with lower melting point, and the solid mixture can be transformed into a two-phase liquid system with an aqueous phase and an oily phase in the presence of aqueous isopropyl alcohol. An emulsion was prepared after adding surfactant to the two-phase liquid system and an O/W cream was prepared based on the emulsion for enhanced transdermal delivery of ibuprofen and ketoprofen. The eutectic mixture was also developed into two other O/W creams, a W/O cream and a gel to investigate the effect of vehicles and bases on drug permeation. Drug release testing was conducted to compare the fluxes of ibuprofen and ketoprofen in the emulsion, creams, gel and two commercial creams using shed snake skin as the model membrane. The emulsion showed the highest fluxes, while the O/W cream had higher fluxes than both W/O cream, gel and commercial products. The stability of the selected O/W cream was investigated using centrifugation, three cycles of freeze-thaw and microscopic examination. The selected cream formulation was also stored at temperatures of 25 and 40 °C for six months and examined periodically for organoleptic characteristics, content of drugs, particle sizes and apparent viscosity. The product was found to be stable in the period of six-month storage.

Keywords: Ibuprofen; Ketoprofen; Enhanced transdermal drug delivery; Eutectic; Cream; Gel; Semi-solid formulation; Stability

1. Introduction

Ibuprofen and ketoprofen are among of the most widely used non-steroidal anti-inflammatory drugs (NSAIDs) in treating of rheumatoid arthritis and related diseases (Lawrence et al., 1998). Traditional oral dosage forms of NSAIDs usually upset the stomach and cause nausea. Long-term use can result in stomach ulcer and kidney toxicity. Topical or transdermal delivery of these drugs offers several advantages over the traditional oral administration method. It not only avoids the hepatic first-pass effect, gastric irritation and renal side effects, but also enhances therapeutic efficacy at the site of action and therefore would have better patient compliance. Extensive research has been done to develop these drugs into topical formulations to overcome the adverse effects associated with oral doses for prolonged periods (Rovensky J et al,2001. Vaile JH, Davis P, 1998. Chlud K, 1991. Valenta C et al. 2000).

There are many factors that may influence drug permeation through the skin barrier of stratum corneum, including solubility, lipophilicity, ionization, molecular weight or size, stability and hydrogen bonding ability. Among them, one particularly important factor is the intrinsic solubility of drug in skin lipids, which is closely related to its melting point, lipophilicity, entropy of fusion, and membrane density. The melting points of some anti-emetic drugs have been shown to be inversely proportional to their lipophilicity ($\log P$) and solubility in skin lipids and, therefore, to their transdermal flux (Calpena et al., 1994). Based on ideal solution theory, a relationship between transdermal permeation and melting point of the permeant was proposed as follows (Kasting et al. 1987):

$$S_{ideal} = \frac{\rho}{1 - \{1 - \exp[\frac{\Delta S_f}{RT}(T_m - T)]\}} \frac{M_1}{MW} \quad (1)$$

where ρ is density of skin lipids, M_1 is average molecular weight of skin lipids, MW is molecular weight of the penetrant, T_m is melting point in degrees Kelvin, ΔS_f ($\Delta S_f = \Delta H_f / T_m$) is entropy of fusion of the penetrant and ΔH_f is heat of fusion. S_{ideal} was then entered into a proposed model to predict the maximum flux (J_m) from molecular weight and melting point using:

$$\log (J_m / S_{ideal}) = \log(D_0 / h) - (\beta / 2.303)v \quad (2)$$

where D_0 is a parameter related to diffusion coefficient D by $D = D_0 \exp(-\beta v)$, where v is molecular van der Waals volume and β is a parameter related to the skin properties. v is property of the permeant while D_0 and β are properties of the skin. For rigid molecules, ΔS_f is slightly varying and is approximately 13.5 EU or 56.5 J mol⁻¹ K⁻¹ (Yalkowski and Valvani, 1980). According to Equation (1), S_{ideal} increases significantly when melting point decreases over 10 °C. It also follows that there should be a significant increase in transdermal flux J_m with decreasing melting point, and thus higher S_{ideal} , assuming all other factors being equal.

The melting temperature-membrane transport (MTMT) concept (Touitou et al., 1994), again based on the ideal solution theory, has been proposed to predict the relative transdermal fluxes of chiral isomers with different melting points. This concept shows that the ratio of maximum fluxes of enantiomer mixtures is equal to the ratio of their lipid solubility. The solubility, in terms of mole fraction X of a penetrant in a given solvent, was then related to the melting temperature (T_m) and enthalpy of fusion (ΔH) as shown:

$$\ln X = - \frac{\Delta H}{R} \left(\frac{T_m - T}{T \cdot T_m} \right) \quad (3)$$

where R and T are gas constant and temperature of the solution, respectively. These equations clearly show that a reduction in the melting point of a penetrant will increase its solubility in skin lipids and thus enhances transdermal permeation. Therefore, if one can reduce the melting point of a drug without causing unfavorable changes to other physicochemical parameters, then this should enhance transdermal flux. A method by which the melting point of a compound can be reduced is eutectic formation (Grant et al., 1982; Ford et al., 1989). Eutectic is a Greek word meaning “most fusible” or “most easily melted”. A binary eutectic is a mixture of two compounds which do not interact with each other to form a new chemical entity, but which at certain ratios inhibit crystallization process of one another, resulting in a system with a lower melting point than either of the compounds.

Previous studies showed that ibuprofen and ketoprofen formed a binary eutectic with a lower melting point than that of both drugs in previous studies (X. Yuan et al. 2003). A two-phase liquid system with an aqueous phase and an oily phase was obtained from the eutectic mixture in the presence of aqueous isopropyl alcohol and showed higher *in vitro* permeation rates of ibuprofen and ketoprofen than other reference preparations. In this study, the two-phase liquid system of binary eutectic mixture was developed into an emulsion and a O/W cream in a hope to achieve enhanced transdermal drug delivery as compared to the commercial products. The eutectic mixture was also formulated into two other O/W creams, a W/O cream and a gel with different bases to compare the effect of different vehicle, polymer and formulation type on the

percutaneous absorption. The drug content, viscosity, particle size and apparent viscosity of a select O/W cream formulation were also investigated after being stored for six months.

2. Materials and methods

2.1 Materials

The following chemicals were obtained from commercial suppliers and used as received: ibuprofen, ketoprofen, methyl paraben, mineral oil, oleic acid, limonene, isopropyl myristate, cetyl alcohol, propylene glycol, polyoxyl 40 stearate, Tween 80, stearyl alcohol (Sigma Chemical Co., St. Louis, MO), isopropyl alcohol (IPA), HPLC grade acetonitrile, sodium acetate, dibasic sodium phosphate, phosphoric acid, sodium hydroxide (J. T. Baker Chemical Co., Phillipsburg, NJ), Pemulen® TR1-NF, Carbopol® 980NF (The BF Goodrich Co., Cleveland, OH) and Cremphor® EL, Pluronic F-127 (BASF corporation, Mount Oliver, NJ), Arlacel 165 (ICI Americas Inc., Wilmington, DE), petrolatum white, spermaceti (Gallipot Inc., St Paul, MN). Two commercial cream products of 10% ketoprofen and 10% ibuprofen were purchased from Your-Druggist Pharmacy (Coral Springs, FL). Distilled, deionized water was prepared by Milli Q system (Millipore Corporation, Bedford, MA). Shed snake skin was donated by the Sandy Creek Nature Center (Athens, GA).

2.2 Preparation of formulations

The compositions of emulsion, creams and gel formulation of the same amount of binary eutectic mixture of ibuprofen (2.83 %) and ketoprofen (4.24 %) are shown in Table 6.1. To prepare the emulsion of the eutectic mixture, ibuprofen and ketoprofen were dissolved in IPA at first. An appropriate amount of citrate buffer (0.05 M, pH 4.0) was added to the solution and to obtain a two-phase liquid system with an aqueous phase and an oily phase. Then the two-phase liquid system was emulsified by adding the surfactant of Cremophor® EL. The obtained emulsion was passed three times through a homogenizer (KU-1, Erweka-Apparatebau, Germany). To prepare O/W cream I, ibuprofen, ketoprofen and methyl paraben were dissolved first in IPA. Then 3.0 % Carbopol® 980NF was dispersed in water and stirred well for 5 hours, and 50 g of dispersion was used to mix with the solution of drugs. Cremophor® EL and Pemulen® were used as surfactant and co-surfactant. The appropriate amounts of water and solution of sodium hydroxide (30 %, w/v) were added, with final pH 4.0. Similar procedures were followed to prepare O/W cream II, the drugs were mixed with oleic acid, propylene glycol, cetyl alcohol, limonene and IPA first. Then the mixture was heated to 70 °C to dissolve the drugs before mixing with Carbopol® dispersion. To prepare the O/W cream III, ibuprofen, ketoprofen and methyl paraben were mixed with isopropyl myristate, oleic acid, propylene glycol, stearyl alcohol, IPA and petrolatum in a beaker. The mixture was then heated to 70 °C to dissolve the drugs. Polyoxyl 40 Stearate, Cremophor and Tween 80 were added as surfactants. To prepare the W/O cream, ibuprofen, ketoprofen, methyl paraben were mixed with spermaceti, IPA, oleic acid, petrolatum and mineral oil in a

beaker. The mixture was heated to 70 °C to dissolve the drugs, and melt the spermaceti, before it was emulsified by the surfactants Arlacel 165 and Pemulen. All the above mixtures were well stirred and homogenized three times using the Erweka homogenizer. To prepare the Pluronic gel of the eutectic mixture, Pluronic F-127 polymer was dispersed in buffer, then stirred for 1 hr and left in the refrigerator overnight to get a homogenous dispersion. Ibuprofen, ketoprofen and methyl paraben were mixed with oleic acid and IPA in a beaker. After the drugs were dissolved, the solution was mixed with Pluronic F-127 dispersion and stirred well. A transparent gel was obtained and centrifuged (IEC, Needham Heights, MA) at 5000 rpm for 30 min to eliminate the trapped air bubbles.

2.3 Viscosity and particle size analysis of the selected O/W cream

Appropriate amounts of the emulsion and the eutectic cream were removed and examined under a Leica TCS SP2 Spectral Confocal Laser Microscope (Leica Microsystems, Bensheim, Germany). 0.5 g of the cream was dispersed in 5 ml of diluent, which was citrate buffer (0.05M, pH 4.0) with the surfactant Cremphor. 1 ml of dispersion was injected into the mixing chamber of a NICOMP-732 dynamic light scattering particle sizer (Particle Sizing Systems, Santa Barbara, CA) for particle size analysis.

The apparent viscosity of the cream was measured at ambient temperature (25 °C) using a Brookfield viscometer (Brookfield Engineering Laboratories, Inc., Stoughton, MA). A No. 7 spindle was used and the rotation speed of the spindle was set at 10 rpm.

2.4 In vitro drug release testing

The permeation rates of ibuprofen and ketoprofen in the prepared emulsion, creams, gel and two commercial creams were determined and compared with each other using shed snake skin as a model membrane. A large whole piece of skin was cut into small circular pieces of the size that fitted to the Franz diffusion cells. The skin samples, which were left in the distilled water for 30 min to allow for complete hydration, were mounted onto the diffusion cells with the stratum corneum side facing the donor compartment. Three grams of the prepared emulsion and equivalent amounts of prepared creams and gel, commercial ibuprofen and ketoprofen creams were carefully applied onto the skin surface and the donor compartments were covered with Parafilm® (American National Can, Neenah, WI). The receptor compartments of diffusion cells (Dayton Electric Mfg. Co., Chicago, USA) were filled with 0.05 M phosphate buffer (pH 7.4) and maintained at 32 ± 1 °C by circulating water from a thermostat pump (Haake, Model F4391, Berlin, Germany). The receiver phase was continuously stirred at 300 rpm using a star head magnetic stirring bar. The effective diffusion area of the skin was 2.0 cm^2 , and the volume of the receptor compartment was 6.0 ml. Each sample test was replicated for three times. During 8 hours of the diffusion test, 200 μl of the receptor phase was periodically removed into the HPLC autosampler vials using a micro-syringe and immediately replaced with fresh buffer solution. Then 20 μl of the internal standard solution and 1.0 ml of 20% ACN solution were added into the vial. The steady state flux, J_{ss} ($\mu\text{g}/\text{cm}^2/\text{hr}$) of ibuprofen and ketoprofen were calculated using Fick's first law:

$$J_{ss} = \Delta M/S \cdot \Delta t = P \cdot C_d = D \cdot K \cdot C_d/h \quad (4)$$

$$D = h^2 / 6 \cdot L \quad (5)$$

where S is the effective diffusion area (cm^2) and $\Delta M/\Delta t$ is the amount of drug penetrating through the membrane per unit time at steady state ($\mu\text{g}/\text{hr}$); P is the permeability coefficient (cm/hr); C_d is the drug concentration in donor phase ($\mu\text{g}/\text{ml}$); D is the diffusion coefficient (cm^2/hr); K is the partition coefficient between vehicle and skin; h is the membrane thickness (cm); and L is the lag time (hr). One-way ANOVA was performed using SAS statistical package (SAS Institute Inc., Cary, NC) to determine significant differences among the J_{ss} values found for different preparations.

2.5 Stability studies of the selected O/W cream

Two glass jars each containing 100 g of the selected formulation, O/W cream I, were sealed and left at $-15\text{ }^\circ\text{C}$, and three cycles of freeze-thaw for the examination of organoleptic characteristics, crystal formation, coalescence of oily phase and separation of aqueous and oily phases were carried out. Separation of the two phases and the homogeneity was also studied by centrifuging (IEC, Needham Heights, MA) the cream in tubes at speeds ranging from 2000 to 5000 rpm for half an hour.

Another four glass jars with the cream were sealed and stored two each at 25 and $40\text{ }^\circ\text{C}$ for the long-term stability study. After being stored for three and six months, one jar at each temperature was taken and appropriate amounts of samples were removed and subjected to the drug content determination, particle size analysis, viscosity measurement and examination of organoleptic characteristics, homogeneity, crystal formation, aqueous

and oily phase separation. For drug content determination using HPLC, 0.1 g of each cream was dissolved in 100 ml of the HPLC mobile phase, which was 50:50 (v/v) acetonitrile : sodium phosphate buffer (0.025 M, pH 2.0), in a volumetric flask. The solution was agitated and sonicated for 30 minute to extract the drugs. Then 5 ml of the solution was withdrawn using a syringe and filtered using a 0.45 μm PTFE Whatman filter disk (Whatman Group, Kent, UK). 1 ml of the filtered solution was taken and diluted to 10 ml. Then 1 ml of diluted solution and 20 μl of the pentobarbital acid internal standard solution were added into the autosampler vial and vortexed well prior to HPLC analysis. Microscopic examination was performed to determine if there was any crystal formation. Particle size distribution of the sample was analyzed by a NICOMP dynamic light scattering particle sizer and apparent viscosity of the sample was measured using a Brookfield viscometer following the procedures described earlier.

2.6 HPLC analysis of ibuprofen and ketoprofen

The Waters HPLC system (Waters, Milford, MA) consisted of a Model 616 solvent delivery pump, a Model 600S controller, a Model 717plus autosampler equipped with a temperature-controlled rack, a photo-diode array UV detector, and a Millennium data station. Ibuprofen, ketoprofen and internal standard pentobarbital acid were separated on a Waters C18 analytical column (250 \times 4.6 mm I.D., 5 μm) at ambient temperature. The mobile phase was 50:50 (v/v) acetonitrile : phosphate buffer (0.025 M, pH 2.0). The flow rate was set at 1.0 ml/min. Absorbance was monitored at 223 nm using a photo-diode array UV detector. The automated injection volume was 20 μl for each sample. Weekly calibrations using the peak height ratios of drugs to internal standard were obtained for different concentrations from 20 ng/ml to 2 mg/ml. HPLC separation

was achieved within 10 minute run and the chromatogram of analysis is shown in Figure 6.6. The retention time of ibuprofen, ketoprofen, methyl paraben and the internal standard were 7.6, 3.3, 1.8 and 2.3 minute, respectively.

3. Results and discussion

3.1 Preparation of formulations

In previous studies (X Yuan et al, 2003), ibuprofen and ketoprofen were found to form a binary eutectic, mutually depressing their melting points at ambient temperature. After the addition of aqueous IPA, the mixture formed a two-phase liquid system containing an aqueous phase and an oily phase. It was found that oily phase had very high drug concentrations of both ibuprofen and ketoprofen. The composite phase diagram was obtained to study the phase changes of the drugs at different ratios in the mixture systems. Different preparations of drugs were chosen from the phase diagram to compare *in vitro* membrane permeation using Franz diffusion cells and shed snake skin as the model membrane. The results showed that the preparation of the binary eutectic two-phase liquid system provided the highest permeation rates of both ibuprofen and ketoprofen among all the test preparations.

In this study, the emulsion prepared from the binary eutectic two-phase liquid system was further developed into an O/W cream formulation. The binary eutectic of ibuprofen and ketoprofen was also developed into two other O/W creams with different vehicles and into a pluronic gel. For the cream formulation, the drugs and preservative were dissolved in the organic solvent at first to avoid the solid crystals being left over

after simple mixing. For emulsion and O/W cream I, the amount of IPA required to get the binary eutectic two-phase liquid system was obtained from the composite phase diagram obtained in a previous study (X. Yuan et al., 2003). Carbopol 980NF, which is a crosslinked polymer of acrylic acid, requires a long time to be completely dispersed. Therefore, the dry powder of Carbopol polymer was dispersed in water and stirred well for 5 hours before the dispersion was mixed with the solution of drugs and preservative. Pemulen were added as a polymeric emulsifier in this cream formulation, since Pemulen and Carbopol polymers are usually used in combination for thickening topical lotions, creams and gels. In addition, Pemulen can help form occlusive layers in a short time after the cream has been applied. As oleic acid was reported to be an enhancer for permeation of NSAIDs, the same amount of oleic acid was added in the O/W cream II, III and W/O cream and gel. Three passes of formulation through the homogenizer yielded good homogenization and small particle sizes of cream, which helped improve the percutaneous absorption. Glass jars used for storing the creams were sealed to prevent the evaporation of vehicle from the cream.

3.2 Particle size analysis and viscosity determination of the select O/W cream

The O/W emulsion made from the binary eutectic two-phase liquid system was observed under a Leica Spectral Confocal Laser microscope. It was found that some oily droplets were dispersed in the external aqueous phase, as shown in Figure 6.1. The majority of drugs were distributed in the oily phase and accounted for 73 % of total weight of oily phase (X. Yuan et al. 2003). Very high concentration and maximum

thermodynamic activity of the drugs were achieved in the oily phase and therefore provided enhanced transdermal drug delivery. Oily droplets were still found in the O/W cream I based on the emulsion of binary eutectic two-phase liquid system under microscopic examination as shown in Figure 6.2. The particle size distribution of the oily droplets in the select cream, O/W cream I, was determined using the particle sizer and is shown in Figure 6.3, and the Gaussian distribution (with intensity, volume and number weighting) was used to describe it. The results showed that the particle sizes had normal distribution, with the mean diameter of 661.5 nm in number weighting (Table 6.2). The obtained sub-micron oily droplets could provide large contact surface area with the skin after being applied topically, and therefore could improve percutaneous absorption of drugs in formulation (Friedman D.I. et al, 1995).

The obtained O/W cream I was very viscous, therefore the smallest spindle (No. 7) of the Brookfield viscometer was used and the rotation speed of the spindle was set at low speed to measure more accurately. The cream was stored in glass jars at ambient temperature for three days to equilibrate prior to the viscosity measurements using Brookfield viscometer. The apparent viscosity of the cream was determined to be $56.3 \pm 1.4 \text{ (cps)} \times 10^3$ ($n = 3$) at ambient temperature.

3.3 In vitro drug release testing

The permeation profiles of ibuprofen and ketoprofen from the emulsion, creams and gel formulations are shown in Figures 6.4 and 6.5. The permeation rates of drugs were calculated using linear regression analysis of steady state portion of the plot and

Fick's first law. The obtained results (Table 6.3) showed that the emulsion gave the highest permeation rates for both ibuprofen ($36.6 \mu\text{g}/\text{cm}^2/\text{hr}$) and ketoprofen ($32.8 \mu\text{g}/\text{cm}^2/\text{hr}$) than other formulations. The fluxes of ibuprofen and ketoprofen from the O/W cream I, which were based on the binary eutectic two-phase liquid system, were 22.3 and $19.1 \mu\text{g}/\text{cm}^2/\text{hr}$, respectively. Lower fluxes of drugs in the cream than these in the emulsion were most likely due to the rheological difference of cream and emulsion. The polymer of the thickener in the cream hindered the free flowing of the drugs dispersed in the viscous matrix. However, the fluxes of ibuprofen and ketoprofen in O/W cream I were 1.49 and 1.44 - fold higher than those obtained from the commercial ibuprofen and ketoprofen creams, which were 15.0 and $13.3 \mu\text{g}/\text{cm}^2/\text{hr}$, respectively. The enhanced percutaneous absorption of the drugs could be explained by the lower melting point of the binary eutectic and high concentration and maximum thermodynamic activity of drugs in the oily phase in the cream. The differences between the fluxes of ibuprofen and ketoprofen in emulsion, O/W cream I and commercial creams were tested to be statistically significant ($P < 0.05$) using one-way ANOVA performed by SAS statistical package.

Both O/W creams II and III had lower fluxes of ibuprofen (18.9 and $16.6 \mu\text{g}/\text{cm}^2/\text{hr}$) than that in O/W cream I ($22.3 \mu\text{g}/\text{cm}^2/\text{hr}$). In addition to IPA, propylene glycol, cetyl alcohol and oleic acid were used as vehicles in O/W cream II. As a result, it reduced the thermodynamic activity of ibuprofen in the oily phase and weakened the driving force of the drugs in permeation, although oleic acid, an unsaturated fatty acid, was known to be a penetration enhancer. However, O/W cream II and III had slightly higher fluxes of ketoprofen (21.1 and $23.5 \mu\text{g}/\text{cm}^2/\text{hr}$) than the O/W cream I (19.1

$\mu\text{g}/\text{cm}^2/\text{hr}$). The synergistic effect of propylene glycol and oleic acid on enhancing permeation of ketoprofen could attribute to the increase (Kim CK and et al. 1993). But the differences between the fluxes of ketoprofen in O/W cream I and II were not statistically significant ($P > 0.05$) using ANOVA performed by SAS statistical package.

In the W/O cream, the drugs had high partition coefficients in the oily petrolatum base and mineral oil, the driving force of drugs to permeate through stratum corneum was significantly reduced. The continuous oil phase also retarded water diffusion and reduced the hydration of skin. Therefore, this W/O cream had relatively lower fluxes of ibuprofen ($10.7 \mu\text{g}/\text{cm}^2/\text{hr}$) and ketoprofen ($12.6 \mu\text{g}/\text{cm}^2/\text{hr}$) than O/W creams. The gel formulation showed the lowest fluxes of both ibuprofen and ketoprofen, which were 8.4 and $11.7 \mu\text{g}/\text{cm}^2/\text{hr}$, respectively. This might be due to the rheology of the Pluronic gel, which was very viscous in nature and therefore prevented free flowing of drugs to the skin surface and reduced percutaneous absorption of the drugs. Incorporation of a higher percentage of aqueous alcohol might help improve its rheology characteristics and increase the permeation of drugs.

The above drug release testings showed that the skin could interact dynamically with the contacted environment and vehicles in different formulations. The applied vehicles in emulsion, creams and gel could modify the skin permeability as a result of solvent action and hydration effect on the stratum corneum. Different vehicles and polymers might also give rise to different plasticization or rheology on drug mobility in the formulation and stratum corneum, which is closely related to the drug diffusion coefficient. All of these factors contributed to the different fluxes and permeabilities of drugs in diffusion.

3.4 Stability studies of the select O/W cream

The O/W cream I based on the binary eutectic of two-phase liquid system was selected to carry out stability studies. The homogenized product showed the consistency of a gleaming white cream and was homogenous, non-greasy and smooth in texture. After three cycles of freeze-thaw, the formulation was still a shiny white cream with a homogeneous and non-greasy texture, and no other organoleptic changes were observed. No crystal formation, oily phase coalescence and separation of aqueous and oily phases were observed after visual and microscopic examination. In addition, no separation of two phases was observed after centrifuging the cream at high speed, and the homogeneity of cream was still the same as the original product.

The O/W cream I was examined after three - and six - month storage at room condition (25 °C) and at an accelerated condition (40 °C). It was still a white and homogeneous cream without noticeable organoleptic changes, crystal formation and phase separation after visual and microscopic examinations. At the same time, appropriate amounts of the samples were removed and subjected to drug content determination, particle size analysis, and apparent viscosity measurement, and the obtained results are shown in Table 6.4. The initial contents of ibuprofen and ketoprofen in the cream were 2.81 and 4.23 %, respectively. After storing for three months, 99.29 % of the ibuprofen and 99.05 % of the ketoprofen were recovered in the cream at 25 °C; and 99.64 and 99.29 % were recovered, respectively, at 40 °C. After a six - month storage period, over 99 % of both drugs were recovered in the cream at 25 and 40 °C. In addition, the particle size distribution and bulk apparent viscosity of the eutectic cream did not change significantly

after storing at both 25 and 40 °C as shown in Table 6.5. The results shown above demonstrated that the select formulation of the O/W cream I was stable at both room and accelerated conditions after storage for three and six months.

4. Conclusion

The binary eutectic mixture of ibuprofen and ketoprofen was successfully developed into O/W cream, W/O cream and gel formulations. In vitro drug release testings showed that the emulsion based on the binary eutectic two-phase liquid system had the highest permeation rates of both drugs among all formulations. This was due to the maximum thermodynamic activity and high drug concentration in the oily phase and the different rheology property of the emulsion from that of the cream or gel formulation. The O/W cream based on the two-phase liquid system had higher fluxes than the two commercial creams, which was attributed to the lower melting point of drugs in the binary eutectic in O/W cream and thereafter higher skin lipid solubility. Different vehicles, polymers and rheology of formulation resulted in different permeation rates of drugs in cream and gel formulations. The organoleptic characteristics, drug contents, particle size distribution and apparent viscosity of the select O/W cream did not change significantly during six-month storage period. The studies suggested that the formulation of the O/W cream of the binary eutectic could be employed and optimized for enhanced transdermal delivery of ibuprofen and ketoprofen.

References

Calpena, A. C.; Blanes, C.; Moreno, J.; Obach, R.; Domenech, J. A Comparative In Vitro Study of Transdermal Absorption of Anti-emetics. *J. Pharm. Sci.* 1994, 83: 29-33.

Chlud K. Percutaneous Therapy of Painful Osteoarthritis. *Therapeutische Umschau* 48 (1): 42-45 JAN 1991.

Ford, J. L.; Timmins, P. *Pharmaceutical Thermal Analysis*; John Wiley and Sons: New York, pp. 47-67 1989.

Friedman DI, Schwarz JS, Weisspapir M.. Submicron emulsion vehicle for enhanced transdermal delivery of steroidal and nonsteroidal antiinflammatory drugs. *Journal of Pharmaceutical Sciences* 84 (3): 324-329 MAR 1995.

Grant, D.; Abougela, I. *Physico-chemical Interactions in Pharmaceutical Formulations*. *Anal. Proc.* 19: 545-549 1982.

Kasting, G. B.; Smith, R. L.; Cooper E. R. Effects of Lipid Solubility and Molecular Size on Percutaneous Absorption. *Pharmacol. Skin.* 1987, 1: 138-153.

Kim CK, Kim JJ, Chi SC, Shim CK. Effect of fatty-acids and urea on the penetration of ketoprofen through rat skin. *International Journal of Pharmaceutics* Vol 99, Iss 2-3, 109-118, 1993.

Lawrence, R. C., Helmick, C. G., Arnett, F. C., 1998. Estimates of the prevalence of arthritis and selected musculoskeletal disorders in the United States. *Arth. Rheum.* 41: 778-799.

Rovensky J, Micekova D, Gubzova Z, Fimmers R, Lenhard G, Vogtle-Junkert U, Schreyger F. Treatment of knee osteoarthritis with a topical non-steroidal antiinflammatory drug. Results of a randomized, double-blind, placebo-controlled study on the efficacy and safety of a 5% ibuprofen cream. *Drugs under Experimental and Clinical Research.* 27 (5-6): 209-221 2001.

Touitou, E.; Chow D. D.; Lawter J. R. Chiral Beta-blockers for Transdermal Delivery. *Int. J. Pharm.* 104: 19-28 1994.

Vaile JH, Davis P. Topical NSAIDs for musculoskeletal conditions - A review of the literature. *Drugs* 56 (5): 783-799 NOV 1998.

Valenta C, Wanka M, Heidlas J. Evaluation of novel soya-lecithin formulations for dermal use containing ketoprofen as a model drug. *Journal of Controlled Release* 63 (1-2): 165-173 JAN 3 2000.

Yalkowski, S. H.; Valvani, S. C. Solubility and Partitioning. I. Solubility of Nonelectrolytes in Water. *J. Pharm. Sci.* 69: 912-922 1980.

Yuan, X. Capomacchia, A.C. Enhanced membrane permeation NSAIDs based on the binary eutectic of two-phase liquid system. To be submitted to *Journal of Pharmaceutical Development and Technology*. 2003.

Yuan, X. Capomacchia, A.C. Physicochemical studies of binary eutectic of ibuprofen and ketoprofen and mathematical models for enhanced transdermal drug delivery. In preparation to be submitted to *International Journal of Pharmaceutics*. 2003.

Table 6.1. The composition (%) of formulations of binary eutectic

Components	O/W	O/W	O/W	O/W	W/O	Pluronic
	emulsion	cream I	cream II	cream III	cream	Gel
Ibuprofen	2.83	2.83	2.83	2.83	2.83	2.83
Ketoprofen	4.24	4.24	4.24	4.24	4.24	4.24
IPA	22.2	22.2	5.0	2.0	5.0	12.0
Isopropyl myristate	—	—	—	5.0	—	—
Carbopol 980NF	—	1.5	1.5	—	—	—
Cremophor EL	0.5	0.5	0.5	2.0	—	—
Pluronic F-127	—	—	—	—	—	20.0
Pemulen	—	1.0	0.5	—	2.0	—
Oleic acid	—	—	2.0	2.0	2.0	2.0
Spermaceti	—	—	—	—	5.0	—
Mineral oil	—	—	—	—	40.0	—
Propylene glycol	—	—	2.0	10.0	—	—
Cetyl alcohol	—	—	1.0	—	—	—
Stearyl alcohol	—	—	—	16.0	—	—
Limonene	—	—	0.5	—	—	—
Petrolatum	—	—	—	20.0	20.0	—
Arlacel 165	—	—	—	—	4.0	—
Polyoxyl 40 Stearate	—	—	—	2.0	—	—
Tween 80	—	—	—	2.0	—	—
Methyl paraben	—	0.5	0.5	0.5	0.5	0.5

Table 6.2. Particle size of the oily droplets in the cream at 25 °C

Weighting	Mean Diameter (nm)	Std. Deviation (nm)	Percentage (%)
Intensity	1481.1	924.6	62.3
Volume	2185.3	1361.4	62.3
Number	661.5	412.1	62.3

Table 6.3. Fluxes of ibuprofen and ketoprofen in formulations through the model membrane (n = 3)

Preparation	J_{ss} of ibuprofen ($\mu\text{g}/\text{cm}^2/\text{hr}$)	J_{ss} of ketoprofen ($\mu\text{g}/\text{cm}^2/\text{hr}$)
Emulsion	36.6	32.8
O/W cream I	22.3	19.1
O/W cream II	18.9	21.1
O/W cream III	16.6	23.5
W/O cream	10.7	12.6
Gel	8.4	11.7
Ibuprofen cream	15.0	—
Ketoprofen cream	—	13.3

Table 6.4. Stability of the eutectic cream (n = 3)

Time (month)	Temperature (°C)	Ibuprofen (%)	Ketoprofen (%)	Particle size (nm) ^b	Viscosity (cps × 10 ³)
0	25	2.81 ± 0.08	4.23 ± 0.05	661.5 ± 412.1	56.3 ± 1.4
	40 ^a	2.81 ± 0.07	4.23 ± 0.06	674.3 ± 454.3	55.2 ± 1.6
3	25	2.79 ± 0.05	4.19 ± 0.02	678.4 ± 450.6	57.2 ± 1.7
	40	2.80 ± 0.04	4.20 ± 0.09	697.5 ± 452.2	53.4 ± 1.3
6	25	2.80 ± 0.06	4.21 ± 0.07	694.7 ± 464.9	59.4 ± 1.5
	40	2.81 ± 0.07	4.23 ± 0.05	715.5 ± 482.4	51.3 ± 1.6

^a The cream was stored in the oven (40 °C) for an hour before measurement.

^b The number weighting of the Gaussian distribution for particles size analysis was used.

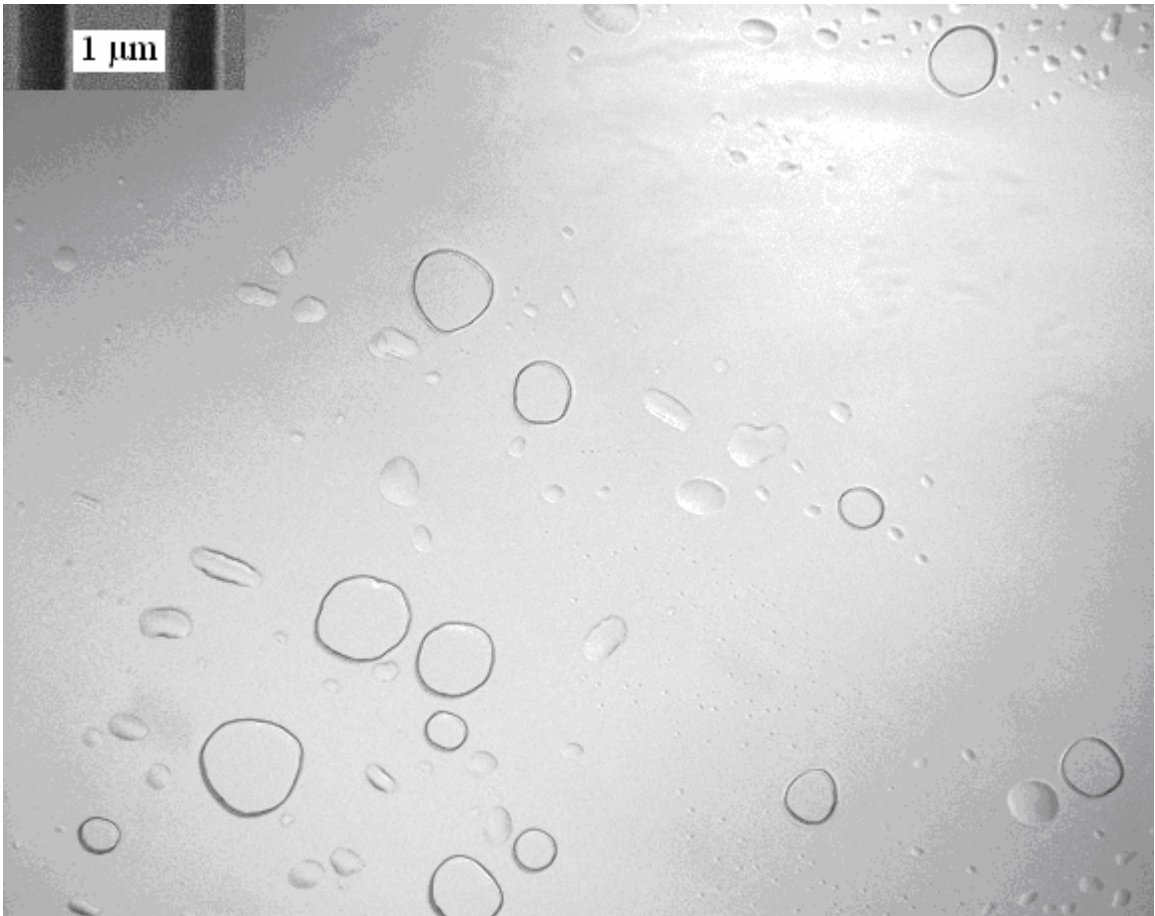


Figure 6.1. Photomicrography of oily droplets in the emulsion from the binary eutectic two-phase liquid system

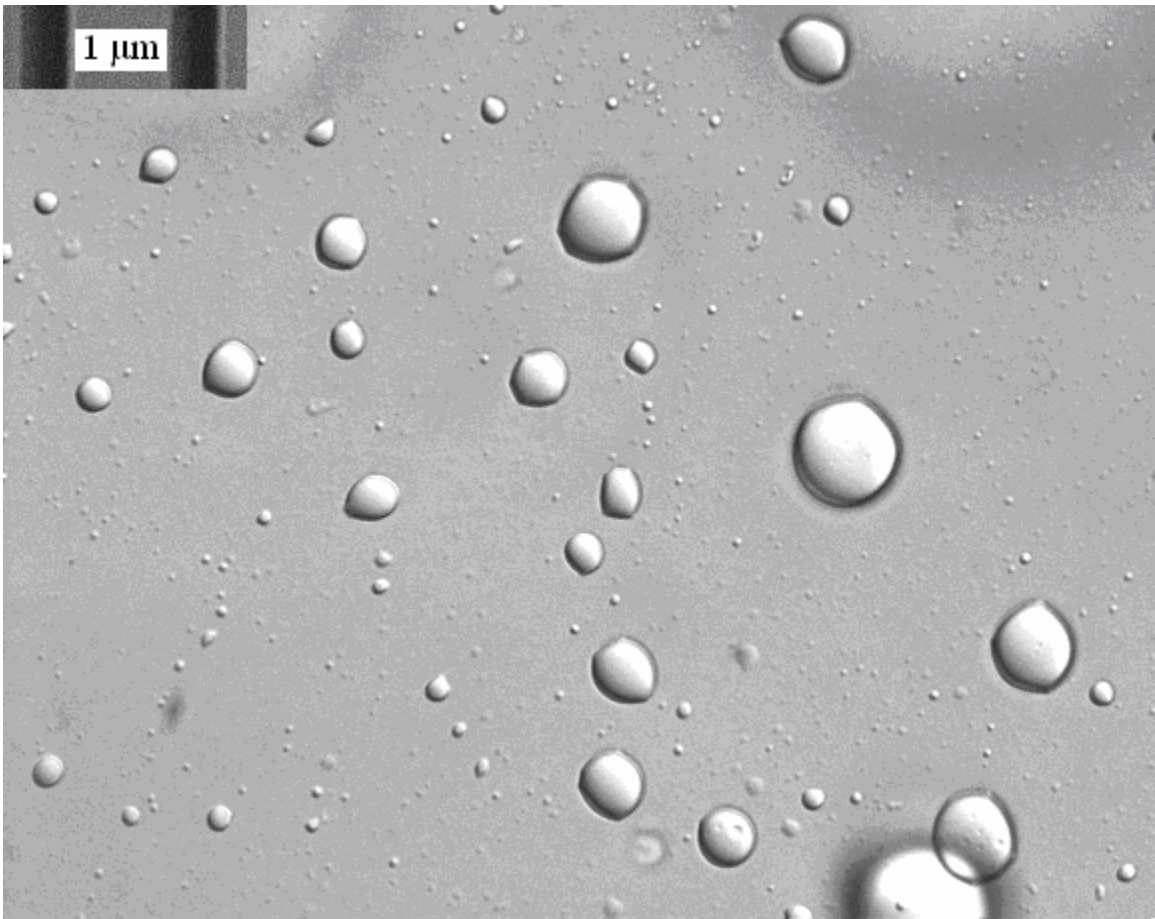


Figure 6.2. Photomicrography of oily droplets in the cream from the binary eutectic two-phase liquid system

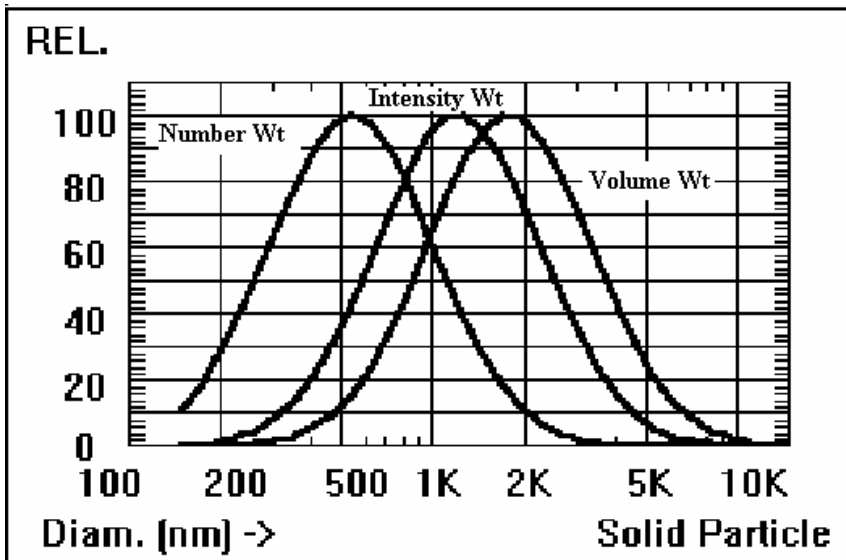


Figure 6.3. The Gaussian distribution of particle sizes in the cream

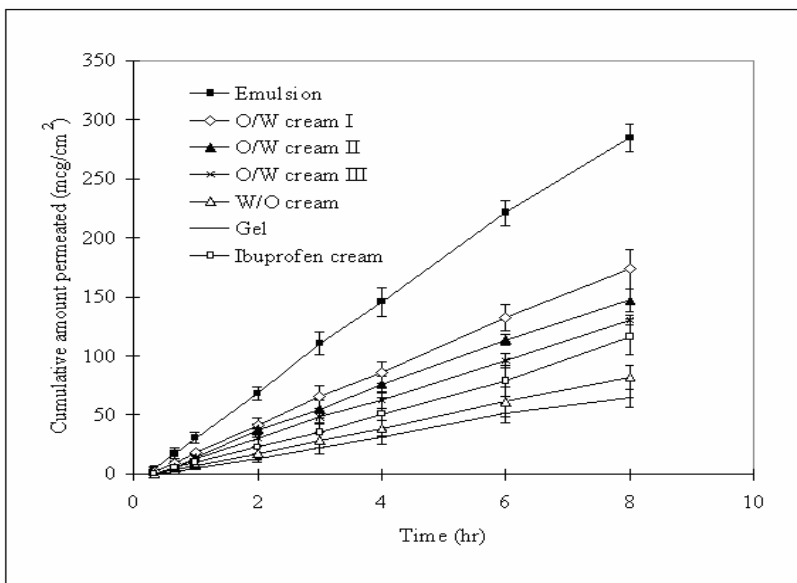


Figure 6.4. Permeation profiles of ibuprofen from different formulations through shed snake skin (n = 3, error bar = SD)

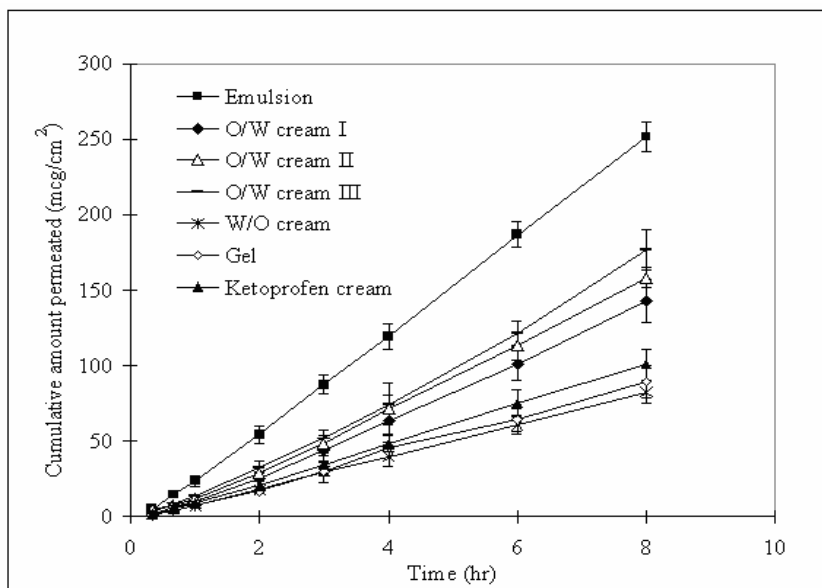


Figure 6.5. Permeation profiles of ketoprofen from different formulations through shed snake skin (n = 3, error bar = SD)

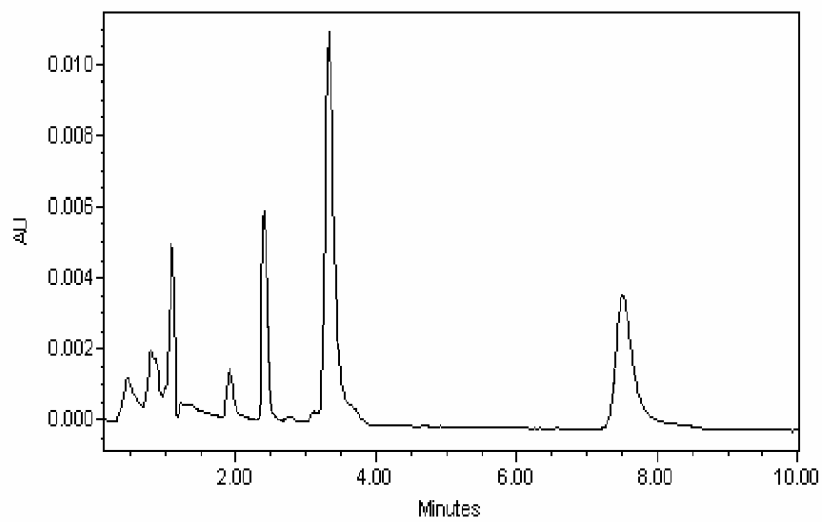


Figure 6.6. HPLC profile of ibuprofen (7.6 min), ketoprofen (3.3 min), methyl paraben (1.8 min) and internal standard (2.3 min) in the *in vitro* diffusion samples

CHAPTER 7

CONCLUSIONS

The eutectic formation of ibuprofen in the presence of another non-steroidal anti-inflammatory drug (NSAID) significantly depressed the melting points of these compounds with reduced enthalpy and entropy of fusion in the binary eutectic. The addition of aqueous IPA to the binary mixture completely transformed the solid drugs into the oily state and resulted in a two-phase liquid system at ambient temperature. The preparation of the binary eutectic two-phase liquid system of these drugs significantly enhanced their membrane transport as compared to other reference preparations. It was confirmed that the melting point of a drug is inversely related to its membrane permeation due to increased lipid solubility of the drug when melting point is reduced. Using the thermodynamic data obtained from DSC studies, the two proposed mathematical models based on the ideal solution theory correctly predicted the increases of the steady state fluxes of these drugs as a result of melting point depression. The enhanced permeation was attributed to the lower melting point of the binary eutectic, and the high drug concentration and maximum thermodynamic activity in the oily phase of two-phase liquid system. The binary eutectic two-phase liquid system was shown to be stable at different temperatures and no impurities or degradation was found after being stored for a period of time. The pure enantiomers and eutectic of ibuprofen have lower melting points than racemic ibuprofen, therefore they have higher solubility in the skin lipids and demonstrate higher percutaneous absorption. The increasing trend of total ibuprofen flux, as a result of lower melting point of the eutectic and enantiomers, was also indicated by two theoretical models and was confirmed by diffusion experimentation. The same methodology can be applied to other chiral drugs, which have lower eutectic points than their racemates and enantiomers, to achieve enhanced

transdermal delivery of the drugs without modifying the chemical structures or adding chemical enhancers. The binary eutectic mixture of ibuprofen and ketoprofen was successfully developed into three O/W creams with different vehicles, a W/O cream and a gel formulations. The emulsion based on the two-phase liquid system of the eutectic mixture had the highest permeation rates of both drugs among all formulations. Different vehicles, polymers and rheology of formulation caused different permeation rates of drugs in different formulations. The organoleptic characteristics, drug contents, particle size distribution and apparent viscosity of the select O/W cream did not change significantly after three- and six- month storage. The select O/W cream formulation of binary eutectic mixture could be further investigated and optimized. The above studies suggested that the two-phase liquid system of binary eutectic mixtures of NSAIDs or other categories of drugs could be used in the transdermal or topical formulation development for enhanced percutaneous absorption.

APPENDIX:

DETERMINATION OF CARBAMAZEPINE IN UNCOATED AND FILM-COATED
TABLETS BY HPLC WITH UV DETECTION

Xudong Yuan*, H. W. Jun, J. W. McCall. Published in the Journal of Analytical Letters.
Vol. 36. No. 6. pp. 1197 – 1210. 2003.

Abstract

A simple and reliable method for the determination of carbamazepine in uncoated and film-coated tablets has been developed and validated by high-performance liquid chromatography with ibuprofen as the internal standard. The tablets were weighed and ground individually, and were extracted in methanol using method of sonification. The extract was diluted and purified using 0.45 μ m membrane filter. Separation was achieved on an Econosphere C18 5 μ analytical column with a mobile phase of 28:72 acetonitrile:sodium phosphate buffer. Detection was at UV 230 nm using a photodiode array detector. The mean retention times of carbamazepine and ibuprofen were 4.2 and 12.3 min, respectively. Peak height ratios were fit to a least squares linear regression for calculation of standard regression equation. The linear calibration range was from 5.0 to 25.0 μ g / ml with the lower limit of detection (LLOD) of 18 ng/ml and the lower limit of quantitation (LLOQ) of 60 ng/ml. This simple and convenient method produced good linearity, precision and accuracy and avoids using methylene chloride as the mobile phase. A modified USP method was also carried to analyze the drug content in the tablets. These results were compared statistically, and no difference was found between the new method and the modified USP method, while the new method is more convenient and is suitable for stability and dissolution studies of this drug.

Key words: Carbamazepine; Antiepileptic; High-performance liquid chromatography; HPLC; Photodiode array; Tablet; Film-coated

1. Introduction

Carbamazepine (5-carbamoyl-5H-dibenz[b,f]-azepine) is a tricyclic neutral lipophilic compound, which is widely used in partial epilepsy, trigeminal neuralgia and as an adjunct to neuroleptic therapy in psychosis ^[1]. Due to its favorable therapeutic profile, it has become one of the most used anticonvulsant drugs. It is nearly completely metabolized in the body ^[2], forming over 30 metabolites ^[3]. Many methods have been proposed for the simultaneous determination of carbamazepine in biological fluids, mostly in plasma or serum ^[4]. These include high-performance liquid chromatography (HPLC), gas chromatography (GC), gas chromatography-mass spectrometry (GC-MS), and immunoassays, such as fluorescence polarization immunoassays (FPIA) ^[5] or enzyme-multiplied immunoassay (EMIT) ^[6]. Because of heat instability and lack of specificity of carbamazepine for immunoassay, HPLC is the method of choice in most analysis of plasma and serum samples.

Carbamazepine is usually prepared as tablet, film-coated tablet or suspension dosage forms, and the tablet forms are most commonly used. The USP gives the monograph for the determination of carbamazepine in the tablet using HPLC with ultraviolet detection ^[7]. The quantitation method is to use peak height ratio of the reference concentration over the theoretical concentration level. If the concentration of sample preparation does not vary too much from the theoretical value, it is accurate enough to quantify the concentration. But if the concentration of the sample varies a lot from the theoretical value, for example, in stability or dissolution studies, this method would not be accurate for the measurement. In this study, an alternative analytical HPLC

method was developed and validated. It employs the regression equation method from a series of standard solutions with different concentration levels to calculate drug contents, which gives not only the accurate measurement of carbamazepine concentration near the theoretical concentration, but also a linear concentration range necessary for stability studies. Another potential problem associated with the USP method is that two phases could separate during the preparation of the mobile phase, which is the mixture of water, methanol, and methylene chloride (40:30:3). The reason could be that the room temperature is too low or the mobile phase is not well mixed, filtered and degassed. In the newly developed method, the mobile phase is only composed of acetonitrile and phosphate buffer (28:72), which does not show the similar problem found in the USP method.

2. Experimental

2.1 Reagents and materials

Tegral 200 (200 mg carbamazepine) scored uncoated tablets were supplied by Chemical Industries Development, S.A.A. (Giza, Egypt), and Tegretol CR 400 (400 mg carbamazepine) film-coated divitabs were supplied by Novartis Pharma AG (Basle, Switzerland). The following chemicals and solvents were used as received from commercial suppliers: carbamazepine, ibuprofen, phenytoin (Sigma Chemical Co., St. Louis, MO), sodium dibasic phosphate (J. T. Baker Chemical Co., Phillipsburg, NJ). HPLC grade methanol and acetonitrile, methylene chloride were purchased from Sigma

(Sigma Chemical Co., St. Louis, MO). Deionized and filtered water was obtained from Milli Q water purification system from Millipore (Bedford, MA).

2.2 Apparatus and conditions and application software

The HPLC system was primarily a Waters Alliance™ 2690 separation module (Waters, Milford, MA) consisting of a controller, a solvent delivery pump, a autosampler equipped with a temperature-controlled rack, a Waters 996 photodiode array detector, and a Waters Millennium³² version 3.05.01 data station was used. Carbamazepine was separated on an Alltech Econosphere C18 analytical column (250 × 4.6 mm I.D., 5µm, Alltech Associates, Deerfield, IL) at ambient temperature. The mobile phase was 28:72 (v/v) acetonitrile:0.02 M sodium phosphate buffer (pH 7.8). The flow rate was set at 1.0 ml/min. Absorbance was monitored at 230 nm using a photodiode array UV detector. The injection volume was 20 µl for each sample.

SAS 8.1 statistical software (SAS Institute Inc., Cary, NC 27513) was used to perform a one-way ANOVA test.

2.3 Standard solutions

Stock, working and internal standard solutions were prepared in methanol. 100 mg carbamazepine was weighed accurately and dissolved in methanol in a 100 ml volumetric flask. The volume was made up to 100 ml to get 1000 µg / ml stock solution. 1 ml was taken into a 10 ml volumetric flask and the volume was made up to get 100 µg /

ml stock solution. Then 0.5, 1.0, 1.5, 2.0 and 2.5 ml of this stock solution were taken into 10 ml volumetric flask, and methanol was used to dilute to 10 ml to get 5, 10, 15, 20 and 25 $\mu\text{g} / \text{ml}$ carbamazepine stock solution. 4000 μg ibuprofen was weighed accurately and dissolved in methanol in a 100 ml volumetric flask. The volume was made up to 100 ml to get 40 $\mu\text{g} / \text{ml}$ internal standard solution. 5 ml each of standard solutions of carbamazepine were mixed with 5 ml of internal standard solution of ibuprofen in each 10 ml volumetric flask to get five standard solutions for calibration.

2.4 Extraction procedure and sample solution preparations

For Tegral 200, 6 tablets were weighed and well ground individually, and were put into a 100-ml volumetric flask. 70 ml of methanol was added, and it was sonicated for about 10 minutes. An appropriate amount of methanol was added to make up to the volume, and was well mixed. After the solution was allowed to stand for about 10 minutes, 2.5 ml of this solution was transferred to a 25-ml volumetric flask, and the solution was diluted with methanol to volume, and mixed. 1.0 ml of this solution was transferred to a 10-ml volumetric flask, and the solution was diluted with methanol to volume, and mixed. Filter disk (0.45 μm) was used to filter and transfer 5.0 ml of this carbamazepine sample solution to a 10-ml volumetric flask. 5.0 ml of internal standard ibuprofen solution was added and mixed to get sample solutions that were subjected to HPLC analysis.

For Tegretol CR 400, 6 tablets were weighed and well ground individually, and were put into a 100-ml volumetric flask. 70 ml of methanol was added, and it was

sonicated for about 10 minutes. An appropriate amount of methanol was added to make up to the volume, and was well mixed. After the solution was allowed to stand for about 10 minutes, 2.5 ml of this solution was transferred to a 25-ml volumetric flask, and the solution was diluted with methanol to volume, and mixed. 0.5 ml of this solution was transferred to a 10-ml volumetric flask, and the solution was diluted with methanol to volume, and mixed. Filter disk (0.45 μm) was used to filter and transfer 5.0 ml of this carbamazepine sample solution to a 10-ml volumetric flask. 5.0 ml of internal standard ibuprofen solution was added and mixed to get sample solutions that were subjected to HPLC analysis.

In order to study the recovery and inter-day and intra-day precision, three concentration levels of carbamazepine were spiked in the extraction of Tegral 200 tablets. Five Tegral 200 tablets were weighed and ground together to give a mixture of powder. The average tablet weight was around 270 mg. 135, 180 and 270 mg of powder were taken respectively in a 100-ml volumetric flask, and 20 ml of 1000 μg / ml carbamazepine standard solution was spiked in for each sample. 50 ml of methanol was added and the same procedures were followed as the extraction for Tegral 200 tablets to get three spiked sample solution. Another 135, 180 and 270 mg of powder was taken separately and the extracts were used as the control.

2.5 Calibration curves

1.5 ml of standard solution for each concentration level of calibration (5, 10, 15, 20 and 25 $\mu\text{g}/\text{ml}$) was taken into the vial of autosampler and subjected to HPLC analysis.

Calibration curve was obtained by plotting the peak height ratios of carbamazepine to internal standard ibuprofen *versus* the nominal concentrations. The regression equation was calculated by the least-squares method using linear regression.

2.6 Method validation

The precision and accuracy of the method were evaluated by repetitive analysis of spiked sample solutions. The intra-day analyses were done for the spiked sample solutions with three concentration levels by five consecutive injections within a day (n=5). The inter-day analyses were done for the spiked sample solutions with three concentration levels by one injection each day for four days (n=4). The lower limits of detection and quantitation were derived from multiple measurements in the low concentration range. The level of three times the noise level was defined as the lower limit of detection (LLOD) and the level of ten times the noise level was used as the lower limit of quantitation (LLOQ).

2.7 Data analyses

Peak height ratios (carbamazepine over ibuprofen) were evaluated by least-squares linear regression analyses. The formula used to calculate the “unknown” concentrations is as follows: $y = Ax + B$, where A is the slope, and B is y-intercept, x is the peak height ratio and y is the concentration ($\mu\text{g} / \text{ml}$).

2.8 USP method

The USP method for analyzing the carbamazepine tablet was adopted here to compare with the new method. 6 Tegral 200 and 6 Tegretol CR 400 tablets were weighed and finely ground. The powder was transferred to a 100-ml volumetric flask, 70 ml of methanol was added. It was shaken by mechanical means for about 30 min and sonicated for about 2 min, then it was diluted with methanol to volume and mixed. The solution was allowed to stand for 10 min, and 10 ml of the clear solution was transferred to a 100-ml volumetric flask, and was diluted with methanol to volume and mixed. 10 ml of this solution was transferred to a 100-ml volumetric flask, and 10 ml of internal standard solution (600 μg / ml phenytoin) was added, then it was diluted with mobile phase (water:methanol:methylene chloride 40:30:3) to volume and mixed. The standard solutions were 20 and 40 μg / ml carbamazepine for Tegral 200 and 6 Tegretol CR 400 tablets, respectively. The quantity, in mg, of $\text{C}_{15}\text{H}_{12}\text{N}_2\text{O}$ in the portion of tablets was taken by the formula $10C(R_U/R_S)$, in which C is the concentration, in μg per ml, of USP Carbamazepine RS in the standard preparation, and R_U and R_S are the ratios of the analyte peak response to the internal standard peak response obtained from the assay and standard preparations, respectively.

3. Result and discussion

3.1 Chromatography

The specificity of the assay of carbamazepine is demonstrated in Fig. 1, which shows the spectrum of carbamazepine and ibuprofen extracted from the chromatography by photodiode array detection. No endogenous excipient peaks in Tegral 200 and Tegretol CR 400 tablets were found to interfere with detection of carbamazepine and ibuprofen. Validation data were collected over four consecutive days. HPLC chromatograms of the standard carbamazepine, sample preparation from the uncoated and film-coated tablets with internal standard ibuprofen are shown in Fig. 2. The mean retention times of approximately 4.2 and 12.3 min were consistently observed for ibuprofen and carbamazepine, respectively, throughout all analytical runs.

3.2 Linearity of calibration standard curves

Calibration curve data (Table 1) and calibration curve parameters for carbamazepine demonstrated that the calibration curves were linear in the concentration range from 5.0 to 25.0 $\mu\text{g} / \text{ml}$. The linear regression equation is $y = 25.448x + 0.1764$ with correlation coefficient of 0.9996 showing good linearity (Fig. 3). The molar absorptivity for carbamazepine is 16659, while for ibuprofen is 5817.7 under optimized chromatographic conditions at the 230 nm detection wavelength. The assay has the

necessary sensitivity and linearity to cover the concentration range of carbamazepine expected in the tablet dosage form. HPLC analytical data for carbamazepine in Tegral 200 and Tegretol CR 400 tablets using the new developed method (n = 6) are shown in Table 2.

3.3 Precision and accuracy

Since it's difficult to find the blank tablet with excipients only, known concentration of carbamazepine were spiked into the powder of the drug to give three concentration levels and another three corresponding powder samples were used as the control. The precision and accuracy data are shown in Table 4. The intra-day coefficients of variation were found to be within 0.26 to 0.40% for three drug concentration levels, while the inter-day coefficient of variation ranged from 0.35 to 0.45%. The accuracy was expressed as the percentage deviation between the mean concentration found for the added drug, which equals to the difference of drug concentration between spiked samples and the control, and the theoretical added drug concentration, which equals to $2 \mu\text{g} / \text{ml}$ ($20 \text{ ml} \times 1000 \mu\text{g} / \text{ml} \div 10000$). For these three concentration levels, the intra-day accuracy ranged from -0.29 to 0.12%, while the inter-day accuracy ranged from -0.51 to 1.23%.

3.4 Lower limit of detection and quantitation

The lower limit of detection (LLOD) for this assay 18 ng/ml was determined by the concentration of three times the noise level. The lower limit of quantitation (LLOQ) for this assay 60 ng/ml was determined by the concentration of ten times the noise level.

3.5 Comparison to the modified USP analytical method

The data obtained using the USP analytical method is shown in Table 3. A one-way ANOVA is performed to check statistically for the difference of these two analytical methods. SAS 8.1 statistical software was used to perform a one-way ANOVA using LSD, SNK, Tukey, Duncan and Scheffe tests at $\alpha = 0.05$. The data showed that $P = 0.9321$ for Tegral 200 tablets and $P = 0.8931$ for Tegretol CR 400 tablets, which are both larger than default α value 0.05. Thus there is no statistically difference between these two methods at significance level $\alpha = 0.05$, and LSD, SNK, Tukey, Duncan and Scheffe tests all suggest the same result. This means that the new analytical method is comparable to the modified USP method.

4. Conclusion

A reversed phase HPLC analytical method using a photodiode array detector was developed and validated for the assay of carbamazepine in the uncoated and film-coated carbamazepine tablet dosage forms. This method is comparable to the modified USP

method since no statistical difference was found between them and also eliminate methylene chloride from the mobile phase composition (which is important given the cost and environmental considerations pertaining to the use of this chlorinated solvent). This procedure is also suited for the stability and dissolution studies of carbamazepine tablet. No modification of a regular HPLC system was required.

References

- [1] VanValkenburg, C.; Kluznik J.C.; Merrill R. New Uses of Anticonvulsant Drugs in Psychosis. *Drugs* **1992**, 44, 326-335.
- [2] Faigle J.W.; Feldmann K.F.; Levy R.; Mattson R.; B. Meldrum; Penry J.K.; Dreifuss F.E. *Antiepileptic Drugs*, Raven Press, New York, 3rd ed., **1989**; 491-504.
- [3] Lertratanangkoon K.; Horning M.G. Metabolism of Carbamazepine, *Drug Metab. Dispos.* **1982**, 10, 1-10.
- [4] Burke J.T.; Thenot J.P. Determination of Antiepileptic Drugs, *J. Chromatogr.* **1985**, 340, 199-241.
- [5] Chai C.; Killeen A.A. Ther. Carbamazepine Measurement in Samples from the Emergency Room, *Drug Monit.* **1994**, 16, 407-412.
- [6] Martens J.; Banditt P. Validation of the analysis of carbamazepine and its 10,11-epoxide metabolite by high-performance liquid chromatography from plasma: comparison with gas chromatography and the enzyme-multiplied immunoassay technique, *J. Chromatogr.* **1993**, 620, 169-173.

[7] U.S. Pharmacopoeia / National Formulary. Prepared by the Council of Experts and published by the board of Trustees. The United States Pharmacopoeial Convention, Inc., Rockville, MD. **1995**, 265-267.

Table 1

Data for the new HPLC method

	1	2	3	4	5
Concentration ($\mu\text{g/ml}$)	5.0	10.0	15.0	20.0	25.0
Ratio ^a	0.1937	0.3762	0.5877	0.7823	0.9726
Slope			25.448		
y-intercept			0.1764		
R ² ^b			0.9996		
LLOD ^c			18		
LLOQ ^d			60		

^a Ratio = Peak height ratio of carbamazepine / ibuprofen , n = 3

^b R² = correlation coefficient

^c LLOD = lower limit of detection (ng/ml)

^d LLOQ = lower limit of quantitation (ng/ml)

Table 2

HPLC analytical data for carbamazepine in Tegral 200 and Tegretol CR 400 tablets using the new developed method (n = 6)

Tegral 200	Weight (mg)	Ratio ^a	Concentration ($\mu\text{g/ml}$) ^b	Content (mg) ^c	Percentage (%) ^d	% of content ^e
1	272	0.8100	20.79	207.9	103.95	74.78
2	278	0.7704	19.78	197.8	98.92	72.73
3	272	0.7431	19.09	190.9	95.44	70.17
4	267	0.7379	18.95	189.5	94.77	70.99
5	270	0.7551	19.39	193.9	96.96	71.82
6	271	0.7434	19.09	191.0	95.48	70.46
Average	271.7	0.7600	19.52	195.2	97.58	71.84
S.D.	3.61	0.0271	0.69	6.90	3.45	1.72
R.S.D. ^f	1.33	3.57	3.54	3.54	3.54	2.40

Tegretol CR 400	Weight (mg)	Ratio ^a	Concentration ($\mu\text{g/ml}$) ^b	Content (mg) ^c	Percentage (%) ^d	% of content ^e
1	601	0.7859	20.18	403.5	100.88	67.14
2	608	0.7855	20.27	403.3	100.83	66.33
3	609	0.7713	19.81	396.1	99.03	65.04
4	615	0.7653	19.65	393.1	98.28	63.92
5	612	0.7866	20.19	403.9	100.98	66.00
6	608	0.7828	20.10	401.9	100.46	66.10
Average	608.8	0.7796	20.03	400.3	100.08	65.75
S.D.	4.71	0.0090	0.25	4.57	1.14	1.12
R.S.D. ^f	0.77	1.16	1.23	1.14	1.14	1.71

^a Ratio = Peak height ratio of carbamazepine / ibuprofen , n = 3

^b Concentration = Carbamazepine concentration in the preparation solutions

^c Content = Calculated carbamazepine content in the tablet

^d Percentage = The percentage of carbamazepine found in the labeled weight of drug

^e % of content = The percentage of carbamazepine in the tablet

^f R.S.D. = The percentage of standard deviation in the average value

Table 3

HPLC analytical data for carbamazepine in Tegral 200 and Tegretol CR 400 tablets using the modified USP method (n = 6)

Tegral 200	Ratio ^a	Content (mg) ^b	Percentage (%) ^c
1	1.42	203.4	101.7
2	1.40	202.0	101.0
3	1.33	190.4	95.2
4	1.31	187.6	93.8
5	1.37	196.2	98.1
6	1.35	193.4	96.7
Average	1.36	195.5	97.8
S.D.	0.042	6.29	3.14
R.S.D. ^d	3.07	3.22	3.22

Tegretol CR 400	Ratio ^a	Content (mg) ^b	Percentage (%) ^c
1	2.69	398.8	99.7
2	2.73	404.8	101.2
3	2.69	398.8	99.7
4	2.68	397.2	99.3
5	2.71	401.6	100.4
6	2.69	398.8	99.7
Average	2.70	400.0	100.0
S.D.	0.02	3.00	0.75
R.S.D. ^d	0.74	0.75	0.75

^a Peak Height Ratio = carbamazepine / internal standard phenytoin

^b Content = Calculated carbamazepine content in the tablet

^c Percentage = The percentage of carbamazepine found in the labeled weight of drug

^d R.S.D. = The percentage of standard deviation in the average value

Table 4

Precision and accuracy of carbamazepine assay in the spiked samples

	Spiked ($\mu\text{g/ml}$) ^a	Un-spiked ($\mu\text{g/ml}$) ^b	Concentration found ($\mu\text{g/ml}$) ^c	R.S.D. (%) ^d	Accuracy (%) ^e
Intra-day	12.04	10.05	1.99	0.26	- 0.29
variability	15.36	13.36	2.00	0.40	0.12
(n = 5)	22.12	20.12	2.00	0.27	- 0.26
Inter-day	12.06	10.07	1.99	0.40	- 0.51
variability	15.39	13.36	2.03	0.45	1.23
(n = 4)	22.09	20.12	1.97	0.35	- 1.49

^a Spiked = Calculated spiked samples concentration

^b Un-spiked = Calculated un-spiked samples concentration

^c Concentration found = Calculated added concentration, which equals to spiked concentration minus the un-spiked concentration

^d R.S.D. (%) = The percentage of standard deviation in the average value

^e Accuracy (%) = The percentage deviation between the mean concentration found and the theoretical added concentration (2.0 $\mu\text{g/ml}$)

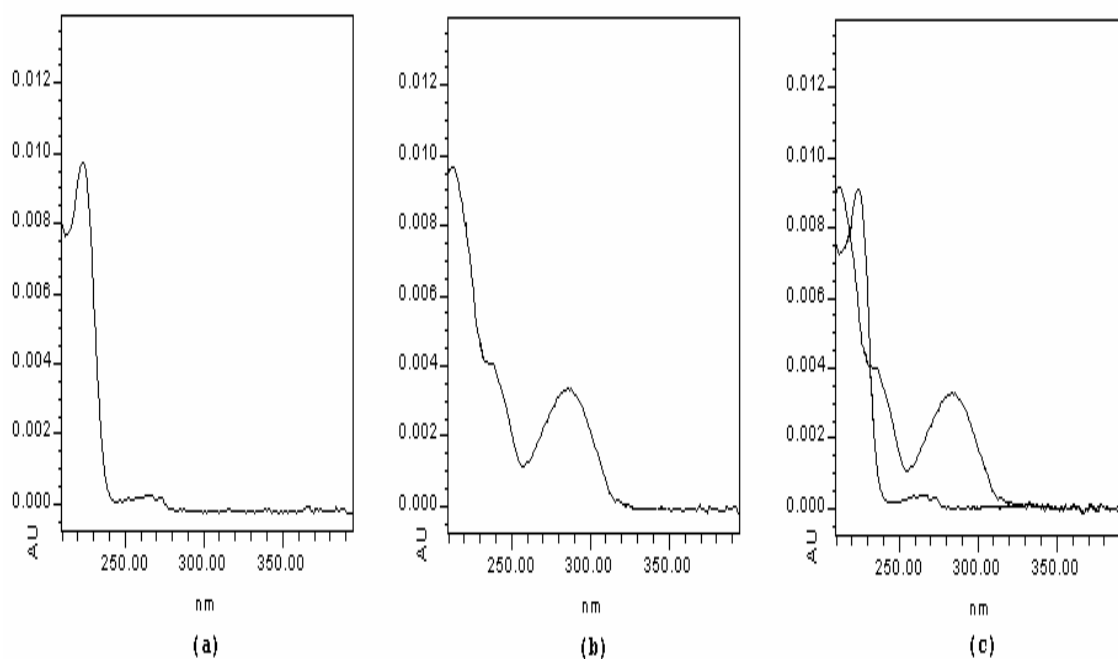


Figure 1. Specificity of UV spectra of carbamazepine and ibuprofen. (a) UV spectra of standard ibuprofen (0.0970 M); (b) UV spectra of standard carbamazepine (0.0424 M); (c) UV spectra of carbamazepine and ibuprofen extracted from the chromatogram of carbamazepine sample (Tegra 200) preparation spiked with ibuprofen.

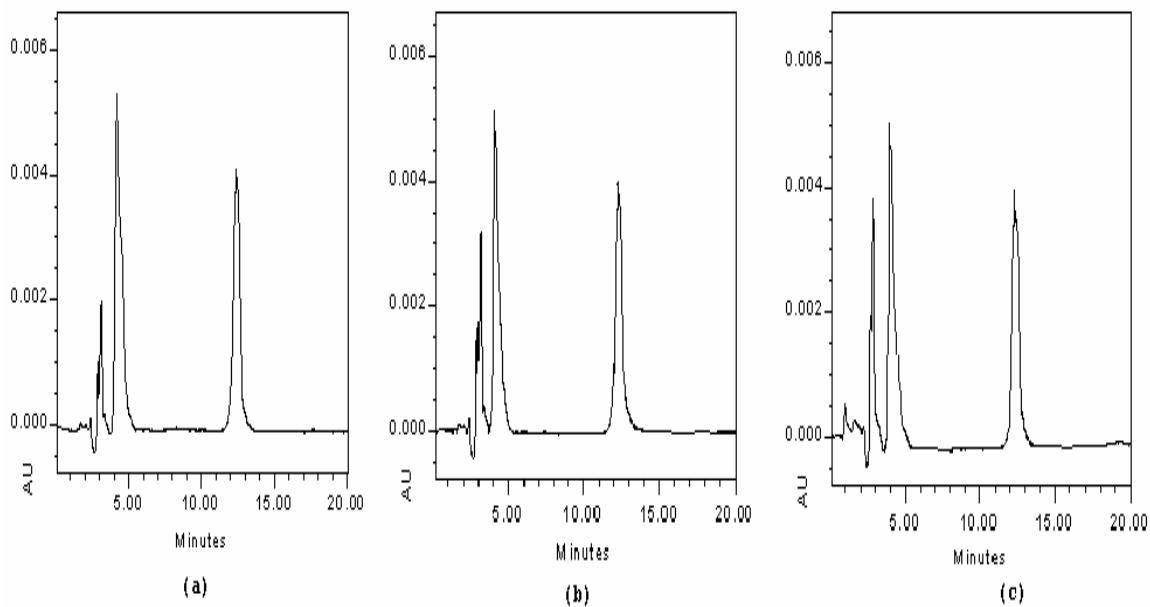


Figure 2. HPLC chromatograms (C18 5 μ column; acetonitrile:sodium phosphate buffer = 28:72, 230 nm, 1 ml/min) (a) HPLC of carbamazepine (0.0847 M) with internal standard ibuprofen (0.0970 M) (b) HPLC of a sample preparation from the uncoated Tegral carbamazepine tablet (c) HPLC of a sample preparation from the film-coated Tegretol carbamazepine tablet.

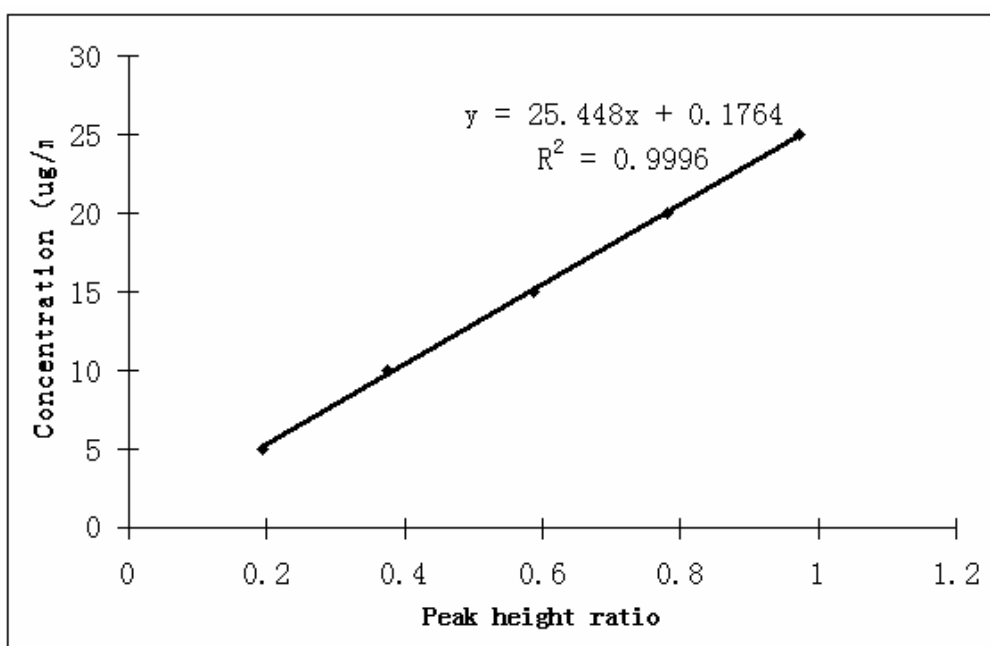


Figure 3. Calibration graphs with standard regression equations and correlation coefficients (R^2). (Peak height ratio = carbamazepine / ibuprofen)